Edited by:

ROBERT HOFMANN, WIEBKE KIRLEIS, JOHANNES MÜLLER, VITALII RUD, STANISLAV TERNA†, MYKHAILO VIDEIKO

From Ros to Prut:

TRANSFORMATIONS OF **TRYPILLIA SETTLEMENTS**

VOLUME I



From Ros to Prut:

TRANSFORMATIONS OF TRYPILLIA SETTLEMENTS VOLUME I



Edited by:

ROBERT HOFMANN, WIEBKE KIRLEIS, JOHANNES MÜLLER, VITALII RUD, STANISLAV ŢERNA \dagger , MYKHAILO VIDEIKO

From Ros to Prut:

TRANSFORMATIONS OF TRYPILLIA SETTLEMENTS VOLUME I

© 2025 individual authors

This book is published under a Creative Commons Attribution 4.0 International License (CC BY 4.0). This license does not apply to content that is attributed to sources other than the copyright holder mentioned above. Under this license you are free to share and adapt this work, provided the makers are attributed.

For more information about our licenses, please visit https://www.sidestone.com/publishing/creative-commons.



Published by Sidestone Press, Leiden

www.sidestone.com

E-mail: info @ sidestone.nl Phone: (+31)(0)71-7370131

Imprint: Sidestone Press Academics

This book has been peer-reviewed. For more information see www.sidestone.com

Graphic editing: Esther Thelen and Ralf Opitz Copy-editing: Sara Krubeck and Nicole Taylor

Language editing: Moura MacDonagh

Layout & cover design: CRC 1266/Carsten Reckweg and Sidestone Press

Cover image: Susanne Beyer

ISBN 978-94-6427-072-3 (softcover) ISBN 978-94-6427-073-0 (hardcover) ISBN 978-94-6427-074-7 (PDF e-book) ISSN (print) 2590-122 | (e-book) 2950-2438

DOI: 10.59641/j9n462cl

The STPAS publications originate from or are involved with the Collaborative Research Centre 1266, which is funded by the Deutsche Forschungsgemeinschaft (DFG, German Research Foundation; Projektnummer 2901391021 – SFB 1266).

Contents

Foreword of the series editors	5
Foreword of the editors	9
TRYPILLIA RESEARCH DECOLONISATION	13
1. Modern Trypillia Transformation research: decolonising through new research concepts, methods and results Johannes Müller	15
MAIDANESTSKE AND SINYUKHA REGION (REGION A)	21
2. Report on the fieldwork of 2016 in the Trypillia mega-site Maidanetske: Investigations on the development and internal structuring Robert Hofmann, Johannes Müller, Wiebke Kirleis, Mykhailo Videiko, Hans-Rudolf Bork, René Ohlrau, Natalia Burdo, Liudmyla Shatilo, Vitalii Rud, Stefan Dreibrodt, Knut Rassmann, Mariia Videiko	23
3. Geophysical Investigations at Maidanetske Natalie Pickartz, Tina Wunderlich, Erica Corradini, Knut Rassmann, Dennis Wilken, Wolfgang Rabbel	107
4. Geoarchaeological analyses on daub pieces from Maidanetske – A treatise on reconstructing burning temperatures of houses and daub processing Stefan Dreibrodt, Sarah Martini, Robert Hofmann, Marta Dal Corso, Wiebke Kirleis, Johannes Müller	115
5. The geoarchaeological record of the Chalcolithic Trypillian mega-site Maidanetske, central Ukraine Stefan Dreibrodt, Sarah Martini, Robert Hofmann, Marta Dal Corso, Wiebke Kirleis, Johannes Müller	137
6. Worked osseous materials from the site of Maidanetske: is that all there is? Andreea Ţerna	157
7. Plant economy and local environment at the Trypillia mega-site Maidanetske from botanical macro-remains Marta Dal Corso, Wiebke Kirleis	167

8. X-Ray computer microtomography (XRay-µCT) as a fast non-invasive technique for compositional studies of burnt prehistorical materials: results and implications from burnt daub at Maidanetske, central Ukraine Stefan Dreibrodt, Christopher Heilmann, Marta Dal Corso, Pia Bodden, Robert Hofmann, Mykhailo Videiko, Johannes Müller, Wiebke Kirleis, Astrid Holzheid	191
9. Archaeozoological and taphonomic examinations carried out on faunal remains from Ukrainian-German excavations at Maidanetske from 2013 to 2016 Norbert Benecke, Robert Hofmann, Mykhailo Videiko, Johannes Müller	217
10. The contribution of Chalcolithic terrestrial snail shells from Maidanetske to environmental reconstruction Frank Schlütz, Marta Dal Corso, Wiebke Kirleis	251
11. Before Talianki: large Trypillian sites built before the largest mega-sites in the Sinyukha basin Robert Hofmann, Liudmyla Shatilo	257
12. What was the significance of small Trypillia settlements? Report on a test excavation in Moshuriv 1, Sinyukha river basin, Ukraine Robert Hofmann, Liudmyla Shatilo, Mykhailo Videiko	309
13. Trypillia mega-sites vicinity: the chronology of several small sites of the Southern Buh left bank region Mykhailo Videiko, Vitalii Rud, Robert Hofmann, Vladyslav Chabaniuk	323
VOLUME II contains a further 8 chapters, organised into the following sections:)

BUG-DNIESTER INTERFLUVE (REGION B)
PRUT/DNIESTER INTERFLUVE (REGION C)
TRYPILLIA MACROSCALE
CONCLUSION

MAIDANESTSKE AND SINYUKHA REGION (REGION A)

2. Report on the fieldwork of 2016 in the Trypillia mega-site Maidanetske: Investigations on the development and internal structuring

Robert Hofmann, Johannes Müller, Wiebke Kirleis, Mykhailo Videiko, Hans-Rudolf Bork, René Ohlrau, Natalia Burdo, Liudmyla Shatilo, Vitalii Rud, Stefan Dreibrodt, Knut Rassmann, Mariia Videiko

Abstract

In this chapter, we present results of Ukrainian-German fieldwork of 2016 in the Trypillia mega-site Maidanetske, Ukraine. In addition to the continuation of the archaeomagnetic surveys, these field works included excavations in one of the ditches, the investigation of a communal building and different unbuilt open areas of the settlement. In combination with radiometric dating and various scientific investigations, which are presented in other contributions of this volume, important new results on the internal development of the settlement, the use of space, the function of ditches and the architectural and functional differentiation between residential houses and communal mega-structures were obtained during these explorations.

Introduction

This chapter reports on the 2016 field activities in the Trypillia mega-site at Maidanetske, Talne Raion, which at 200 ha in size represents one of the largest Trypillian settlements. It dates in relative chronology to the period Trypillia C1 (*e.g.* Shmaglij and Videiko 2005; Rassmann *et al.* 2014; Müller *et al.* 2017; Müller and Videiko 2016; Ohlrau 2020a). Our fieldwork builds on extensive earlier surveys and excavations and is embedded within Ukrainian-German research on the large Trypillia settlements framework of the Collaborative Research Centre 1266. In addition to archaeomagnetic surveys and excavations in Maidanetske, we excavated test

trenches in the two approximately contemporaneous settlements of Moshuriv 1 and Vijtivka (Chapter 12, this work, Vol. I).

During the 2013 and 2014 campaigns in Maidanetske, systematic investigations focused on uncovering examples of burnt houses (Trenches 51, 92), pits (Trenches 50, 52, 60) and pottery kilns (Trench 80; Müller *et al.* 2017; Müller and Videiko 2016; Ohlrau 2020a). Furthermore, as the backbone of our sampling strategy, we excavated test trenches systematically in order to obtain sampling material for ¹⁴C dating, typo-chronological studies, archaeobotanical, archaeozoological and pedological analyses from different parts of the site (Trenches 70–79 and 94–103).

Thus, while these earlier campaigns were focused primarily at the level of individual households, the 2016 excavations investigated various aspects of the settlement as a whole. We attempted to understand the social organisation within a Trypillia mega-site, on the one hand by investigating a presumed collaborativelybuilt ditch and, on the other hand, through the excavation of a special category of building, a so-called mega-structure. The term 'mega-structure' was introduced by Mykhailo Videiko and John Chapman for a large construction that was investigated in Nebelivka in 2012 (Videiko et al. 2013). Within our research at Maidanetske, the term was adopted and used for all large buildings in highly visible positions (Hofmann et al. 2019). These could be identified mainly in otherwise unbuilt concentric ring-corridors of the giant settlement, which we interpret as public areas in-between residential domestic zones (Rassmann et al. 2014; Ohlrau 2015; Hofmann et al. 2019). In addition to this first and most important criterion, two other criteria are hierarchically used in the identification of mega-structures in archaeomagnetic site plans, namely that these buildings display specific architecture in comparison to domestic dwellings and often have extraordinarily large dimensions. The number of mega-structures is many times lower than that of residential houses. Our excavations aimed to reconstruct the architecture and create an inventory of such a building, in order to decipher its functions for the communal integration and social organisation of the community.

The investigation of unbuilt areas in the centre of the settlement and, for comparison, within the ring corridor, aimed to reconstruct the use of public space within the settlement. This should help clarify whether the central unbuilt areas were used for economic purposes such as animal husbandry, gardening/food production or rather for integrative activities. In addition, the excavation offered the opportunity to investigate and date the temporal relationship of different settlement ground plans in a stratigraphic setting.

Fieldwork strategy 2016

In 2016 we continued the sampling and focused mainly on four targets in the northern and central parts of the site:

- 1. In Trench 111, for the first time in Maidanetske, one of the large building structures was uncovered, situated in a particularly visible position in the main street of the settlement (Figs. 1 and 2A). For this so-called mega-structure, different authors assume public or communal functions, due to the structure's high visibility at regular distances within the public space of the settlement. The investigation of such a building should contribute primarily to the determination of the functions of such buildings.
- 2. Also in Trench 111, there was the chance to examine older settlement remains below the floor of the mega-structure, which have a different spatial layout and indicate a different course of the ring corridor.
- 3. In Trench 110 a section of a ditch was excavated which enclosed the inner (main) part of the settlement (Figs. 1 and 2B). The southern part of a burnt house was included in the excavation area, in order to clarify on the one hand the chrono-

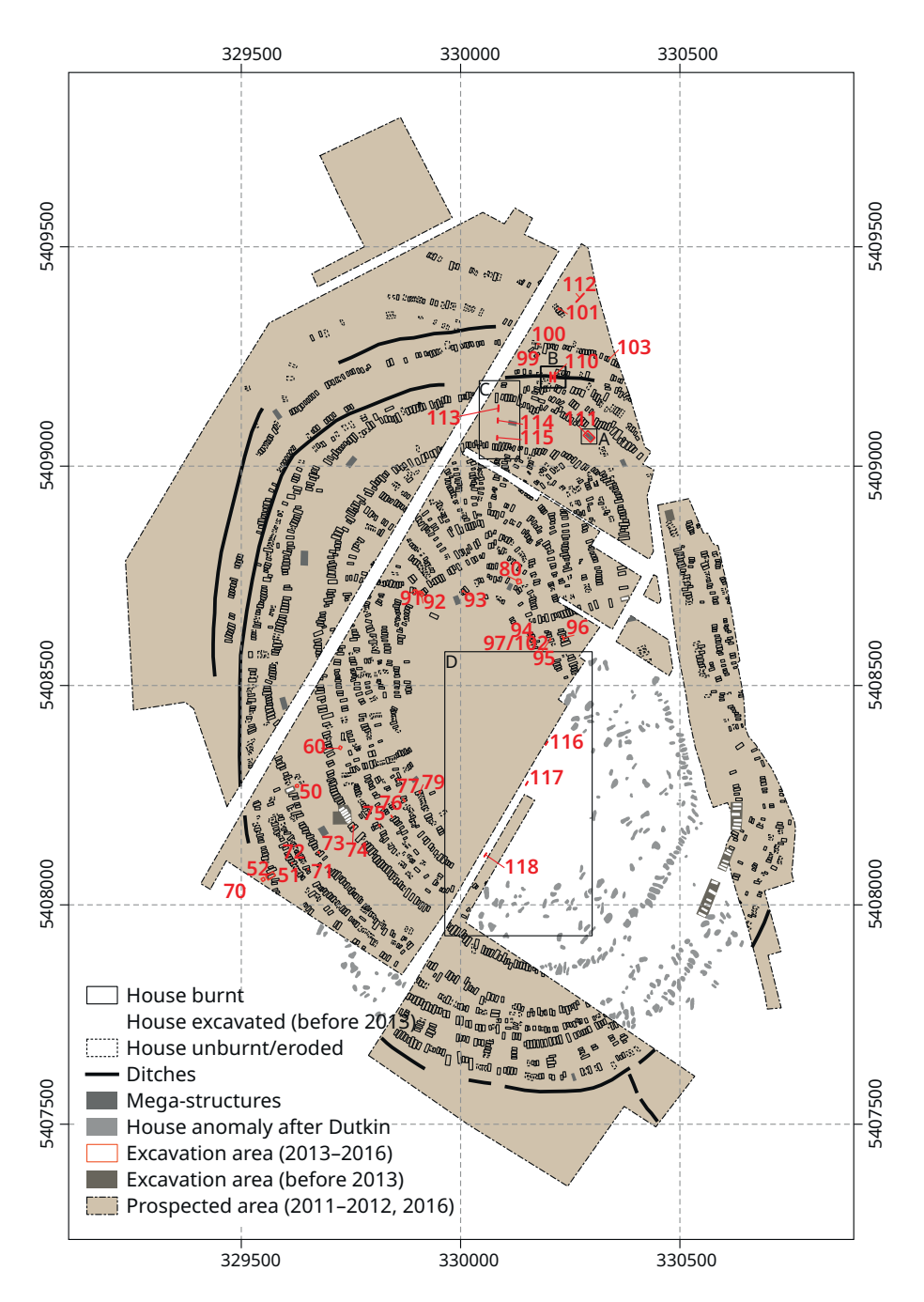


Figure 1. Plan of the Maidanetske mega-site with location of the trenches investigated between 2013 and 2016.

logical (stratigraphic) relationship between the ditch and, on the other hand, the house rows which are situated more to the north, outside the enclosed area. The results and analysis of the excavations in Trench 110 were recently published in detail by René Ohlrau (2020a) as part of his dissertation.

- 4. The excavation in Trenches 113–117 aimed to investigate different kinds of unbuilt areas of the settlement in order to try and establish the purposes for which the large unbuilt space in the centre of settlement was used. To do this, in each case three trenches were excavated in the central unbuilt space (Trenches 116–118) and in the main street of the settlement (Trenches 113–115).
- 5. At the northern periphery of the settlement, in Trench 112, a gully, visible in the terrain surface and running from northwest to southeast into the valley of the Talianki River (Fig. 1) was investigated by geomorphologists. The primary purpose of this was to investigate colluvial deposits but this was unsuccessful.

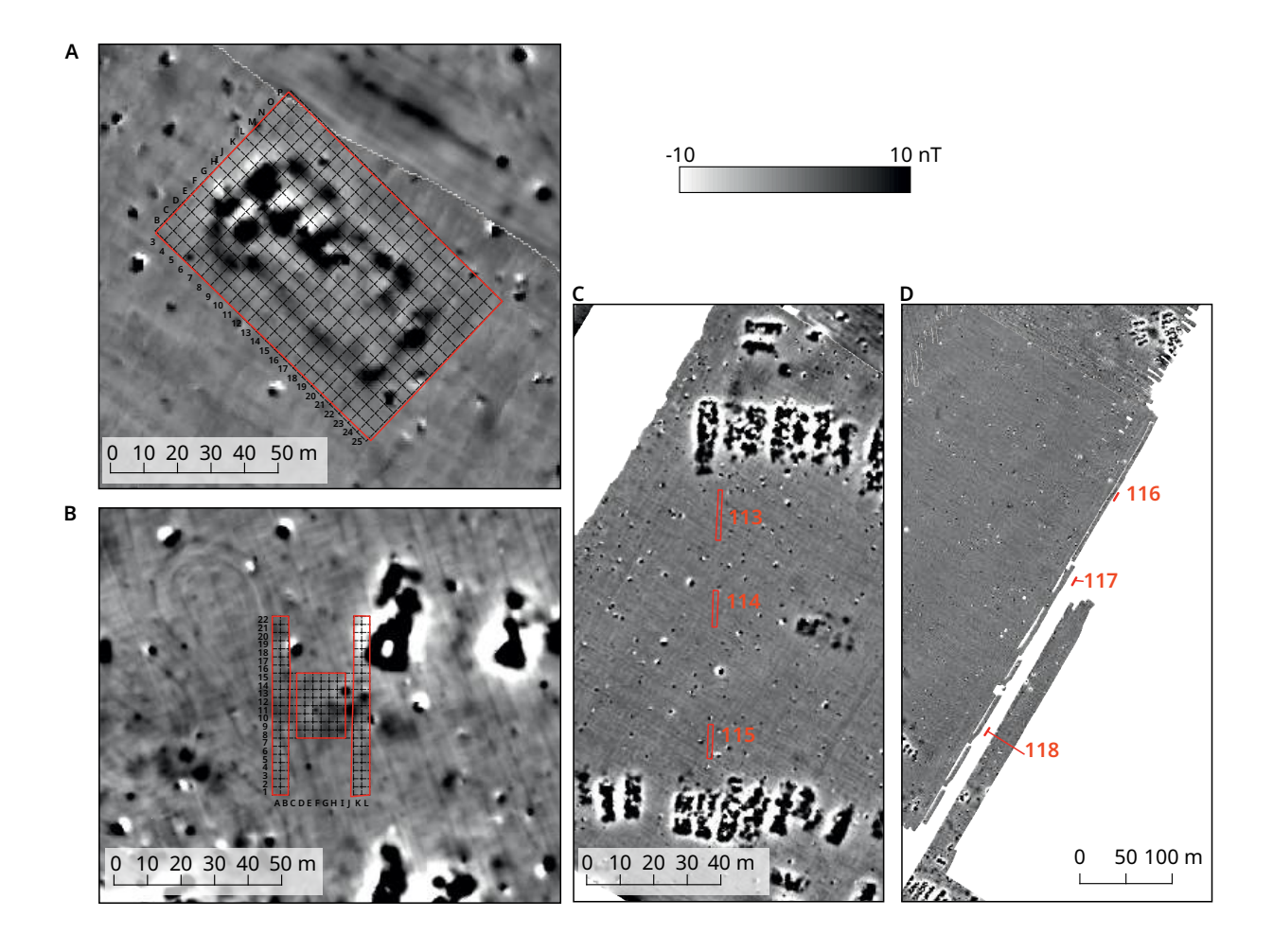


Figure 2. Details of the Maidanetske archaeomagnetic plan with location of anomalies and trenches investigated in 2016: (A) Mega-structure 3 (Trench 111); (B) ditch and house area (Trench 110); (C) within the ring corridor (Trenches 113–115); (D) in the central undeveloped area (Trenches 116–118).

Methods and Materials

Excavation methods and sampling

During the excavations in Maidanetske, we applied a dual excavation strategy based on the results of archaeomagnetic prospection. On the one hand we aimed to investigate examples of selected contexts of different find categories (Chapman *et al.* 2014b; Müller *et al.* 2017, 25–30; Hofmann *et al.* 2018). On the other hand, we sampled systematically different parts of the settlement and different house rings of the settlement, mostly with small test trenches, in order to obtain a representative sample of a Trypillian mega-site for dating, typo-chronological studies and various scientific investigations.

Our excavations were carried out in 'natural layers', which were documented as 'features'. As described in more detail elsewhere, we understand 'features' as units that can be distinguished from one another based on material properties such as the type of soil substrate, their colouring and the type, size and quantity of admixtures contained therein (Hofmann *et al.* 2006, 64–67; Hofmann 2013, 52). The localisation of the finds was performed using xyz coordinates (single finds, samples) and a grid system with a width of one metre. In addition, we assigned finds to features and levels, which usually allows a more precise attribution and interpretation of depositional processes in larger contexts. Descriptions of the properties of features and finds are given in the database of the CRC1266 subproject D1 (Hofmann *et al.* 2023).

In general, a systematic and area-wide sampling of the excavation areas for botanical, zoological and geoarchaeological analyses was carried out, which should enable a reconstruction of activity zones in as much detail as possible and, if necessary, the functional differentiation of the site. The use of the same samples by the different disciplines involved ensures an optimal interdisciplinary synergy of the results. Horizontal sampling for botanical and geoarchaeological investigations took place in every second to fourth quadrat. Selected profiles were vertically sampled in 10 cm steps.

Daub classification

In order to be able to understand the architecture and the materials used for the construction of the buildings, on the burnt daub we documented old surfaces and imprints of woods during our excavations in Maidanetske. The documentation was carried out in two different ways.

On the one hand, we mapped the position, type, direction and dimension of wood imprints on drawings or orthophotos. In addition, we measured the diameters of logs and the width of split wood planks.

However, as focussing on imprints of vanished woods does not adequately consider numerous other types of information on daub such as surface treatments and the thickness of loam covering, we decided to classify the daub fragments further, in addition to the description of features and the documentation of impressions. This kind of documentation of the daub seems to us feasible in terms of the required expenditure of time, and is appropriate for large quantities of daub, which in a Trypillia house can comprise up to several tons. We determined the quantities of the different daub types by weighing and counting them and then used find numbers to link them with further context information. In this way, we were able to assign the quantities to individual quadrats, features, levels and building components. The determined masses contributed to the calibration and advanced analysis of the archaeomagnetic plan of Maidanetske (Pickartz *et al.* 2019; Pickartz *et al.* 2022).

Compared to our earlier attempts, this more flexible classification system of burnt daub that we used in 2016 provides separate classifications of *material types*, on the one hand, and *architectural features*, on the other hand. We assume that the *material types* are the result of specific recipes for the processing of the clay, *e.g.* tempering, *etc.* to prepare for its use in a building. We understand *architectural features* to be any kind of manipulation to a building for architectural reasons. *Architectural reasons* include both technical (construction) and visual requirements (*e.g.* surface finish, imprints, wall decoration).

We defined three material categories and four different architectural features, which could be applied to large quantities of daub within a reasonable time-scale (Tab. 1). Nevertheless, even with this relatively simple classification, one person had to work full-time on the data recording of daub when excavating a burnt building.

From the materials used, we can distinguish compact burnt daub without additives from those that are usually highly porous due to organic tempering. Microscopic and micro-tomographic studies have recently shown that the builders of Trypillia houses added large amounts of cereal chaff to the latter category of material (Chapter 8, this work, Vol. I).

Within this organically tempered category, two variants can be distinguished, which were each used in specific parts of the buildings. For the covering of walls, ceilings and the substructure of floors, the builders usually applied a solid light to medium orange category. A crumbly-yellowish variant was the preferred choice of the builders for podiums and installations. Compact material without macroscopically discernible tempering served for the construction of more heavily stressed surfaces such as floors and fireplaces.

Table 1. Material types of burnt daub: 2016 classification and concordance with the 2013 and 2014 classification (after Müller et al. 2017, 29).

Material type	Type-ID – 2013 and 2014 classification
1. compact (without chaff)	2
2. organic tempered (chaff), light-medium orange	1, 3, 5, 7
3. organic tempered (chaff), yellowish, crumbly	4

Architectural features
1 Amorphous
2 Plain surface
3 Two plain surfaces
4 Split wood
5 Log wood
6 Combination: split wood + split wood
7 Combination: split wood + plain surface
8 Combination: 2x split wood + plain surface
9 Combination: split wood + 2x plain surface
10 Combination: split wood + log wood
11 Combination: 2x split wood + log wood
12 Combination: split wood + log wood + plain surface
13 Combination: log wood + plain surface
14 Combination: log wood + 2x plain surface
15 Combination: log wood + log wood
16 Combination: 2x log wood + plain surface
17 Wattle

Table 2. Classification used for architectural features during the 2016 campaign in Maidanetske.

Five basic types of modifications were considered in the classification of burnt daub which, however, also occur in different combinations (Tab. 2). This included negative imprints of timbers in the form of split wood planks and logs. In addition, flat surfaces and different combinations of surface treatments and negatives of timbers were documented.

Grouping of features

The features were grouped on three hierarchical levels according to a system originally developed for the late Neolithic settlement Okolište in Central Bosnia (Hofmann *et al.* 2006; Hofmann 2013). This system allows comparisons of inventories of certain settlement areas (*layer formations*), the entity of specific feature categories (*layer groups* such as houses, pits, and ditch segments) or parts of specific contexts (*layers* such as part of a house or infilling into a pit). For each context of the grouping level *layers*, the volume of the excavated earth was calculated; this was the basis for the calculation of find densities.

Pottery classification, technology, morphology, and decoration

For classification of Trypillia pottery in the Sinyukha River Basin area, a ceramic typology system is important which was developed in detail by Sergei Ryzhov (1999; 2012) in particular, building on previous works by other authors. This

classification system is based on the nomenclature of ancient Greek pottery. In a slightly modified and simplified form, classification systems with comparable systemisation and nomenclature were also used by, for example, Eduard Ovchynnykov (2014), Renè Ohlrau (2020a) and most recently by Liudmyla Shatilo (2021). A nomenclature which is very different in some ways was recently tested on ceramics from Nebelivka (Caswell *et al.* 2020).

When working on the pottery from the Ukrainian-German excavations in Maidanetske, several authors have followed Sergei Ryzhov's classification system; however, those type descriptions have not been published in detail. In this present chapter, the morphological classification of vessels was based on the classification system of Liudmyla Shatilo (2021) which, unlike the typologies of other authors, fits better to the fragmentary character of the find material discussed here. For the technological characterisation of the fabrics, reference is made to the work of René Ohlrau (2020a).

From a technological point of view, so-called kitchenwares, tablewares and 'container wares' are differentiated in the inventory; each one of these was further differentiated according to their temper and surface colour (Tab. 3). While container wares, which scarcely play any role in terms of quantity, are typically organically-tempered, kitchenwares have grey or grey-brown fabrics, are often tempered with crushed shells and moderate to coarse quartz aggregates, and are predominantly fired in a reducing firing atmosphere. These usually comprise less than 10% and a maximum of 20% of the inventories. As demonstrated by their clustered occurrence in burnt contexts (houses or layers over burnt houses), orange-coloured variants are likely to have undergone secondary re-oxidation during the burning of the structures (Fig. 3). Accordingly, so-called 'kitchenwares' are probably not the remains of cooking vessels or pottery used for other pyrotechnic processes.

In contrast to kitchenware, the usually dark-painted and representative tableware was produced under completely oxidising firing conditions. Tableware forms the majority of the inventories, in most cases at more than 90%. Whitish-yellow to reddish surfaces were achieved through the use of kaolin and partly iron-rich white to reddish firing clays. Since the primary firing of the vessels already took place at relatively high temperatures of 800–1200 degrees Celsius in a new type of double-chamber kiln, the additional secondary firing which occurred when the houses burnt down only led to colour changes under certain conditions. Therefore, we cannot exclude the use of tableware as part of pyrotechnical processes.

Nonetheless, from a technological perspective it is remarkable that the ceramic assemblages from Maidanetske and other Trypillia mega-sites consist predominantly of representative painted vessels suitable for use in the context of ritual food consumption. Ceramic vessels, which were clearly used to prepare food and (less representative) vessels for storage, on the other hand, are clearly underrepresented.

Morphologically, according to Liudmyla Shatilo (2021), a distinction was made between six 'types' and ten 'classes' of vessels, to which categories of functions were tentatively assigned according to Rice (1987), taking into account their volumes and their technological properties (Tab. 4). We are aware that functional assignments made in this way can at best allow insight into past category systems of manufacturers and users (Wotzka 1997) and may not be congruent with the actual use of the vessels. In our view, the comparison of frequencies of these functional categories in find inventories does nevertheless offer, under favourable circumstances, the chance to represent and interpret functional differences between contexts.

Bowls, often in a very crudely manner manufactured cups and very representative goblets were most likely used for the serving of food. We consider the following as storage vessels: pear-shaped vessels (including the associated lids as well as large specimens of the categories krater and krater-like), bi-conical and sphero-conical vessels. The generally smaller amphorae and fine ceramic pots as

Fabric	Description
Table: fine, white	
Table: fine, reddish	
Table: fine, red	
Table: medium, white	
Table: medium, reddish	
Table: medium, red	
Table: low secondary fired	Surface discoloured, fracture orange or reddish, not sintered
Table: strongly secondary fired	Grey-blue, at least surface sintered
Table: secondary fired (slagged)	Caked with a significant proportion of slag
Kitchen: coarse, grey brown	
Kitchen: coarse, orange	
Kitchen: strongly secondary fired	Dark red, porous
Container ware	Very thick-walled, strongly organically tempered
Indefinite: reduced	
Indefinite: uncleaned	

Table 3. Classification of ceramic fabrics used for ceramics during the 2016 campaign in Maidanetske.

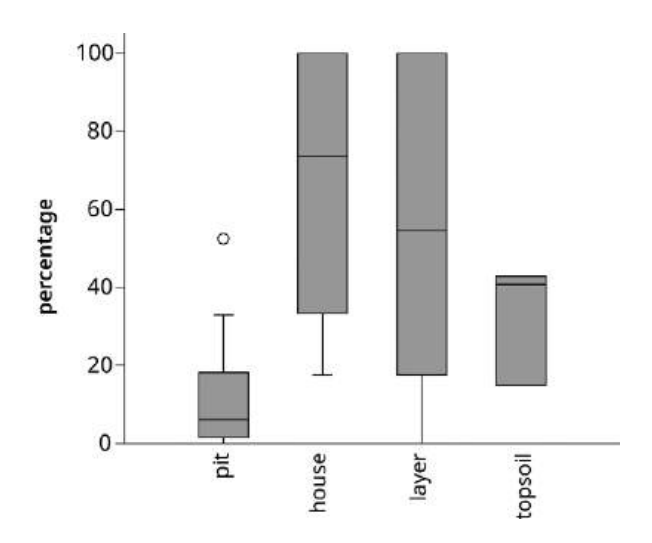


Figure 3. Maidanetske, Trenches 50–111, percentages of orange-coloured so-called kitchenware (among all kitchenwares) in selected types of contexts.

well as smaller bi- and sphero-conical vessels we assume to be serving vessels. Vessels made of kitchenware were probably used to prepare food, although the use of heat can probably be excluded to some extent.

Sergei Ryzhov (1999; 2012) classified decorations at the level of design into so-called 'decoration schemes'. The relevance of this classification for the long-term relative chronology of the Sinyukha River basin was confirmed by Lennart Brandtstätter (2017; cf. Shatilo 2021). In contrast, 'micro' or intrasite chronologies for individual sites have so far relied mainly on the analysis of ¹⁴C dating (Rassamakin 2012; Ohlrau 2020a; Shatilo 2021). Attempts to elaborate 'micro-chronologies' based on vessel shapes and 'decoration traits' have recently been made by René Ohlrau (2020a) for Maidanetske and Liudmyla Shatilo (2021) for Talianki.

Types	Vessel class	Capacity (range in l)	Capacity (median in l)	Kitchenware	Tableware
Bowls		≤2.5 (7)		Processing (without heat)	Transport (serving)
Goblets	Cup	≤0.2			Transport (serving)
Goblets	Goblet	0.2–1			Transport (serving)
Kraters/ krater-like v./	Krater/krater-like	0.1–5 5–54	2.6		Small – transport (serving) Large – storage
pots	Pot		3	Processing (without heat)	Transport (serving)
Pear-shaped v.					Storage
Lids					Storage
	Bi-conical	0.1–5 5–120	6		Small – transport (serving) Large – storage
Biconical/ sphero-conical v./ amphorae	Sphero-conical				Small – transport (serving) Large – storage
	Amphorae	0.3–5 6.6–35	1.4		Transport (serving) Large – storage

Site formation processes

In order to evaluate the archaeological significance of the find assemblages, we aimed to make a taphonomic reconstruction of the depositional processes. In accordance with the terminology introduced by Ulrike Sommer (1991), an attempt is made to distinguish between primary, secondary and tertiary waste. This classification is based on the logic that, basically, all artefacts remaining in an abandoned settlement constitute 'waste' and that ritually deposited artefacts also belong to it. Just as vessels remaining at the site of their use in a burnt house would be classified as *primary waste*, so would, for example, the remains of a ritual meal remaining at the place of deposition. This is contrasted with *secondary* or *tertiary waste* that has been relocated once or several times. An additional category is so-called *foreign waste* deposited from 'outside'.

The relevant parameters for taphonomic reconstructions in this chapter are, on the one hand, the density of finds in relation to volumes of excavated earth and, on the other hand, the average (mean) artefact weight. The former parameter gives a general impression of where waste was deposited. The average artefact weight serves as a proxy for the degree of fragmentation. Because of their ubiquity, find densities and fragmentations were studied for burnt daub, bones and pottery, while other find categories were too rare to be studied in this way. The combination of find density and fragmentation level potentially allows the identification of primary and secondary waste areas, with the interpretation gaining significance by comparing different find categories. However, one has to take into account that one and the same context may contain different secondary or primary and secondary waste.

Quantification of vessels

Quantifications of vessels are important, since the size of inventories and the percentage of morphological and technological groups within them can provide information on depositional processes and the function of specific contexts. Corresponding quantifications of vessels are a methodical problem especially when – as in the present case – only selective reassembly was performed. In the case

Table 4. Classification and proposed function of vessel categories after Shatilo (2021) based on a regional sample of the Sinyukha river basin.

of the ceramic assemblages from Maidanetske, an attempt was made to quantify vessels using statistical methods. For this purpose, the preserved percentages of rim, belly and bottom fragments were documented. By summing up these proportions, a minimum number of vessels (MNI) is obtained whereby in each case 100% of the rim, belly or base represents one vessel.

Dating

The dating of Maidanetske is based on the analysis and Bayesian modelling of 93 14 C dates from practically all contexts investigated with participation from the Kiel side (Müller *et al.* 2017; Brandtstätter 2017; Ohlrau 2020a; Chapter 19, this work, Vol. II). The analyses were carried out with the OxCal software (Bronk Ramsey 2009) and the IntCal20 calibration curve (Reimer *et al.* 2020). Modelling by René Ohlrau (2020a) resulted in the differentiation of four settlement phases with a total duration of about 350 years between 3990 and 3640 BCE, which we attempted to assign to the different contexts. Partly chronological fuzziness has to be accepted, which makes aoristic divisions necessary in the chronological interpretations. In terms of absolute chronology, the phases date as follows: Phase 1 – 3990–3935 BCE, Phase 2 – 3935–3800 BCE, Phase 3 – 3800–3700 BCE and Phase 4 – 3700–3640 BCE. The highest building density was in Phase 3, with 1700 apparently coexisting houses.

Results

Trench 110 - Ditch and burnt dwelling

The results obtained through excavations and subsequent analyses in Trench 110 have already been presented in detail elsewhere by René Ohlrau (2020a, 106–117, 212–214). These were supplemented by investigations of depositional processes on bones (Chapter 9, this work, Vol. I). Here, these findings are summarised in brief only, to the extent that they are relevant to the questions addressed in this report. The excavations in Trench 110 included a 12 m long ditch section and a small portion of a dwelling (Figs. 4 and 5).

The ditch investigated in the central area of Trench 110 shows an interruption, approximately 3.5 m long which might therefore be seen to be a causewayed enclosure. Should this interpretation prove to be correct, it would question the defensive character of the enclosure and reveal possible references to contemporaneous complexes in the Central European region (*e.g.* Michelsberg, Funnel Beaker). However, it cannot be ruled out at present that the interruption represents a gateway.

The ditches had maximum widths of 2.5 m, depths of 1.0–1.1 m and u-shaped cross-sections partly tending towards a v-shape. Irrespective of the question of the primary function of the enclosure, the dating and the type and quantity of finds from the two ditch segments reveal different biographies and depositional processes. While the backfilling of the western ditch segment took place between 3955–3810 BCE, so in early phases of the settlement, the eastern ditch segment was filled much later, between 3840–3650 BCE. This potentially longer duration of use is matched by much higher amounts of sterile soil material at the bottom of the eastern segment, washed away from the trench walls, compared to the western ditch segment.

The eastern ditch segment is characterised by moderate densities and fragmentations of bones and pottery and therefore most likely represents the remains of demolished houses and 'normal' household waste. In contrast, the find inventory of the western ditch segment shows some special characteristics:

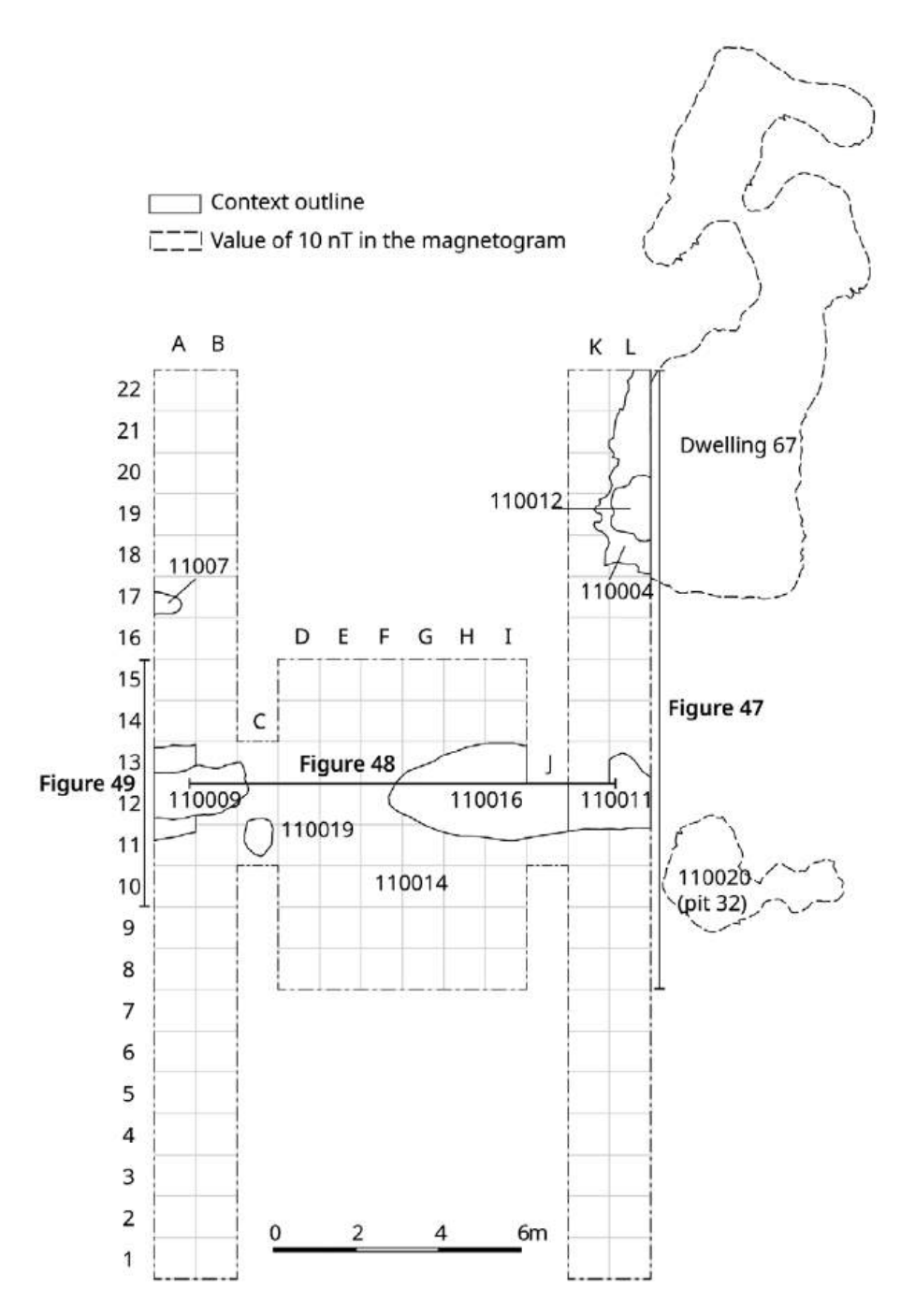


Figure 4. Maidanetske, plan of Trench 110 with location of contexts and profiles (after Ohlrau 2020a, Fig. 46).

the deposition of a *bucranium*, a significantly higher density and lower degree of fragmentation of bones and pottery, and the upside-down deposition of vessels.

The burnt house partly uncovered in the north of Trench 110 over an area of 5×1 m differed from other houses in Maidanetske, having an architecture without a platform raised from the ground (Fig. 5). The usage time of this house was dated to between 3700–3635 BCE (68.2%), the final phase of the settlement. Pit 20 associated with this house cut into the fill of the eastern ditch segment of the ditch, indicating that this may have already been backfilled when the house was built.

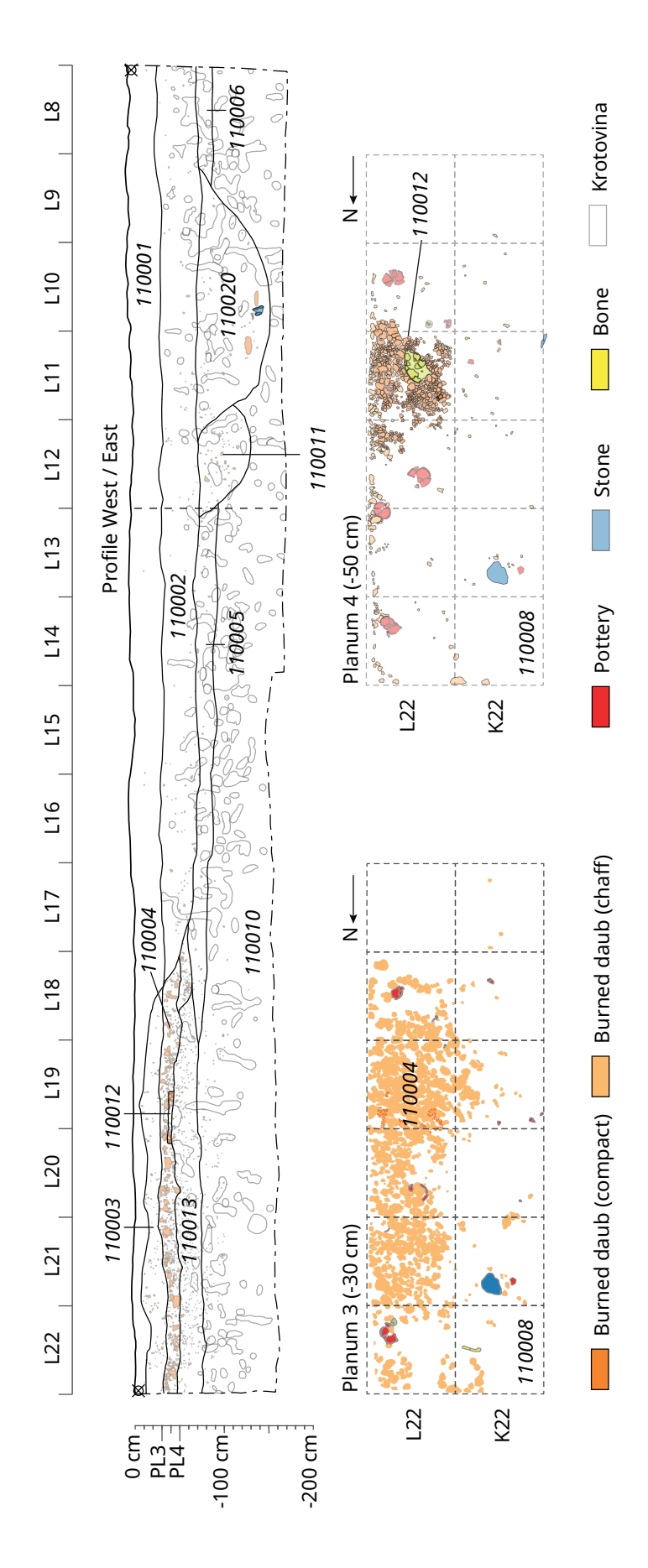
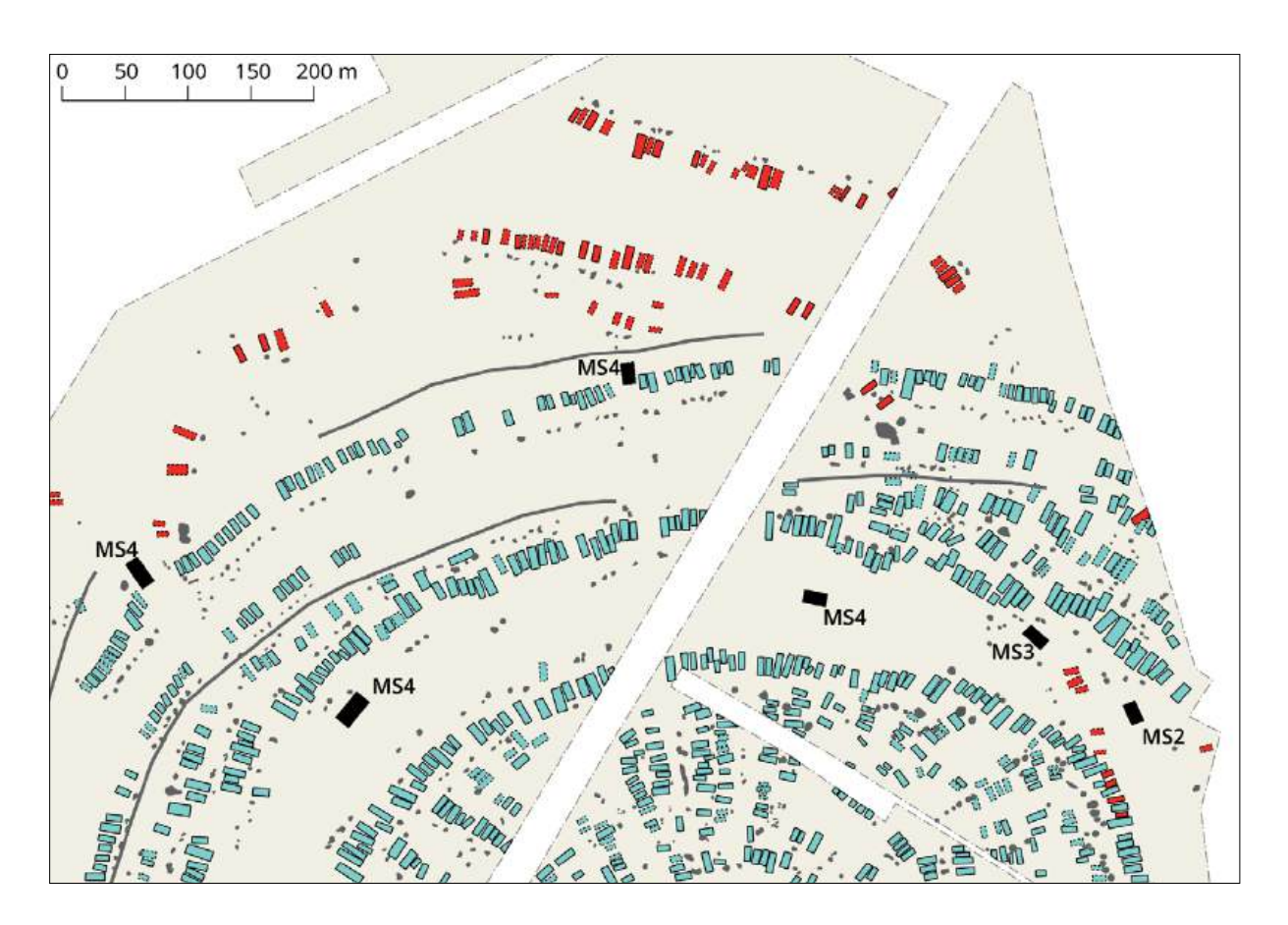


Figure 5. Maidanetske, eastern profile and plana of House 67 in Trench 110 (after Ohlrau 2020a, Fig. 47).



Trench 111 – Excavations in the area of Megastructure 3 in the ring corridor

Situation in the vicinity of Mega-structure 3

In the north of the Maidanetske 1¹ site, two ring-shaped settlements overlap each other (Fig. 6). To the North of the settlement plan drawn up of Maidanetske 1b there are two parallel rows of houses, which probably represent the ring corridor of an older(?), only partly completed or later partly cleared settlement Maidanetske 1a. Due to the many houses of settlement Maidanetske 1b, the continuation of the rows of houses of this second complex to the south is not easily visible.

Mega-structure 3 is located close to the northern boundary of the 70–90 m wide ring corridor of the presumably younger settlement Maidanetske 1b. Apparently in order to create enough space for the mega-structure, the very irregular northern 'building line' of the ring-corridor drop-back at the border of two house clusters northwest of the mega-structure. However, similar drop-backs also occur elsewhere and therefore this does not necessarily have anything to do with the positioning of mega-structures.

Within the ring-corridor of settlement 1b, approximately 25 m southeast of Mega-structure 3, a row of at least six burnt dwellings runs with interruptions in a northwest-southeast direction. Associated with each house is a pit located about 10 metres to the southwest, perhaps defining the back area of each building.

Figure 6. Interpretation of the archaeomagnetic plan of the northern part of Maidanetske. Different colours indicate the affiliation of individual houses to the settlements Maidanetske 1a (red) and 1b (turquoise). Megastructures are marked in black.

While the Trypillia B2/C1 period settlement we investigated is labelled Maidanetske 1, Maidanetske 2 represents an alternative name of the Grebenyukiv Yar site, which lies on the opposite side of the Maidanetske village.

Twenty metres northeast of the houses described, the ruins of another megastructure, Mega-structure 2, are located within the ring corridor. Judging by its orientation, this mega-structure belonged to the above-mentioned row of houses.

The houses located within the ring corridor of the settlement Maidanetske 1b and the associated Mega-structure 2 most likely represent remains of the older settlement Maidanetske 1a, which have been preserved in unbuilt areas. If one continues the row of houses to the northwest, it can be connected easily to the house rows in the north. This hypothetical connecting line also runs through the area of Mega-structure 3.

In contrast to the northern one, the southern house row of the ring corridor shows a much more consistent structure, although here again one cannot speak of a 'building line' in the strict sense. Anomalies first occur where the row of houses coming from the inside of the ring corridor meets the more southward-turning boundary row of the ring corridor. Anomalies occur at the point where the row of houses coming from the inside of the ring corridor joins the southern boundary of the ring corridor. The houses located here are standing closer together and some of them show a larger offset in the longitudinal direction.

As a preliminary result of the analysis of the plan of the archaeomagnetic survey, we would highlight the overlapping of two different Trypillia settlements in the north of the Maidanetske site, with partly different courses of the ring corridor. While the ring corridors of the two settlements show different courses in the north and west, they join the same course in the east. Unfortunately, we cannot track further to the south the ground plan of the presumably older settlement Maidanetske 1a (which we can in general identify only very fragmentarily). In order to clarify the described anomalies of the settlement ground plan and to date the two settlements of Maidanetske, targeted archaeological excavations were carried out in 2016.

Criteria for the choice of the excavation area

In order to be able to manage the excavation in a reasonable time-scale, we chose to investigate Mega-structure 3, one of the smallest mega-structures, located within the ring corridor of Maidanetske, in the north of the settlement and detected through archaeomagnetic surveying at the beginning of the 2016 field campaign (Fig. 2A).

Besides its size, the shape of the anomaly was a second selection criterion: we deliberately did not choose a mega-structure with empty interior space for excavation, which is the most frequent type in Maidanetske. Instead, with Mega-structure 3 we chose an example which showed in its northwestern part extensive deposition of burnt daub in several spatial concentrations of high magnetisation, in contrast to the 'magnetically empty' southeastern part. In view of the almost find-free mega-structure in the Dobrovody settlement (cf. Korvin-Piotrovskiy *et al.* 2016), which in the plan of the archaeomagnetic survey was indicated only by linear anomalies of the exterior walls, we regarded these remains of overbuilding as a possible location for a more extensive inventory. The obtaining of such a substantial inventory seemed to be useful to determine the functions of such a building.

The third criterion was the spatial proximity of the excavation area and presumed overlap with the above-mentioned remains of the row of houses belonging to a possible older settlement, Maidanetske 1a. Accordingly, this offered a chance to clarify and date the chronological relationship between the two settlements Maidanetske 1a and 1b in a direct stratigraphical manner.



Stratigraphy

The excavation area of Trench 111 measured 23×15 m and comprised the megastructure itself and the surrounding open space (Fig. 7). The daub of the megastructure was buried under a 0.5 m thick Chernozem layer (Feature 111001; Fig. 8). Analogous to other excavation areas, this layer was divided into a thicker black upper part and a thinner more greyish horizon directly above the daub.

The upper and major part of the burnt daub package consisted of small pieces of highly fragmented debris of the rising walls of the mega-structure building. Over the entire area of the mega-structure, this collapse lay on a rammed earth floor with thicknesses ranging from a few millimetres to several centimetres (Feature 111010).

The rammed earth floor of the mega-structure rested on a humus-rich layer embedded in some places with numerous medium-sized pieces of daub and large pottery, ranging from fragments up to complete vessels (Feature 111025). In most parts of the mega-structure this layer could not be clearly distinguished from the more or less sterile buried humus underneath (Feature 111030). The two layers together had a thickness of between 0.4–0.8 m and have been exposed to intensive bioturbation.

In the southwestern section of the excavation area five pits were dug into the ground in the context of pre-mega-site settlement activities. Most of these pits were clearly situated below the floor of the mega-structure. Remarkable from the stratigraphic point of view is, among others, Pit 33 which was located below the central installation platform of the mega-structure (Quadrats J–K/10–12). This pit, which contained a filling of massive lumps of daub, was superimposed by a humusrich levelling layer which seems to be identical to Feature 111025. Accordingly, there is a high probability that the find-rich layer below the mega-structure is the result of levelling the building ground for the construction of the mega-site. As an alternative interpretation to the theory of a levelling layer, an artificial mounding in the area of the mega-structure may have to be considered (Chapter 5, this work, Vol. I).

Figure 7. Maidanetske, Trench 111, overview (Planum 2).

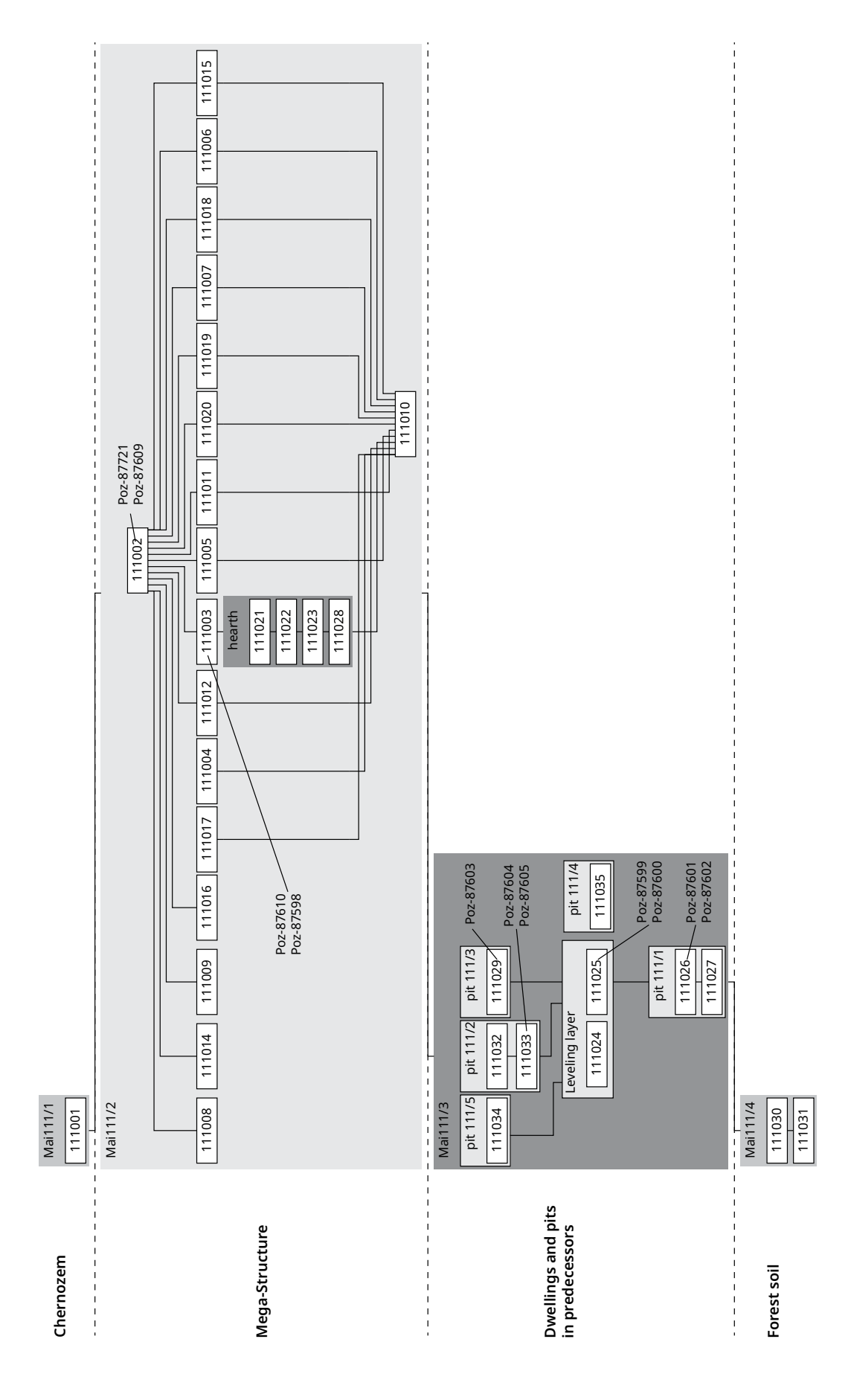


Figure 8. Maidanetske, stratigraphy of Trench 111 shown in a Harris matrix.

Architectural features	Organic tempered (chaff)	Compact (without chaff)	Crumbly yellow	Without material classification
1 Amorphous	438.3	134.3	8.5	
2 Plain surface	208.8	98.7	6.5	0.5
3 Two plain surfaces	88.4	9.7	1.7	
4 Split wood	144.8	3.4	0.5	
5 Log wood	31.0	2.7	1.4	
6 Combination: Split wood + split wood	33.5	1.0		
7 Combination: Split wood + plain surface	58.7	1.2		
8 Combination: 2x split wood + plain surface	18.0			
9 Combination: Split wood + 2 x plain surface (2x)	3.4			
10 Combination: Split wood + log wood	6.0			
11 Combination: 2 x split wood + log wood	0.6			
12 Combination: Split wood + log wood + plain surface	14.7			
13 Combination: Log wood + plain surface	7.8	0.9		
14 Combination: Log wood + plain surface (2x)	0.2			
15 Combination: Log wood + log wood	2.1			
16 Combination: 2 x log wood + plain surface	0.6			
17 Wattle	0.1			
Vitrified daub		1.6		28.7
Non-classified	12.7	12.2	1.0	1.7
Total	1070.2	265.6	19.6	30.9

However, in the cases of the other pits the stratigraphic relation between the levelling layer or platform mound and the pit filling is not entirely clear because of heavy bioturbation. Indeed, in the case of Pit 35, the height and inclination of ceramic fragments indicate that the pit had been dug into the levelling layer. However, we cannot completely exclude an overlapping of the pit by the levelling layer.

Table 5. Maidanetske, weight (in kg) of material categories and architectural features in burnt daub from features of Mega-structure 3.

Overall it can be said that Mega-structure 3 was built in an area in which stratigraphic evidence clearly indicates an earlier settlement phase. Pit 111/1, perhaps Pits 111/2–111/5, and a massive levelling layer or platform mound with numerous pottery finds belong to this pre-mega-structure occupation.

Mega-structure 3

Architecture of Mega-structure 3

In the archaeomagnetic plan of the Maidanetske settlement, Mega-structure 3 appeared as a northwest-southeast aligned anomaly with a floor size of approximately 190 m 2 (dimensions 19 × 10 m; Fig. 2A). Trench 111 opened over this anomaly measured 23 × 15 m and the daub package of Mega-structure 3 was encountered buried under a 0.5 m thick Chernozem layer.

Within the mega-structure, 1.39 tons of daub were documented (Tab. 5); it was not equally distributed, corresponding to the high and low magnetised areas visible

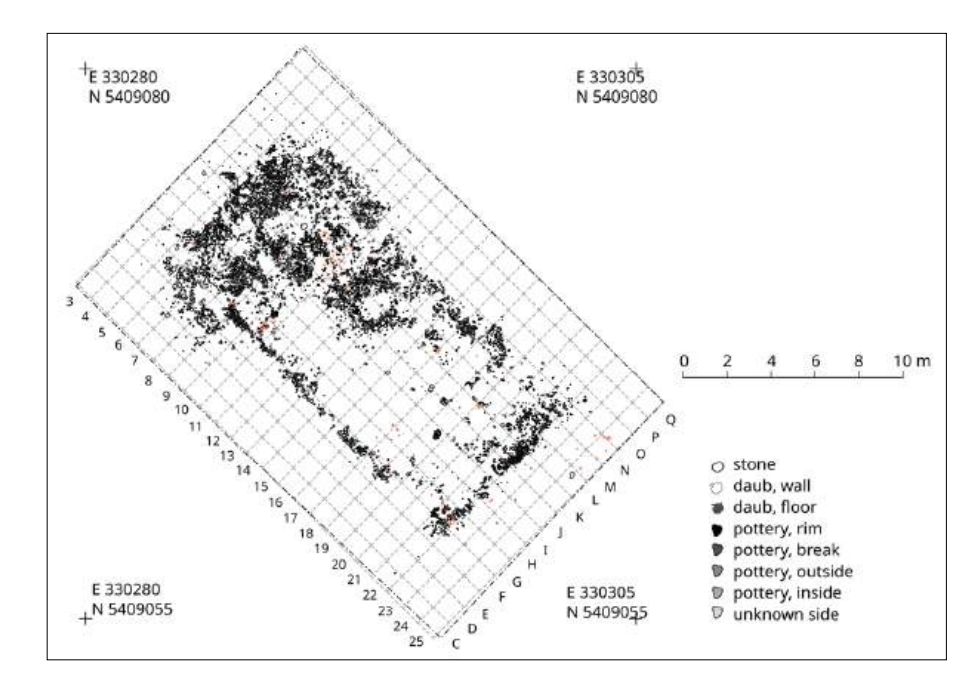


Figure 9. Maidanetske, Megastructure 3 in Trench 111, drawing of daub from collapsed walls, floor, and pottery.

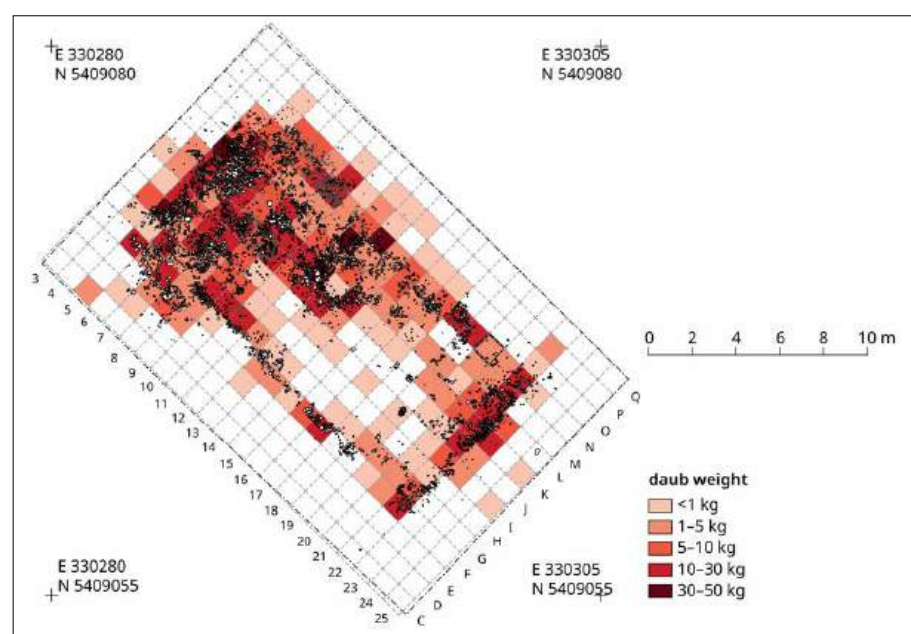
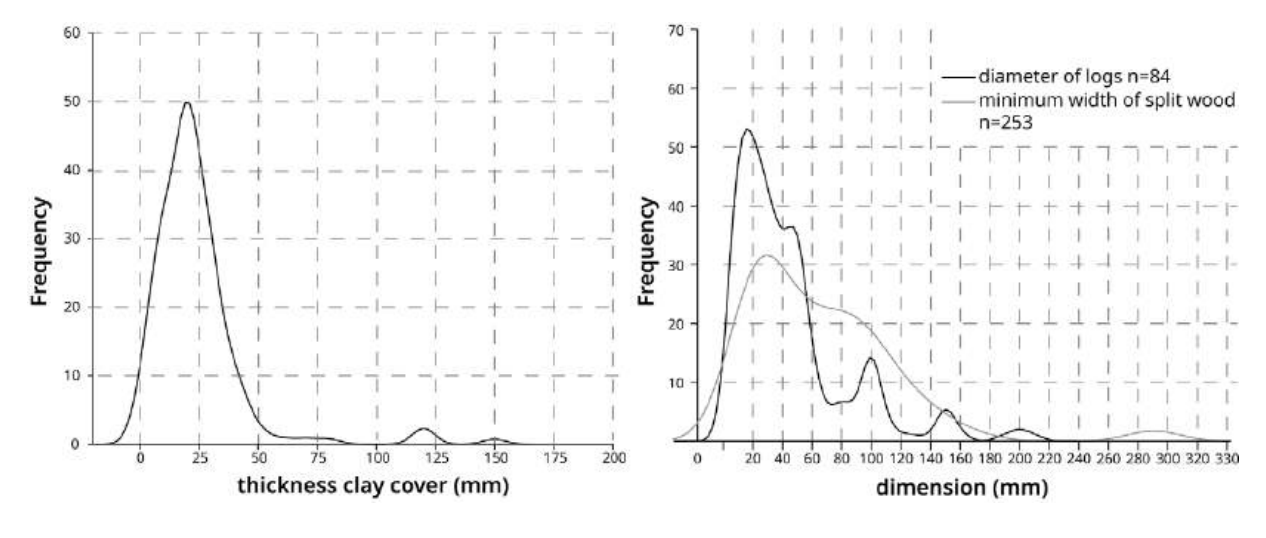


Figure 10. Maidanetske, weight of daub belonging to Megastructure 3 in Trench 111.

in the archaeomagnetic plan (Figs. 9 and 10; Pickartz *et al.* 2019). In some parts of the exterior walls and in the northwestern half of the building, concentrations in quantities of between 10 and 50 kg/m 2 were found. In contrast, a particularly low amount of daub in the range of up to 1 kg/m 2 was documented in the southern quarter of the structure and the surrounding open space. In consequence, an internal division into northwestern and southeastern parts is clearly apparent.

The mega-structure was outlined by a lightweight outer wall made of clay-covered split and logwood timbers. Due to various post-depositional processes, the preservation of this construction was variable in quality. Based on analysis of negative imprints and the measurements of the burnt daub cover, the wall is estimated to have been about 15–20 cm thick (Fig. 11a). As building timber, ash (*Fraxinus* 75%, n=44) and oak (*Quercus* 19%, n=11) were used with dimensions generally less than 10 cm (Fig. 11b; Dal Corso *et al.* 2019). From the wood imprints,



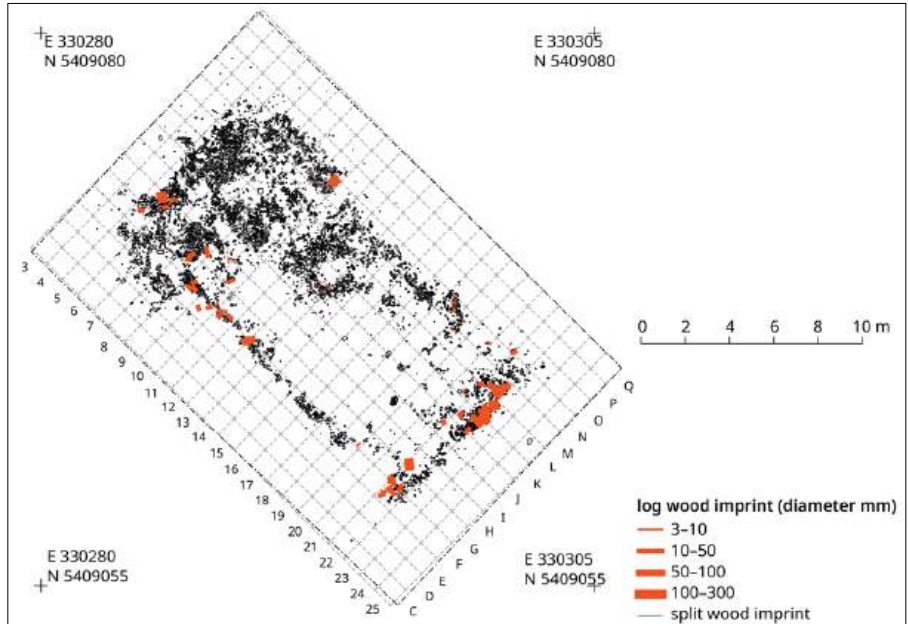


Figure 11 (above). Maidanetske, kernel density distributions of architectural details from Mega-structure 3: left – thickness of the clay covering on construction timbers; right – diameter of logs and minimum width of split wood timbers.

Figure 12. Maidanetske, mapping of type, dimension and direction of split wood imprints within the debris of Mega-structure 3.

both narrow sides and parts of the southwestern longitudinal part of the wall were constructed with log timbers, while the other parts of the wall were constructed mainly with split wood (Fig. 12).

At the southern ends of the longitudinal walls daub-free areas about 1.4 m wide are interpreted as possible entrances. The southeastern narrow side of the mega-structure was particular massive, indicated by the largest diameters of log timbers. A daub concentration 7 m south of the northwestern narrow end might indicate the remains of an interior wall dividing the mega-structure in two parts. The internal wall probably reached 4 m across the house, but 3.50 m remained daub-free, perhaps as a passageway between the two parts of the structure. A small entrance about 1 m wide may also have existed directly north of the interior wall on the northeastern longitudinal side.

The orientation of the negative imprints in the split wood suggests that the timbers were aligned horizontally in the walls of the southeastern part and vertically in the walls of the northwestern part of the mega-structure (Fig. 12). The lack of postholes could indicate a construction with horizontal beams as wall foundations. In the northwestern corner the daub remains with vertically oriented negative imprints

might be remains of a gable wall which collapsed into the internal space of the megastructure. The height of the original external wall can be reconstructed to about 3.5 m. Also, daub remains of the internal wall suggest an original height of 3–3.5 m.

Below small-sized and chaff-tempered wall debris, remains of a burnt rammed earth floor were found in the entire area of the mega-structure (Figs. 9, 13 and 14). This floor layer, mostly only poorly burnt and in parts only 1 cm thick, was preserved exclusively in those places which were also covered by wall debris; it was particularly badly preserved (due to low firing intensity) in the southeastern part of the structure. The floor under the debris of the exterior walls was in better condition and the floor layer was up to several centimetres thick (Figs. 15 and 16). At the outer edge of the wall debris, even in the locations with better preservation, the floor layer suddenly stopped. Here, the floor layer was slightly raised upwards where it would have originally met the outer walls had they been preserved in place. In consequence, it is suggested that all 190 m² of the mega-structure's interior were originally covered with a rammed earth floor. The outer edge of this rammed earth floor marked the position of the exterior walls that are not preserved.

In the northwestern part of the building different installations existed. Within the interior space only a few remains of furnishings were recovered. However, spatial concentrations of a specific yellowish kind of daub in the northwestern part of the building might indicate destroyed furnishing elements. In normal dwellings such as House 44 similar material was used for the construction of bins and podiums (Müller *et al.* 2017, 174).

An oval area 2.2×1.3 m, situated within the mega-structure, 3–5 metres away from the northwestern narrow end along the longitudinal axis, marks a fireplace which was raised above the rest of the floor by several extra layers of tamped and burnt earth (Figs. 17 and 18). Corresponding installations are a standard element of Trypillia houses (Pickartz *et al.* 2019). Since they are sometimes decorated, they are frequently interpreted as altars. In the installation of Mega-structure 3 at Maidanetske, at least three successive screed layers lie one above another and testify to a longer-lasting use of the building. In contrast, no signs of floor renewals were determined in the remaining parts of the mega-structure.

The southeastern part of the mega-structure has dimensions of 10×7 m, measuring from the base of the interior wall, which probably collapsed in a southeastern direction. No archaeological features could be detected. In this respect, the southeastern part of the mega-structure is empty, but artefact distributions describe different activity zones.

Find inventory of Mega-structure 3

Mega-structure 3 produced a large find inventory including pottery, non-pottery ceramic objects, ground stone and flint artefacts as well as various zoological and plant remains (Tab. 6). The most numerous finds were ceramic vessels, many of which were clearly broken *in situ* on the floor in primary find situations (Fig. 19). We do not see why the view defended by our British colleagues assumes *a priori* that inventories are not functional but 'constructed' (Gaydarska *et al.* 2020)². We rather assume as a preliminary that we can interpret the composition and arrangement of the inventory as a 'living assemblage' in a functional context. Of course, this does not completely exclude the possibility that parts of the inventory represent subsequently deposited so-called 'foreign waste'.

² Arguments for this claim are: 1. lack of any functionally coherent pottery groups; 2. overrepresentation of certain vessel parts; 3. too many vessels.



Figure 13. Mega-structure 3 after uncovering the floor plaster (Planum 3b).



Figure 14. Detail photo of the fragmentarily preserved floor plaster of Mega-structure 3.



Figure 15. Remains of floor preserved under the debris of the south-western longitudinal wall of Mega-structure 3, on the right side stopping abruptly at the position of the former wall.



Figure 16. Maidanetske, central fireplace in Quadrats I–J/8–10 after removal of overlying wall remains.

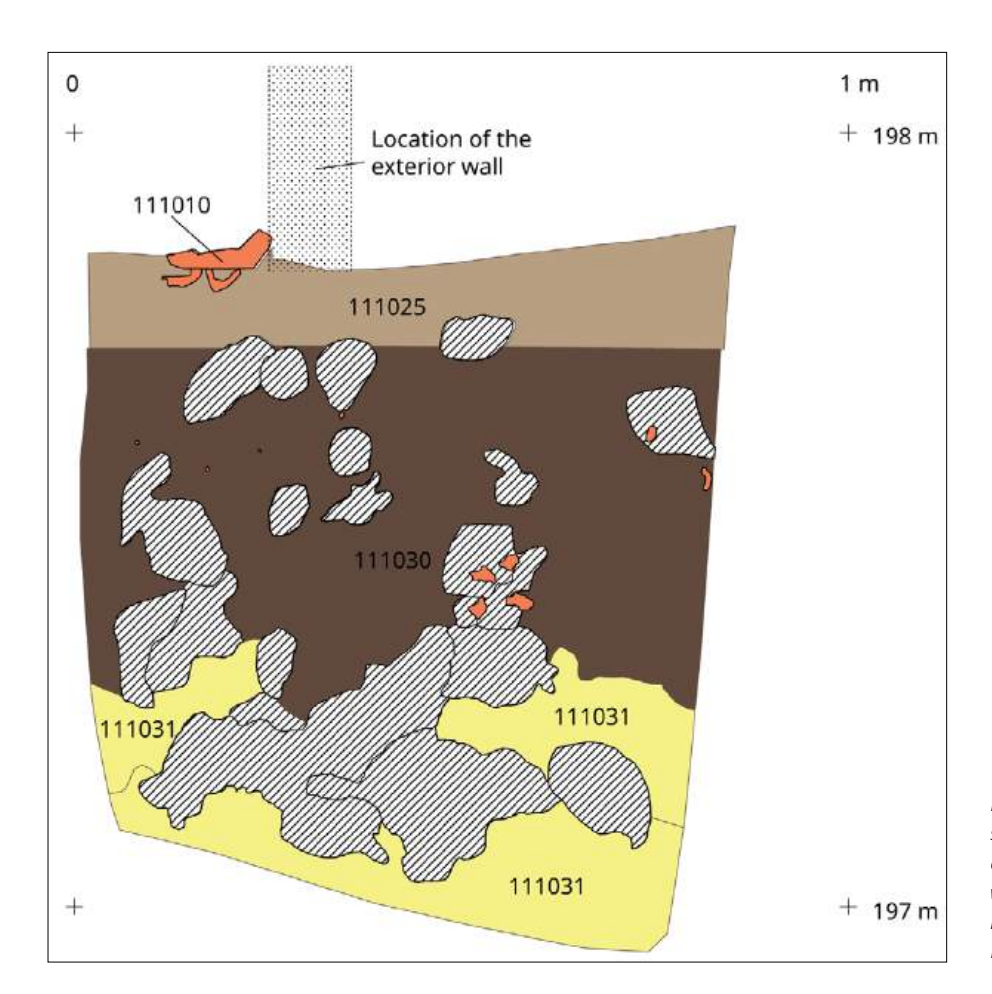


Figure 17. Profile 6 shows the stratigraphic situation at the outer edge of the floor plaster, which here connected to the non-preserved external wall of Mega-structure 3.

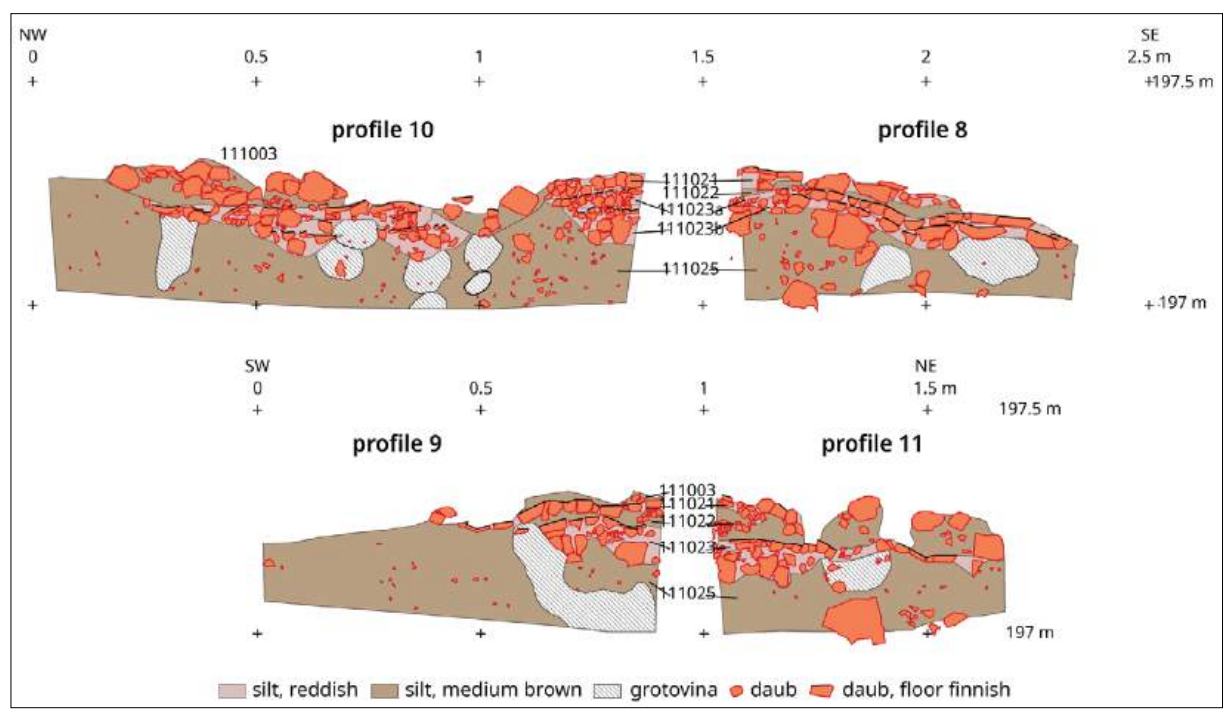


Figure 18. Maidanetske, profile sections through the fireplace of Mega-structure 3 (Profiles 8-11).

	Number (n)	Weight (kg)
Pottery	1821	39.0
Burnt daub	28259	1386.4
Bone	91	1.0
Flint	4	0.02
Ground stone	31	>70.0
Non-pottery ceramic objects	16	0.6

Table 6. Maidanetske, overview of types and quantities of finds in Mega-structure 3.







Figure 19. In situ situations of vessels on top of the floor plaster of Mega-structure 3.

Pottery

A total of 3071 pottery fragments weighing 85.4 kg were recovered from Trench 111, of which 1821 fragments weighing nearly 39 kg were from the daub package and other layers associated with the mega-structure. This quantity includes the material that was most likely transported by post-depositional processes, such as frost heave, into the Chernozem layer directly above the daub and which was thereby increasingly fragmented. The ceramic material of the mega-structure shows a relatively low average sherd weight overall of 21.4 g and thus a medium to high degree of fragmentation (Tab. 7). This relatively high level of mechanical damage is further confirmed given that surfaces with painting are not preserved on many of the fragments.

From a technological point of view, the proportion of tableware in the inventory ranges from 86 to 92% and of kitchenware from just under 7 to 12%, depending on whether the calculation is made according to the number of fragments or their weight (Tab. 8). Between the different 'layers', the proportions of wares vary considerably in some places of the mega-structure, as can be demonstrated for

Layer formation	Layer group	Layer	Number (n)	Weight (g)	Fragmentation (g)
Mai 111/4	Topsoil	Chernozem	38	738	19
	Mega-structure 3	Layer above wall debris	506	8374	17
Mai 111/3		Wall debris	1140	29872	26
Mdl 111/3		Hearth	166	627	4
		Floor	9	123	14
	Pit 36 (111/4)	Filling	15	567	38
	Pit 35 (111/3)	Filling	260	8878	34
Mai 111/2	Pit 34 (111/2)	Filling	286	12926	45
	Pit 33 (111/1)	Filling	84	3757	45
	111-levelling layer	-	519	18209	35
Unknown	Unknown	Unknown	48	1346	28
Total			3071	85417	28

Table 7. Maidanetske, pottery quantities and fragmentation (average sherd weights) in different parts of Trench 111.

	Calculation by number (n)								Calculati	on by we	eight (kg)			
Layer	Table	Kitchen	Non-classified	Total number	Table (%)	Kitchen (%)	Non-classified (%)	Table	Kitchen	Non-classified	Total weight	Table (%)	Kitchen (%)	Non-classified (%)
Floor	4		5	9	44.4	0.0	55.6	0.1		0.1	0.1	49.6	0.0	50.4
Hearth	33	132	1	166	19.9	79.5	0.6	0.5	0.1	0.0	0.6	82.1	15.5	2.4
Layer above wall debris	467	34	5	506	92.3	6.7	1.0	7.4	0.9	0.1	8.4	88.5	10.4	1.1
Wall debris	1066	57	17	1140	93.5	5.0	1.5	27.3	2.1	0.5	29.9	91.5	6.9	1.5
Total	1570	223	28	1821	86.2	12.2	1.5	35.3	3.0	0.6	39.0	90.6	7.8	1.6

example by a higher proportion of kitchenware near the central hearth and higher proportions of tableware in other parts of the mega-structure.

The inventory of the mega-structure contained a wide range of vessel categories, which are listed in Table 9. A selection of these are documented by drawings in Figures 20–24.

Kitchenware products are represented by profiled pots decorated with rows of punctures on the rim and shoulder (Fig. 23: 4–6) and a sphero-conical bowl with a strongly inwardly turned rim (Fig. 23: 7).

Open shapes made of tableware are represented by at least five conical bowls, partly decorated with variants of the comet-shaped design (Fig. 20: 2, 4–7). In addition, there was at least one sphero-conical bowl (Fig. 20: 8) and two bowls with four feet (Fig. 20: 1, 3), whose upper parts, however, are not preserved.

Other presumed serving vessels include a minimum of two cups (Fig. 20: 9–10), the painting of which has not been preserved, and a minimum of four goblets, one of which has a handle (Fig. 20: 11–14). The upper part of a bi-conical goblet shows a painting of the metopic scheme (Fig. 20: 11). Two cups decorated with vertical groups of lines are finds whose exact origin within Trench 111 is unclear, as they were recovered unstratified from the excavated earth material (Fig. 24: 6–7).

Table 8. Maidanetske, quantity of ceramic wares in different parts of Mega-structure 3.

Vessel classes and type groups	Number (n)	Weight (g)	Summed rim percentages	Summed belly percentages	Summed bottom per- centages	Minimum number of vessels
Bowl	22	910	20		330	4
Bowl, conical	93	5959	482.5		287	5
Bowl, sphero-conical	5	88	34			1
Goblet	1	3			25	1
Goblet, cup	2	52	17		70	1
Goblet, goblet	11	255	75.5	65		1
Amphora	66	1865	203	72	100	3
Bi-conical vessel	106	3455		74	100	1
Closed vessel	181	5884	555.5	431.5	377	6
Krater-shaped	2	116		18		1
Sphero-conical vessel	94	4770	36	56	67	1
Pear-shaped vessel	12	356	126			2
Lid	3	72	17			1
Pot	33	1322	218	155	93	3
Binocular vessel	1	80		10		1
Non-classified	71	2782	214.5	86	777	8

Table 9. Maidanetske, quantification of vessels from Mega-structure 3.

Three smaller pots made of tableware seem to be suitable as transport vessels for serving food as well, because the mouths of these vessels are only half-open (Fig. 21: 1–3). One pot is decorated in the rim zone with painting in the leaf-shaped scheme and has a triangular fillet on the neck.

Parts of at least two pear-shaped vessels belong to the group of closed storage vessels. One is painted on the shoulder with festoons, probably according to the metopic scheme (Fig. 20: 15–17). Also, part of this class of pear-shaped vessels are three lid fragments, including the 'cup-shaped' specimen in Figure 20: 16.

The group of closed vessels is also represented by at least two smaller and one slightly larger amphora (Fig. 21: 4, 5, 8, 10), at least one or perhaps two larger biconical storage vessels (Fig. 21: 9, Fig. 22: 1) and two sphero-conical vessels (Fig. 22: 2, Fig. 23: 1).

In addition, there are at least six vessels that were classified as 'closed' mainly due to the characteristics of the bottom fragments (no engobe inside).

The remarkable sphero-conical vessel in Figure 22: 2 can clearly be considered as an import because of the greyish colour of the clay and a painting scheme which is unusual for Tomashovka settlements. On the shoulder and belly of this vessel there is a band-like zone located in which vertical and festooned metope-like hatched blocks alternate with zones divided by tangents. The triangular zones which are generated by the tangent have fillings with organically curved bundles of parallel thinner and thicker lines and triangular or nodular connections. On the upper side, the main motif of the painting is bordered by a band of triangles.

Comparable painting schemes are found in the Sinyukha catchment area, for example, in settlements such as Kosenivka (Kruts *et al.* 2005, Fig. 58: 11, Fig. 60: 6) and Vilhovets (Ryzhov 1999; Videiko 2020, Fig. 9), which are attributed to the Kosenivka group.

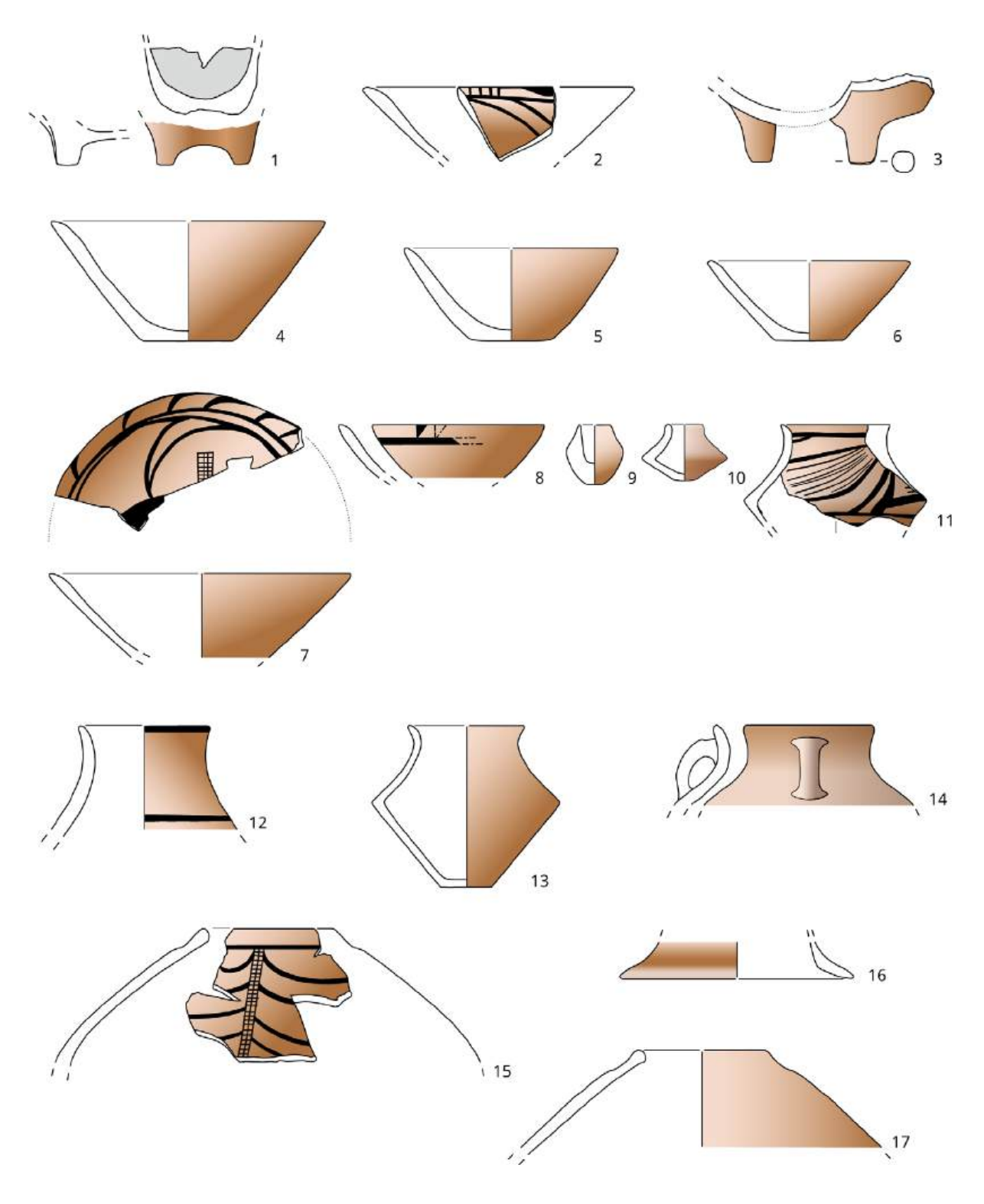


Figure 20. Maidanetske, ceramic inventory of Mega-structure 3: bowls (1–8); miniature vessel (9); cup (10); goblets (11–14); lid (16); pear-shaped vessels (15, 17). Scale 1:4.

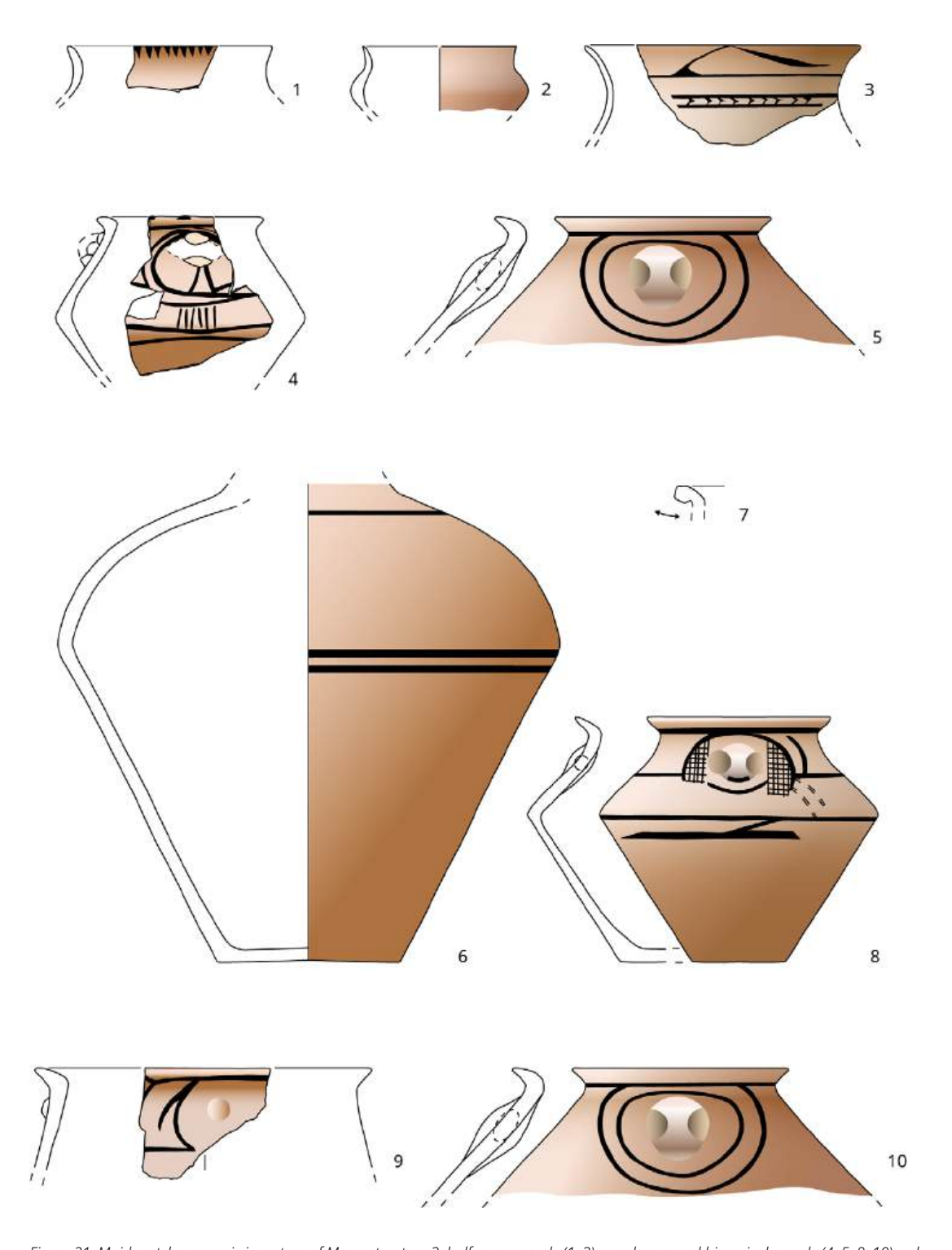
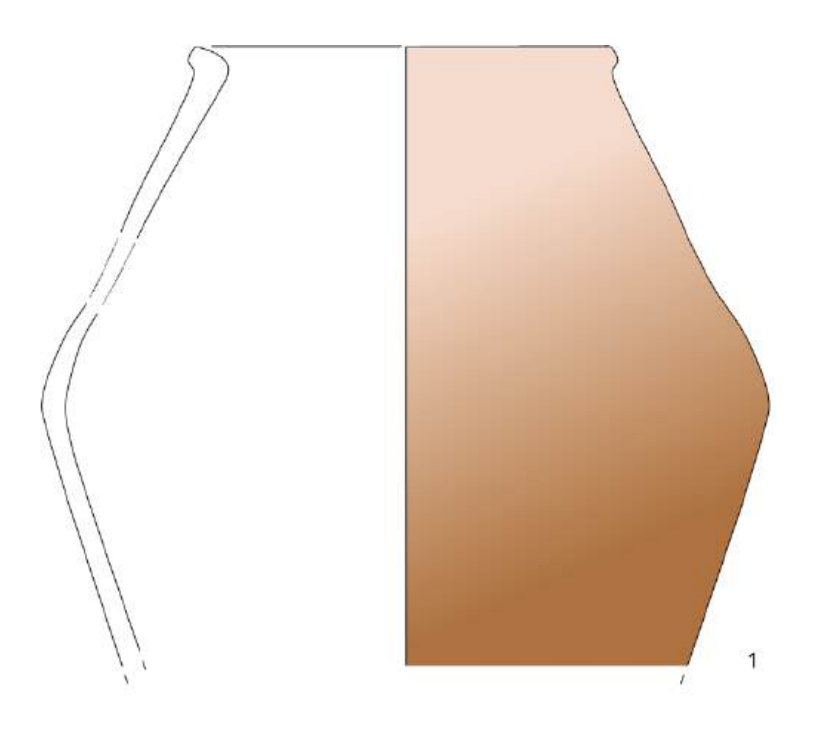


Figure 21. Maidanetske, ceramic inventory of Mega-structure 3: half-open vessels (1–3); amphorae and bi-conical vessels (4, 5, 8–10); spheroconical vessel (6). Scale 1:4.



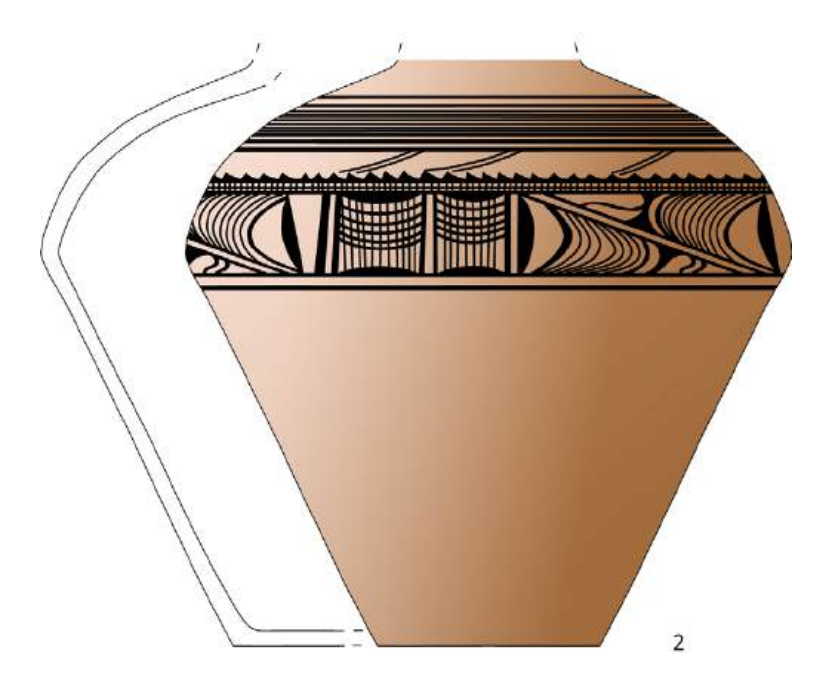


Figure 22. Maidanetske, ceramic inventory of Mega-structure 3: bi-conical vessel (1); sphero-conical vessel (2). Scale 1:4.

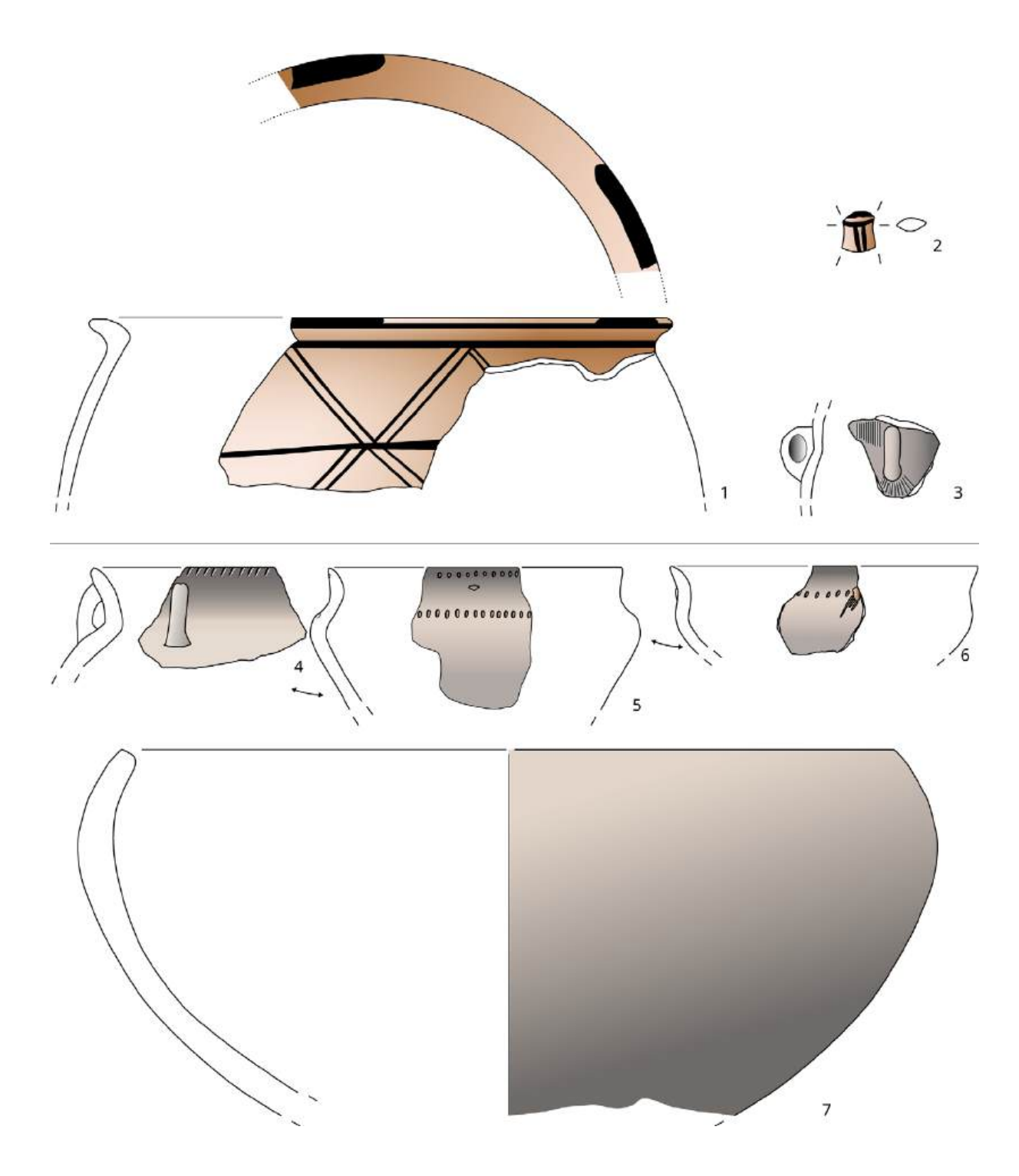
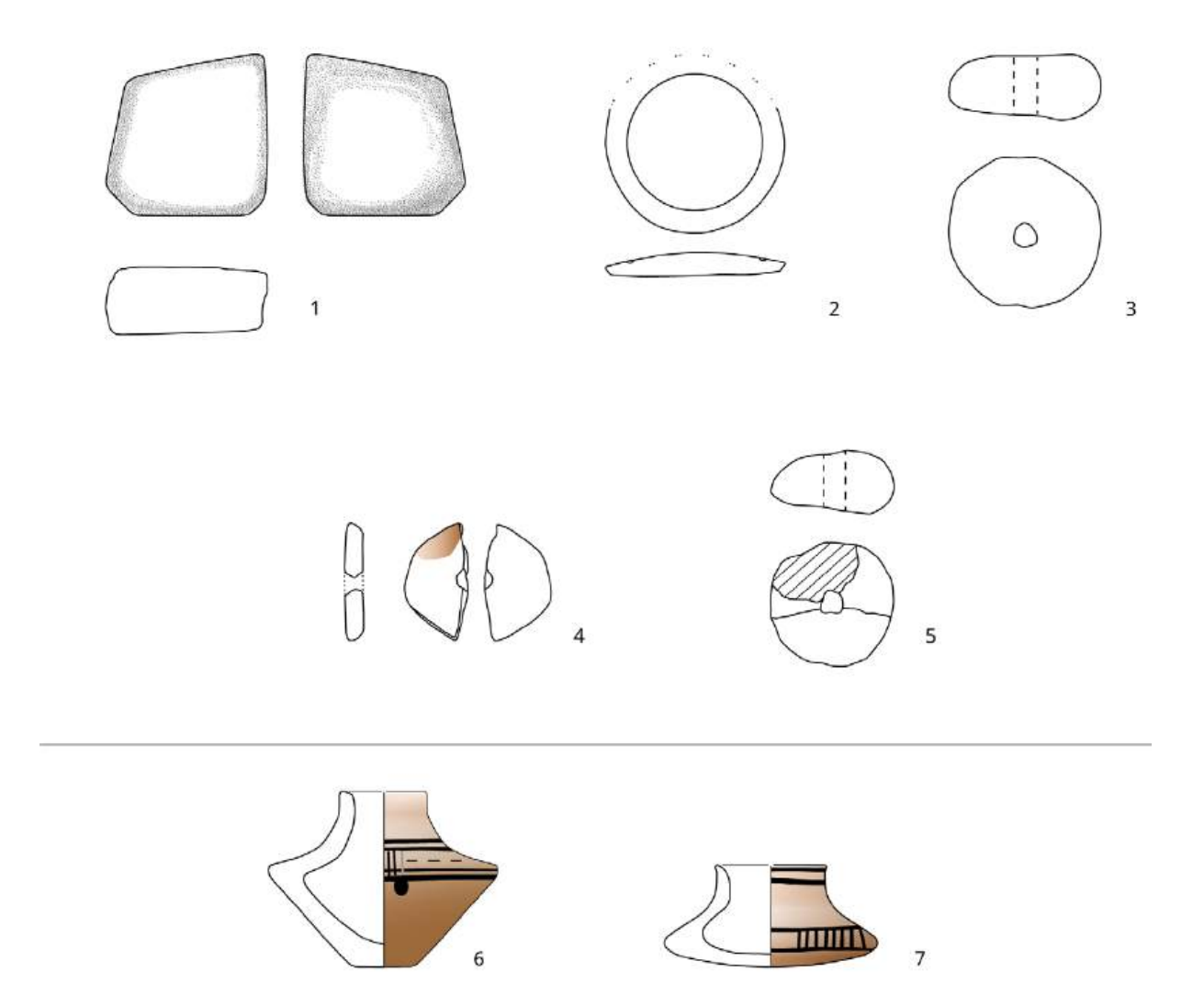


Figure 23. Maidanetske, ceramic inventory of Megastructure 3: sphero-conical vessel (1); decorated handles (2–3); kitchenware pots (4–6); kitchenware bowl (7). Scale 1:3.

Quarry and ground stone artefacts

A total of 19 quarry and ground stone artefacts of different kinds were found in Mega-structure 3 (Tab. 10). At least four and possibly six or more pieces represent millstones or millstone fragments, while the function of nine of the quarry stones is unclear. In addition, there is a boulder with weathered surface, a rubbing stone, a stone slab and a small whetstone. The quarry and grinding stones are mostly made of granite, while the stone slab and the whetstone are made of fine sandstone. For the quarry stones and millstone fragments it is unclear whether they were in primary position at the place of their use or in secondary position as building material.



Flint

Within the layers of Mega-structure 3, a small collection of flint artefacts made of a light brown (local?) raw material, partly whitish-discoloured by fire, was found (Tab. 11; Fig. 25). There were one unmodified flake and four pieces of debris, all with portions of cortex. Tools marked by further modifications were not found.

Non-pottery ceramic objects

A total of 14 non-pottery ceramic objects were found in features attributed to Megastructure 3 (Tab. 12). The largest group is represented by nine mostly fragmentary preserved weaving weights of a round, flattened type with a central perforation (Fig. 24: 3, 5). In addition, a ceramic disc reworked from a vessel bottom (Fig. 24: 2) and an angular-edged pierced sherd with red engobe on one side (closed vessel) were found (Fig. 24: 4). The find inventory furthermore contained three fragments of anthropomorphic figurines. In Quadrat K7 there was a torso of a small female figurine (preserved height 38 mm) with breasts, arm stumps, pierced arms and hips, and clothing indicated by incised lines (Fig. 26: 1). A leg belonging to a considerably larger figurine was found outside the mega-structure in Quadrat M3, broken off at the knee, with carefully sculpted calf and foot (preserved height 55 mm; Fig. 26: 2). An arm fragment was also recovered outside the mega-structure in Quadrat D4.

Figure 24. Maidanetske, ceramic and ground stone inventory of Mega-structure 3: whetstone (1); vessel bottom modified into a ceramic disc (2); loom weights (3, 5); spindle whorl (4); cups (6–7). Scale 1:3.

Find-ID	Feature-ID	Level	Quadrat	Number (n)	Weight (kg)	Category	Material
1110923	111018	3	L22	1	0.24	Boulder (surface weathered)	Granite, fine-grained, red
1111020	111009	4	N9	1	>5	Mill stone fragment (grinder, handstone)	Granite, coarse-grained
1111022	111003	4	16	1	>5	Mill stone fragment (quern, lower)	Granite, coarse-grained
1111028	111003	4	J3	1	>5	Mill stone fragment (quern, lower)	Granite, coarse-grained
1110546	111002	2	J4	2	0.5	Mill stone fragment (unknown position)	Granite, coarse-grained, red
1110008	111002	2	K9	1	0.04	Quartz cube 40 × 38 × 18 mm	Quartz
1110351	111002	2	M16	1	0.10	Quarrystone	Granite, coarse-grained, red
1110362	111002	2	J3-4	1	0.03	Quarrystone	Limestone
1110362	111002	2	J3-4	1	0.20	Quarrystone (perhaps millstone fragment)	Granite, coarse-grained, yellow
1110441	111002	2	E8	1	0.01	Quartz cube 27 × 18.5 x12 mm	Quartz
1110456	111002	2	E8	1	0.08	Quarrystone	Granite, fine-grained, yellowish-gey
1110679	111009	3	O10	1	0.15	Quarrystone	Granite, coarse-grained, red
1110684	111009	3	O10	1	0.10	Quarrystone, perhaps millstone fragment	Granite, coarse-grained, yellow
1110778	111018	3	F22	1	0.09	Quarrystone	Granite, fine-grained, red
1110778	111018	3	F22	1	0.36	Quarrystone	Granite, fine-grained, red
1111024	111003	4	G4	1	>5	Quarrystone	Granite, coarse-grained
1111026	111003	4	J5	1	>5	Rubbing stone	Granite, coarse-grained
1111016	111003	4	K12	1	>5	Stone slab	Sandstone, fine-grained, red
1110274	111002	2	J7	1	0.22	Whetstone with one flat side, $68 \times 70 \times 30$ mm	Sandstone, fine-grained, grey

Table 10. Maidanetske, list of quarrystone and ground stone artefacts found in features attributed to Mega-structure 3.

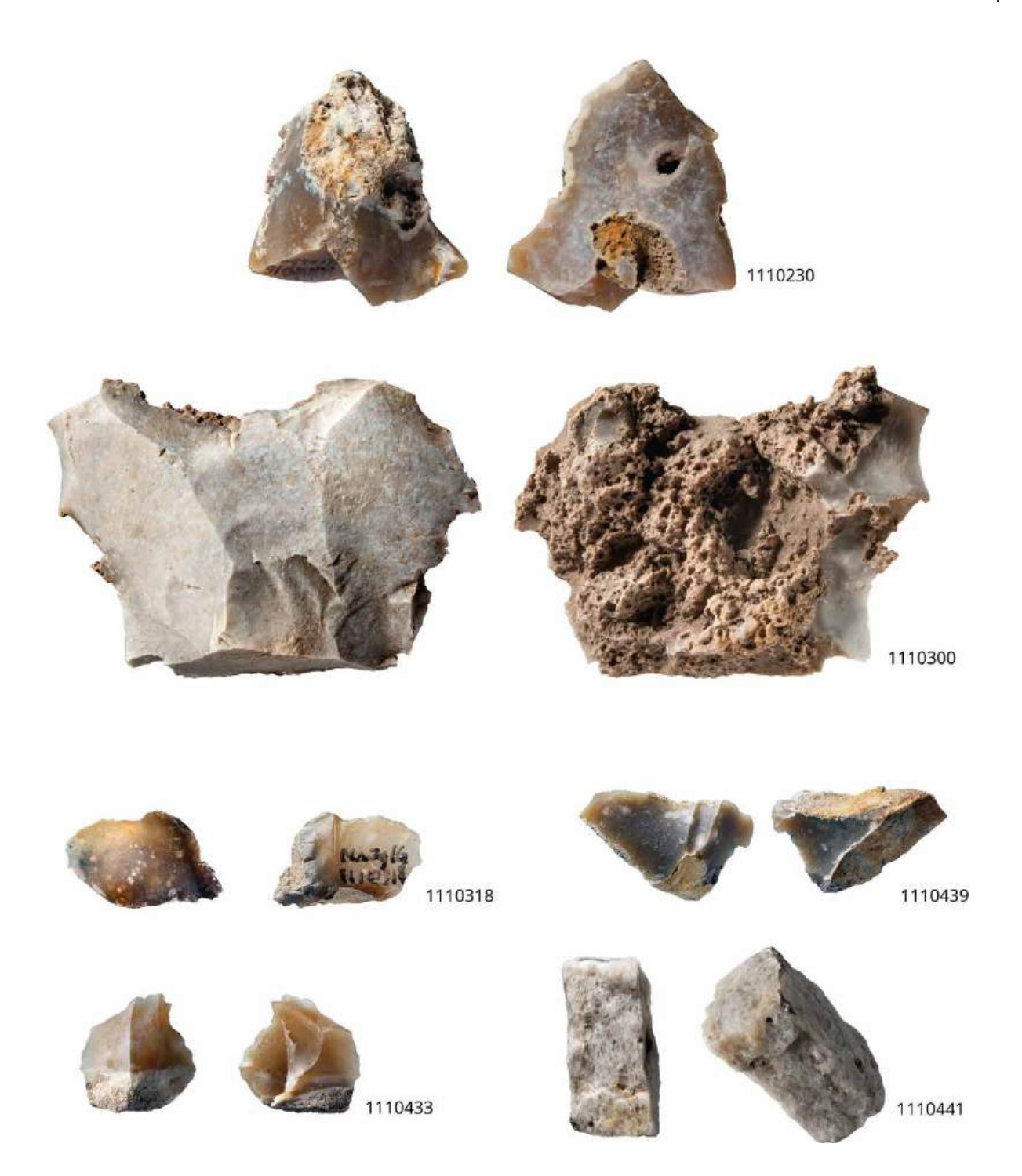
Find-ID	Feature-ID	Level	Quadrat	Description	Number (n)	Weight (g)	Raw mate- rial
1110230	111002	2	C7	Debris with cortex	1	18	Light brown (regional?)
1110300	111002	2	H15	Debris with cortex – missing in database (only photo available)	1	?	Light brown (regional?) whitish discolouration due to fire exposure
1110318	111002	2	J20	Flake with bulbus and cortex remains	1	1	Light brown (regional?)
1110433	111002	2	N23	Debris with cortex	1	1	Light brown (regional?)
1110439	111002	2	I8	Debris with cortex	1	1.5	Light brown (regional?)

Table 11. Maidanetske, list of flint artefacts found in features attributed to Mega-structure 3.

Artefact distribution patterns of Mega-structure 3

Artefact distribution patterns provide information about the depositional processes and activities which took place within the mega-structure. The overall low degree of fragmentation seems to indicate that pottery was fragmented during a primary context of use (Fig. 27).

Pottery is distributed all over the mega-structure (Fig. 28). For example, bowls, which are generally associated with consumption activities, are evenly distributed across the whole interior space of the mega-structure (Fig. 29). Nevertheless, concentrations are visible in the northwestern and the southeastern areas. This



might indicate different activity areas whose character might be detectable by functional differences of the morphological vessel types involved:

Figure 25. Maidanetske, flint artefacts from Mega-structure 3. Scale 1:1.

· Half-closed and closed vessels, which probably had storage functions, are concentrated in both zones described above (Fig. 30). In the northwestern part of the mega-structure they are situated in the northeastern area, east of the fireplace. In the southeastern part they are concentrated in the southern corner beside the postulated entrance.

Find-ID	Feature-ID	Level	Quadrat	Category	Number (n)	Weight (g)	Туре	Degree of preservation (%)	Diameter (mm)	Diameter perforation (mm)	Height (mm)	Thickness (mm)
1110331	111002	2	F6	Spindle whorl	1	11		50	50			8.5
1110474	111002	2	E5	Loom weight (fragment)	1	29	3	25	60		33	
1110576	111003	3	G21	Loom weight	1	63	3	100	55	11	27.5	
1110579	111003	3	I22	Loom weight (fragment)	1	24	3	20	75			
1110579	111003	3	I22	Loom weight (fragment)	1	26	3	20	45		29	
1110611	111003	3	J21	Ceramic disk (fragment)	1	40		65	76			9
1110811	111018	3	I23	Loom weight (fragment)	1	39	3	37	60		25	
1110972	111018	3	H22	Loom weight (fragment)	4	40	3	15	75	6	22.5	
1111571	111018	4a	H23	Loom weight (fragment)	1	83	3	50	75	11	26	
1111572	111018	4a	H23	Loom weight	1	120	3	100	64	9	25	
1111573	111018	4a	H23	Loom weight (fragment)	1	39	3	25	70		28	
1110024	111002	2	K7	Figurine, fragment, torso	1							
1110076	111002	2	M3	Figurine, fragment, leg	1							
1110248	111002	2	D4	Figurine, fragment, arm	2							

Table 12. Maidanetske, list of non-pottery ceramic objects from features attributed to Mega-structure 3.

Kitchenwares, which are usually associated with food processing activities, occur
frequently in the southeastern part but have an additional distribution focus in
the northwestern part of the building, mainly southwest of the fireplace (Fig. 31).

In summary, the patterns of pottery distribution indicate food consumption in all parts of the mega-structure (bowls), food processing southwest of the fireplace and along the southern walls of the southeastern part (kitchenware), and food storage northeast of the fireplace and in the southern corner of the southeastern part. The lower fragmentation rate in these zones supports our view that the activities mentioned took place primarily in these parts of the mega-structure (Fig. 27).

Remains of querns are again mainly concentrated in two zones of the megastructure (Fig. 32). Several fragments were found at the northwestern end of the building partly inside and partly outside the external walls. Another concentration was observed in the central area of the southeastern part of the mega-structure, where the only complete quern was found.

In consequence, the different artefact distribution patterns seem to reflect this dual distribution pattern of the ceramics. We would particularly like to stress the contrast between the only partly preserved querns in the northwestern part and at



least one complete and several fragmented querns in the central southeastern part. This might indicate that cereal processing only took place in the southeastern part of the mega-structure, where slightly more cereal remains were also found (Fig. 33). We interpret the fragmented querns as secondarily appropriated construction material, as might also hold true for a larger number of quarry stones, a boulder, and two unworked stone slabs (Fig. 32). These are distributed in several accumulations along the external walls and along the central axis of the mega-structure.

The spatial distribution of bones clearly reveals another focused activity area in the northwestern half of the mega-structure (Fig. 34). The detailed bone distribution displays a semi-circular density at some distance from the fireplace along the walls. This could indicate that the consumption of meat was restricted to the northwestern part of the mega-structure.

Other ground-stone artefacts include a polishing stone and a whetstone; both of which were found in the northwestern end of the building. From these artefacts, further activities are identified as taking place in the northwestern part, *i.e.* the polishing and the sharpening of tools (Fig. 32). The distribution of the few flint artefacts (three pieces of debris and one flake) reflects again perhaps the two larger activity zones in the northwest and southeast of the structure (Fig. 35). This also holds true for remnants of textile production (Fig. 36). In one concentration six fragments and one complete loom weight were found in the southern corner of the building. A second concentration consisting of a loom weight fragment and a spindle whorl was found in the western corner. The one fragment (foot and calf) of a large anthropomorphic figurine was deposited outside the building along its narrow

Figure 26. Maidanetske, anthropomorphic figurines from Mega-structure 3: (1) Find-ID 1110024; (2) Find-ID 111076. Scale 1:1.

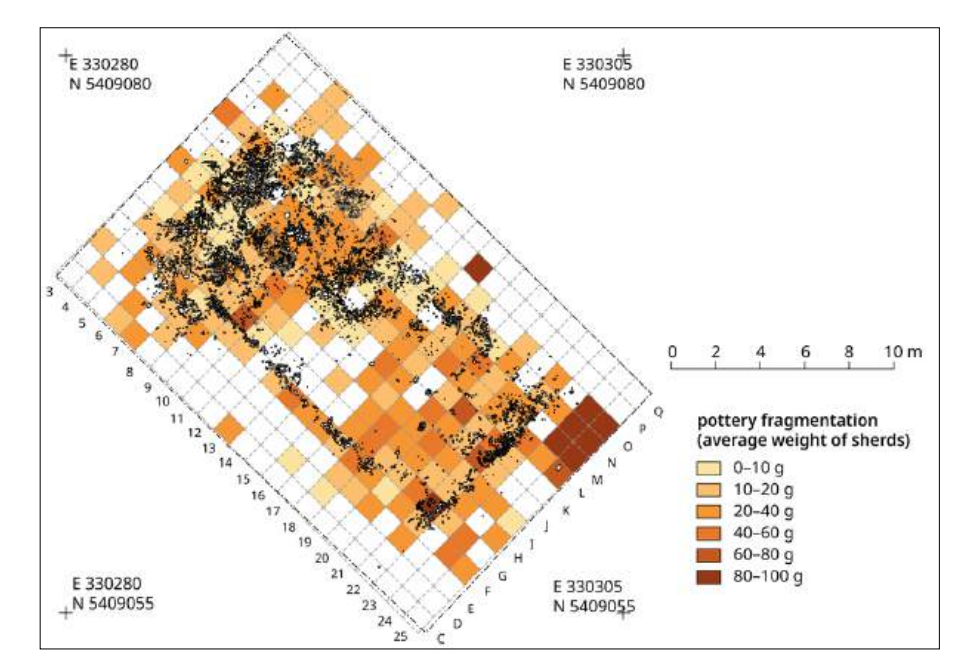


Figure 27. Maidanetske, distribution of ceramic fragmentation (average weight of sherds) in Mega-structure 3.

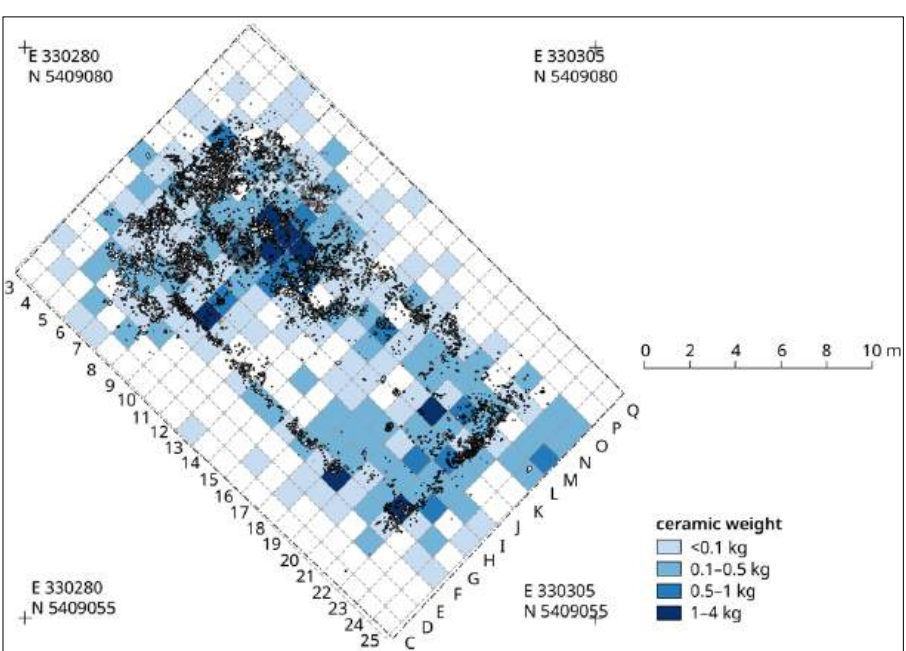


Figure 28. Maidanetske, distribution of ceramics in Mega-structure 3.

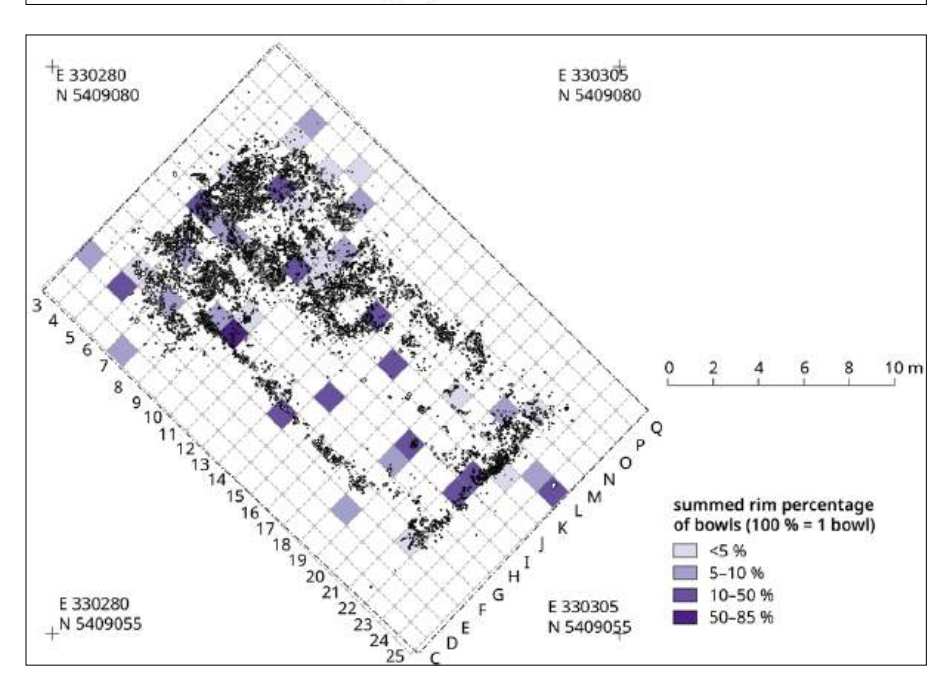


Figure 29. Maidanetske, distribution of ceramic bowls in Mega-structure 3 according to summed rim percentages.

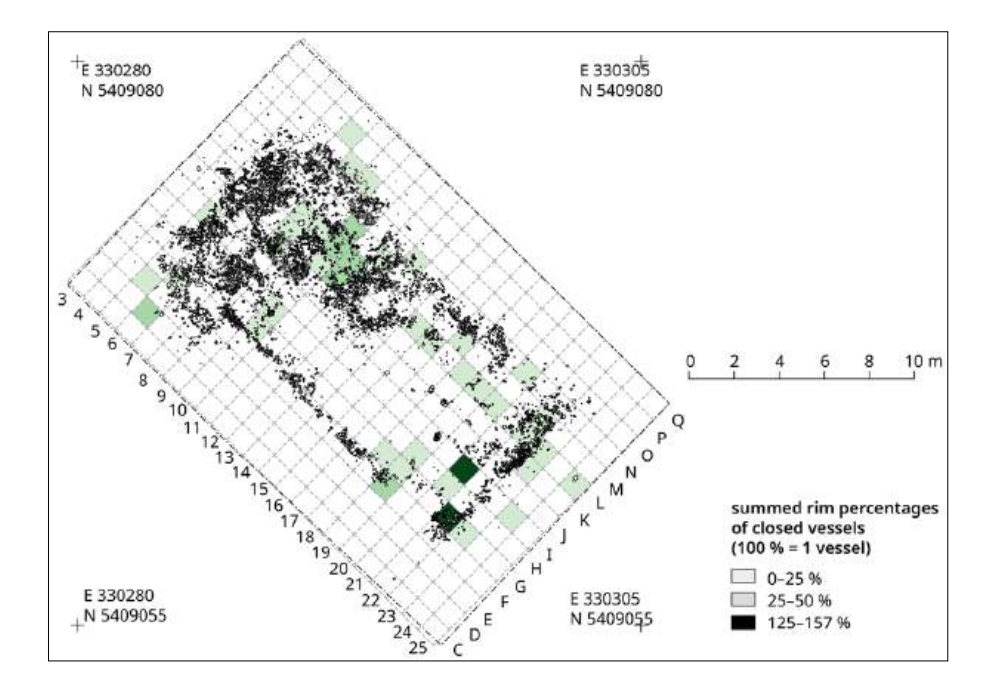


Figure 30. Maidanetske, distribution of closed/halfclosed ceramic shapes in Mega-structure 3.

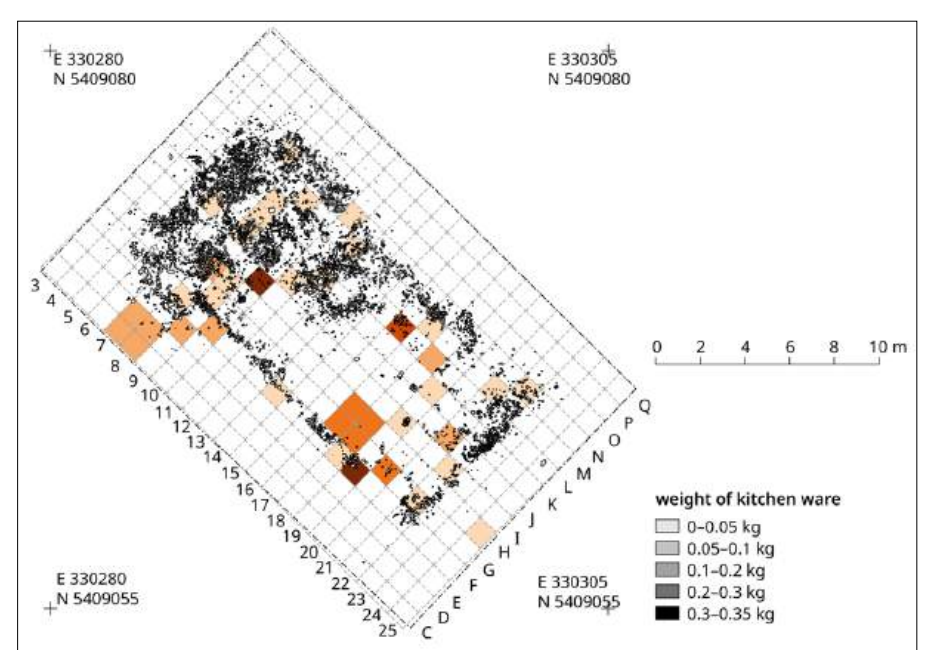


Figure 31. Maidanetske, distribution of kitchenware in Mega-structure 3.

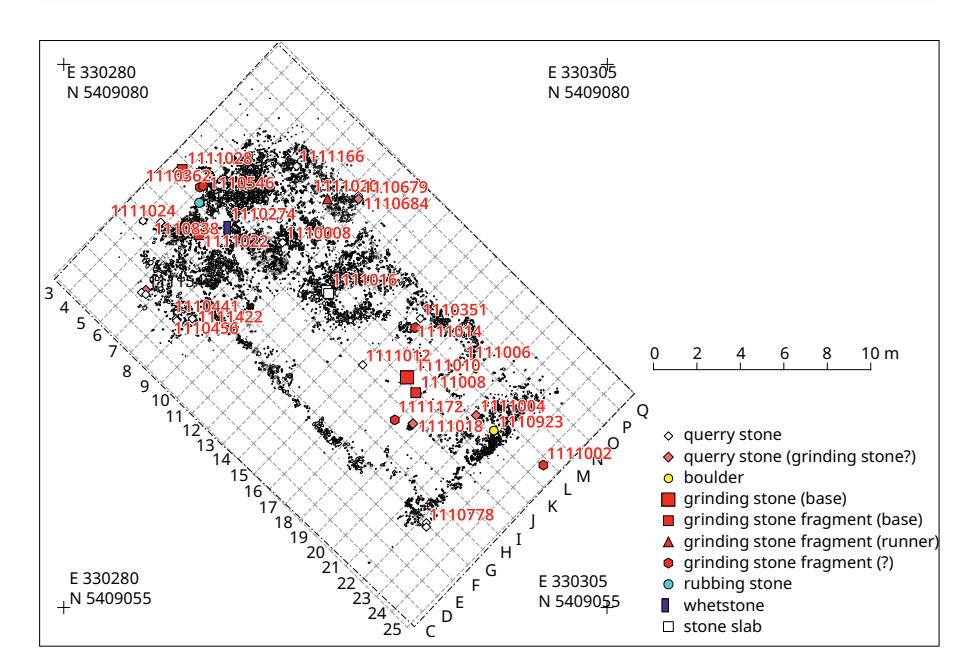


Figure 32. Maidanetske, distribution of ground stone artefacts in Mega-structure 3.

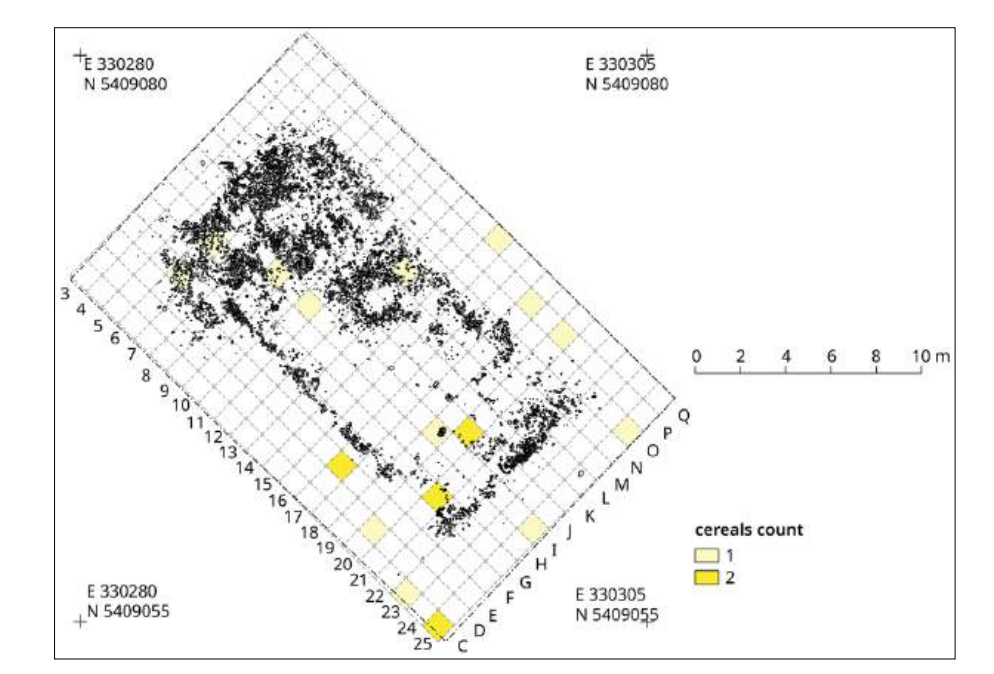


Figure 33. Maidanetske, distribution of charred cereal grains in Mega-structure 3.

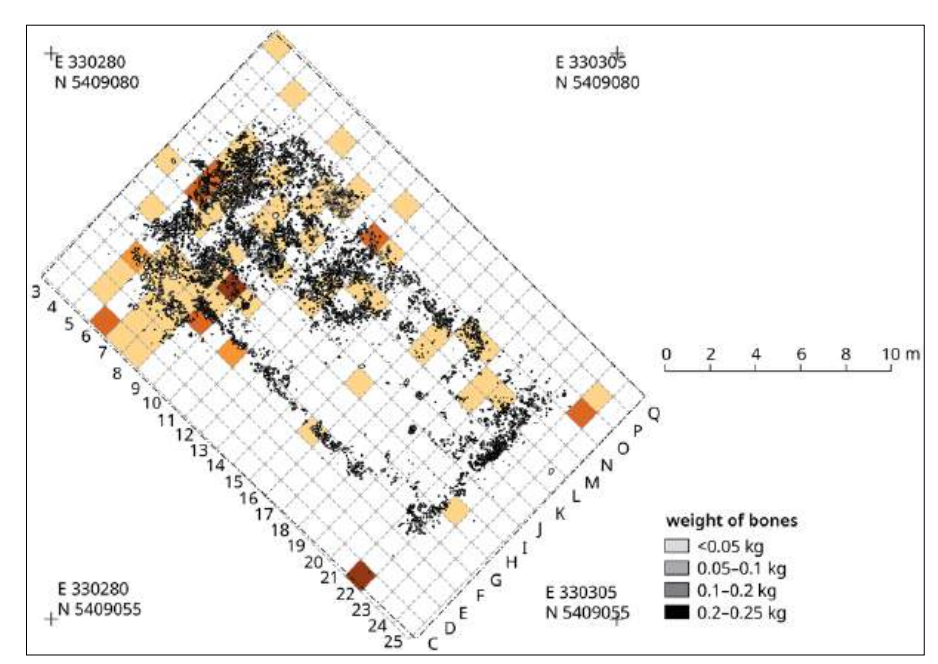


Figure 34. Maidanetske, distribution of animal bones in Mega-structure 3.

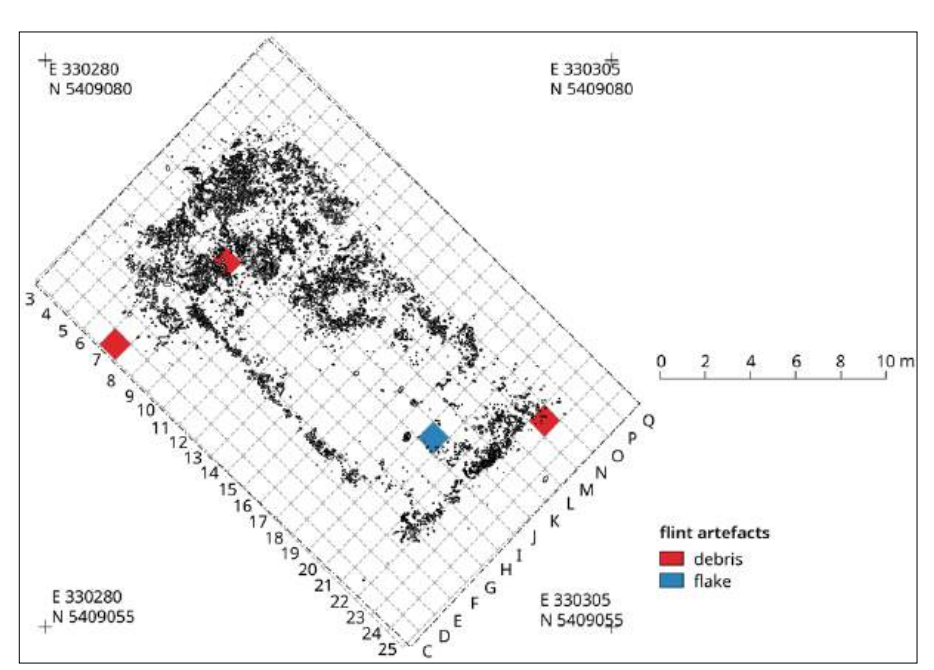


Figure 35. Maidanetske, distribution of flint artefacts in Mega-structure 3.

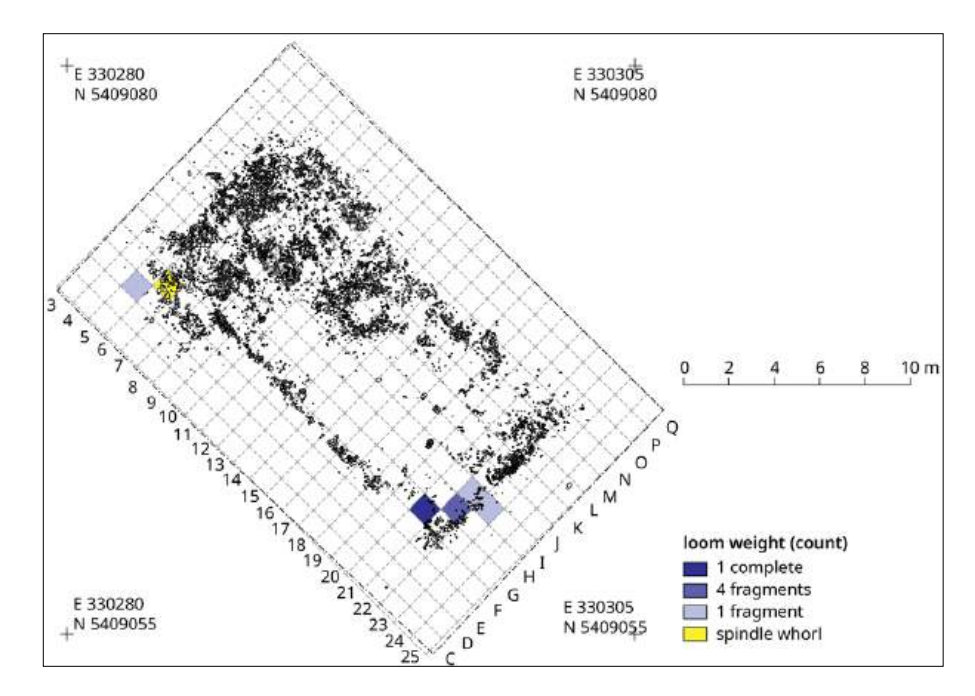


Figure 36. Maidanetske, distribution of remains from textile production in Mega-structure 3.

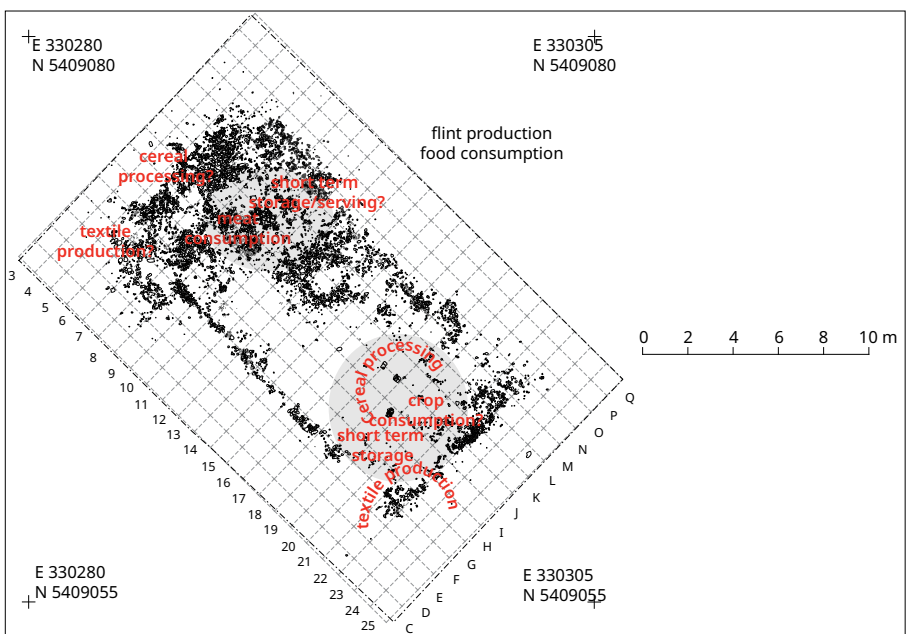


Figure 37. Maidanetske, reconstructed ground plan of Mega-structure 3 with activity zones.

northwestern end and may indicate a certain kind of non-utilitarian practice linked to the northwestern part of the mega-structure.

In consequence, multiple domestic activities could be detected and localised. In the northwestern part of the mega-structure, in addition to pyrotechnical activities at the fireplace, short-term storage, food preparation, meat consumption, textile production, and tool sharpening and polishing were identified. In the southeastern part of the mega-structure cereal processing, short-term storage, food preparation and textile production took place. Food consumption is evident in both areas.

Reconstruction of Mega-structure 3

Comparing the architectural remains and the artefact distribution patterns, the 'dichotomy' between the northwestern and the southeastern part of the megastructure is evident (Fig. 37).

- The ca. 60 m² of the northeastern part were constructed as a more or less closed space with walls up to 3.50 m in height with possible entrances from the outside and a passageway to the southeastern part of the structure. The fireplace is in a central position within this roofed section. The main activities are linked to consumption of cattle and pork meat, tool-sharpening, and storage.
- The ca. 70 m² of the southeastern part were constructed as an enclosed but unroofed space with lower walls up to 1.5 m in height in which cereal processing, but also food preparation, food consumption, short-term storage and textile production took place.

In principle, our interpretation focuses on the difference between a roofed building in which meat consumption and pyrotechnic activities took place, and an appended unroofed enclosure in which activities including cereal processing were performed. The spatial distribution of vessels (except bowls) with their concentration along the exterior walls probably indicates their original alignment. The difference between the roofed and the unroofed part of the mega-structure is reflected in the presence of charred *Stipa* awns in the southeastern part (Fig. 39). Feather-grass (*Stipa*) is a plant of the steppe and might have entered the archaeological record due to its deliberate collection *e.g.* for matting (Anderson and M'hamdi 2014) or attached to the fur of animals that visited spring-summer (Dannath *et al.* 2019; Körber-Grohne 1987; Rivera Núñez *et al.* 2012). The presence of the tiny, charred, *Stipa* awns could be due to a taphonomical bias such as percolation from upper layers, but a direct radiocarbon date from another context in Maidanetske revealed them to be contemporaneous to the site occupation (3969–3794 BCE; Dal Corso *et al.* 2019).

In consequence, the differences in daub quantities between the northwestern and the southeastern part of the mega-structure definitely have architectural reasons and are not due to different degrees of burning. This interpretation is also supported by significant differences in activities between the two parts of the mega-structure.

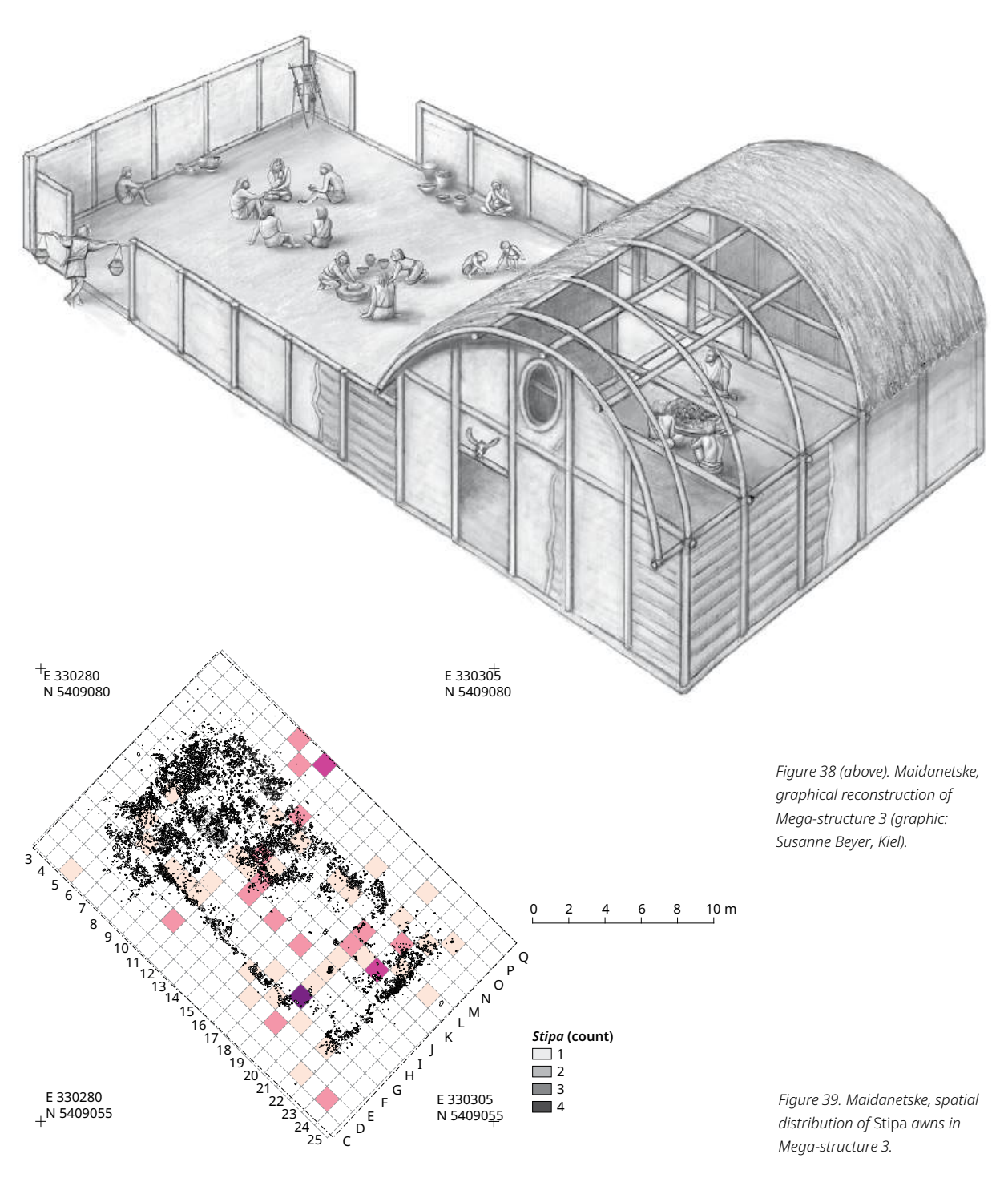
Pre-mega-structure occupation

In this section we describe the archaeological layers, structures and associated finds discovered below the floor of the mega-structure. Since the complete excavation of a 0.4–0.8 m thick horizon would have far exceeded the scheduled time for the fieldwork, we conducted a sampling of smaller areas and documented two profiles. Therefore, there may exist further so far undiscovered features within and under the levelling layer and buried soil.

Levelling layer and buried soil

The rammed earth floor of the mega-structure rested on a humus-rich levelling layer or artificial mound into which numerous medium-sized pieces of daub and large pottery items from fragments up to complete vessels were embedded (Features 111024 and 111025). We could trace these layers in different profiles in most parts of the mega-structure but could not clearly distinguish them from the more or less sterile buried humus (Feature 111030) underneath. In some places at least, the layer superimposed clearly the backfilling of pits. In other cases, the stratigraphic relationship between the levelling layer and pits could not be clarified unambiguously due to the strong bioturbation. Taken together, the two layers had a thickness between 0.4–0.8 m.

It is currently difficult to assess the fact that most of the burnt daub under the floor of the mega-structure is classified as compact material without chaff admixture and one plain surface (Tab. 13). In other contexts of burnt houses, in contrast, organically tempered daub with cereal chaff and different kinds of architectural



features usually represent the most common material category. It seems most likely that the above-mentioned untempered burnt daub fragments are the remains of the floor of the mega-structure, which we incorrectly assigned to the underlying layer.

In the layer below the rammed earth floor of the mega-structure, chaff-tempered daub represents only 15–20% of the material. The most common architectural features on these pieces are fragments with plain surfaces and imprints of split wood planks, while imprints of logs, and other variants, are very rare. Also, the crumbly yellow material which was used in other contexts for the construction of fixed installed containers and interior components showed mainly imprints of split wood planks.

		Cal	culation b	y number	(n)			Cal	culation b	y weight (kg)	
Architectural features	Compact (without chaff)	Organic tempered (chaff)	Crumbly yellow	Material not specified	Total number	Percentage	Compact (without chaff)	Crumbly yellow	Material not specified	Organic tempered (chaff)	Total weight	Percentage
1 Amorphous	1923	453	16		2392	55.0	37.1	0.4		11.2	48.7	44.8
2 Plain surface	1608	48			1656	38.1	43.9			3.0	47.0	43.2
3 Two plain surfaces	1	2			3	0.1	0.0			0.1	0.1	0.1
4 Split wood	10	38	14		62	1.4	1.4	1.4		3.3	6.1	5.6
5 Log wood		8			8	0.2				0.5	0.5	0.4
6 Combination: Split wood + split wood		1			1	0.0				0.2	0.2	0.2
7 Combination: Split wood + plain surface		4			4	0.1				0.8	0.8	0.7
10 Combination: Split wood + log wood		1			1	0.0				0.1	0.1	0.1
Vitrified clay		4		15	19	0.4			0.4	0.1	0.5	0.4
Non-classified	23	104	2	75	204	4.7	0.6	0.1	1.4	2.8	4.8	4.4
Percentage	82	15.2	0.7	2.1			76.4	1.7	1.6	20.3		

Table 13. Maidanetske, frequency of material categories and architectural features of burnt daub in the levelling layer beneath Mega-structure 3.

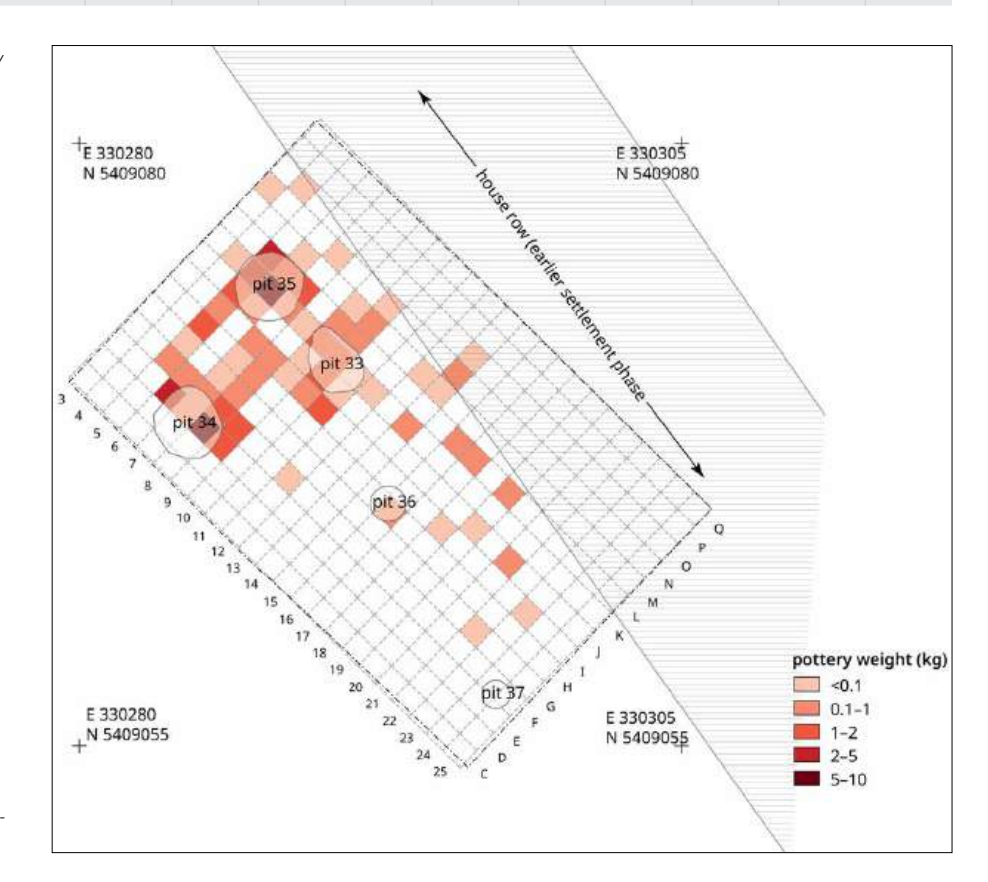


Figure 40. Maidanetske, features of the first building phase in Trench 111 below Megastructure 3, showing the location of pits and a row of dwellings. Additionally, the distribution of pottery in the layers below Megastructure 3 is shown.

	Levellir	ng layer	Pit	: 33	Pit	: 34	Pit	35	Pit	36
	Number (n)	Weight (kg)								
Pottery	519	18.21	84	3.78	286	12.93	260	8.88	15	0.57
Burnt daub	4350	108.68	1616	133.84	118	7.17	116	5.70	43	8.17
Bone (zoology)	80	2.32	3	0.12	237	9.07	31	0.34		
Flint							1	0.06		
Ground stone	10	?			8	1.75				
Non-pottery ceramic objects	3	0.05								

Fabric	Number (n)	Weight (kg)	Number (%)	Weight (%)	Fragmentation (g)
Table	405	12.4	78.0	68.2	31
Kitchen	99	5.1	19.1	28.3	52
Non-classified	15	0.6	2.9	3.5	102
Total	519	18.2			35

Table 14 (above). Maidanetske, overview of type and frequency of finds of the first settlement phase in Trench 111.

Find distribution analysis consistently shows a zone under the northwestern part of the mega-structure where a large amount of waste was disposed of within and in the surrounding area of several pits (Fig. 40). To the southeast is an adjoining zone of much lower waste disposal intensity.

frequency (number, weight) and fragmentation (average sherd weight) of ceramic fabrics in the levelling layer below the floor of the mega-structure in Trench 111.

Table 15. Maidanetske,

Table 14 provides an overview of the spectrum and frequency of finds from the layers under the floor of the mega-structure. Apart from burnt daub, ceramics followed by bones represent the most frequent find categories in the levelling layer.

Nearly 20 kg of ceramic vessel fragments were found within Features 111024 and 111025, which corresponds to a rather low find density of 0.88 kg/m². In fact, the material was concentrated in the areas surrounding Pits 33–35 in the northwest of the excavation trench, while on the other hand, there were larger empty areas. In view of a rather low fragmentation degree with an average sherd weight of 35 g, these find concentrations might be understood as only low to moderately relocated material from primary waste contexts.

From a technological point of view, the relatively high proportion of so-called kitchenwares is remarkable. Depending on the calculation method, this amounted to between 20 and 30% (Tab. 15). In total 60 fragments originate from at least three vessels, a large conical bowl with a vertical rim (Fig. 41: 1) and two pots (Fig. 41: 2–3).

Besides the above-mentioned kitchenware vessels, a broad spectrum of vessel categories of tableware is represented in the find assemblage. Most frequent categories are half or completely closed vessels such as amphorae, bi-conical vessels (Fig. 42: 3–5), followed by bowls (Tab. 16). According to the documented percentages of rim, belly and bottom sherds, the quantity of pottery corresponds, purely statistically, to at least 30 vessels.

The spectrum of vessel forms and decorations is illustrated in Figures 42 and 43, as far as we were able to reconstruct it by means of refitting and graphical documentation. Frequently, it shows conical bowls widely used in Tomashovka contexts (Fig. 43: 1–8), which in one case bears painting with a so-called cometshaped decoration scheme (Fig. 43: 8). Much rarer are bowls with an inwardly bent rim zone like the one shown in Figure 43: 9 which is decorated with the so-called figure-eight-shaped decoration scheme.

 $Compared to bowls, cups and goblets are generally very rare in Trench\,111 whereas they are usually very common in Tomashovka contexts. Only one bi-conical cup,$

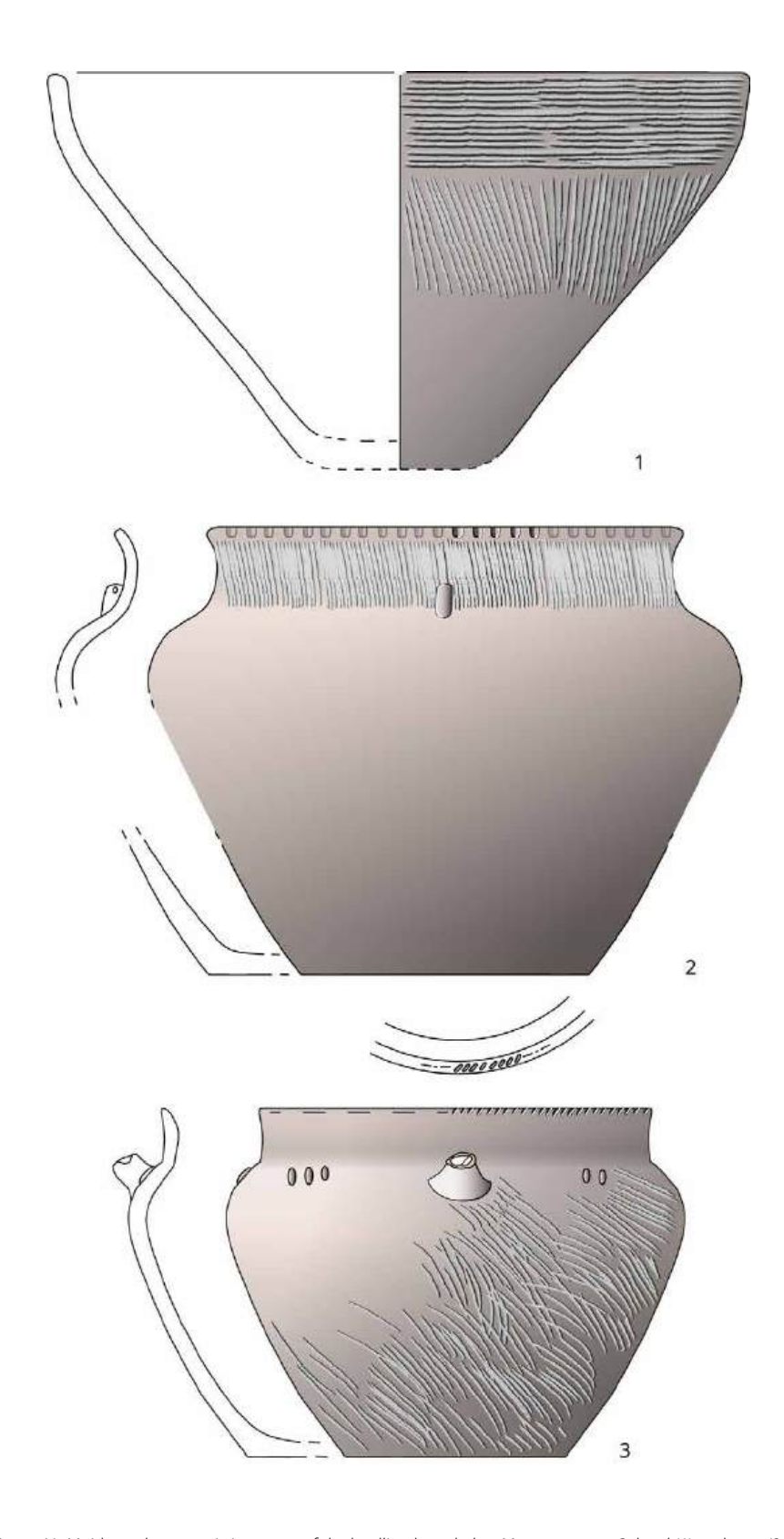


Figure 41. Maidanetske, ceramic inventory of the levelling layer below Mega-structure 3: bowl (1) and pots (2–3) made of kitchenware. (1)–(2) Scale 1:4; (3) Scale 1:3.

Class	Type-group	Number (n)	Weight (kg)	Summed rim percentage	Summed belly percentage	Summed bottom percentage	Minimum number of vessels
Non-classified		132	5.1	146	45	386	4
Amphora		25	1.0	95		200	2
Biconical vessel		4	0.4	15	6		1
Binocular vessel		8	0.3				1
Bowl		14	0.4	13		75	1
Bowl	Conical	30	1.3	318		240	4
Bowl	Sphero-conical	15	0.5	67			1
Closed vessel		214	5.8		125	568	6
Krater		1	0.05	10			1
Krater-shaped		4	0.6		11		1
Goblet		4	0.01	10			1
Goblet	Cup	1	0.1	38		16	1
Goblet	Goblet	4	0.06	10	35		1
Lid		1	0.02	14			1
Pear-shaped vessel		2	0.05	32			1
Pot		60	2.4	85	14	214	3
Total		519	18.2				30

shown in Figure 43: 10, can be assigned to the pre-mega-structural settlement. In addition, larger goblets are only represented by a few fragments.

Apart from the serving vessels described, the find inventory included at least four kraters and krater-like vessels (Fig. 43: 11–13, Fig. 42: 2), one of which has a double wavy line on its rim zone. In addition, there are at least four specimens of amphorae and bi-conical/sphero-conical vessels (Fig. 42: 3–5, 9), a tableware 'pot' (Fig. 42: 1), fragments of a pear-shaped vessel (Fig. 42: 8) and a lid.

In addition to pottery, four fragments of weaving weights of a simple round type with central perforation were found in Features 111024 and 111025 (Tab. 17). The two specimens with Find-ID 1111088 occurred in the south-east of the excavation area directly below a concentration of objects for textile processing; these were assigned to the mega-structure. It seems reasonable to assume that the specimens could have been transported to deeper layers through bioturbation and should actually be assigned to the mega-structure. The other two loom weights were found in the north-west of the area in the immediate vicinity of Pit 35.

A total of 10 quarry and ground stone artefacts of different kinds were found in the 'levelling layer' below Mega-structure 3 (Tab. 18).

Pit 33

Pit 33 (111/1) was situated in Quadrats J–K/9–11, slightly off-centre under the fireplace of Mega-structure 3 (Fig. 44). The pit had an irregular oval shape and dimensions of 2.9 m x 2.0 m x 0.3 m (Fig. 40). It was thus more of a shallow depression than a proper pit. The pit had been dug into the buried humus horizon, Feature 111030, which was probably identical with Feature 111027, which was initially documented as the lower part of the pit filling (Fig. 45).

Table 16. Maidanetske, type and frequency of vessel categories in the levelling layer below Mega-structure 3.

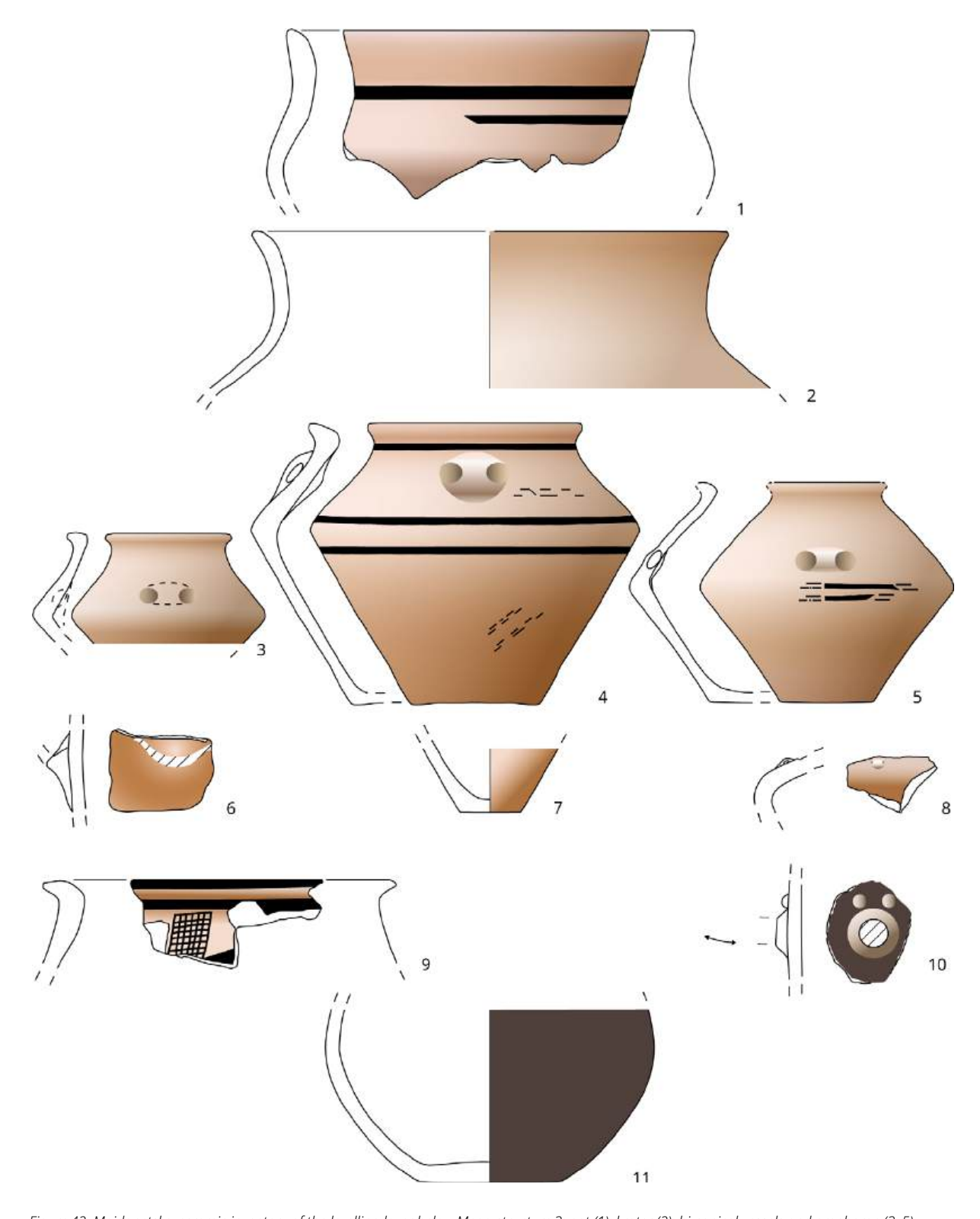


Figure 42. Maidanetske, ceramic inventory of the levelling layer below Mega-structure 3: pot (1); krater (2); bi-conical vessels and amphorae (3–5); handle (6); bottom of a closed vessel (7); bi- or sphero-conical vessel (9); lower part and decorated handle fragment (not Trypillia) of a ceramic vessel (10–11); made of tableware (1–9) and atypical dark burnished black-grey polished ware (10–11). Scale 1:3.

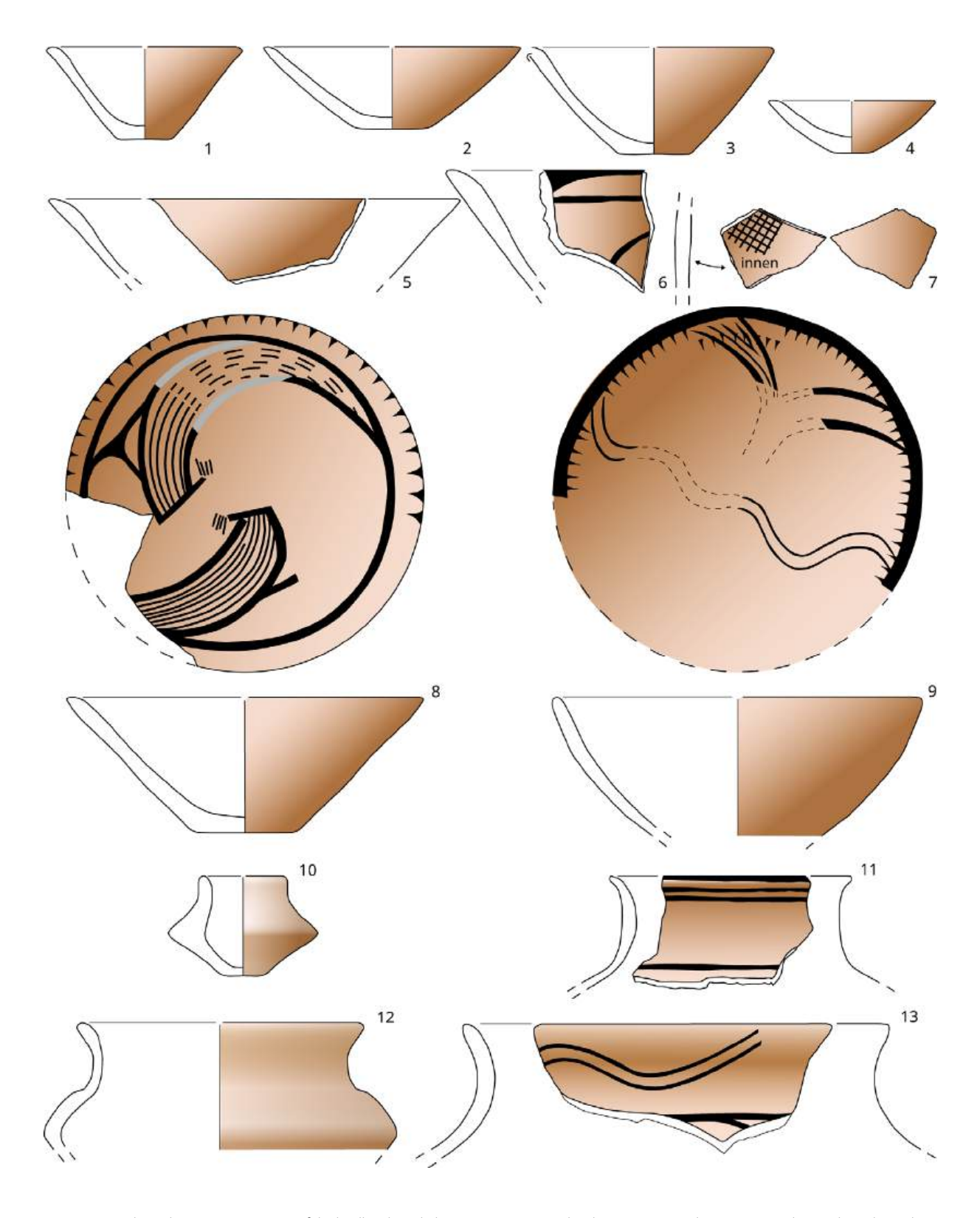


Figure 43. Maidanetske, ceramic inventory of the levelling layer below Mega-structure 3: bowls (1–9); cup (10); kraters (11, 13); krater-shaped vessel (12). Scale 1:3.

Find-ID	Context	Description
1111088	Feature 111025, Level 4b, Quadrat I23	2 loom weight fragments of Type 3, flattened round with central perforation, 26 g, degree of preservation 30%
1111115	Feature 111024, Level 4, Quadrat L6	1 loom weight fragment of Type 3, flattened round with central perforation, 12 g, diameter 50 mm, degree of preservation 25%
1111116	Feature 111025, Level 4, Quadrat L6	1 loom weight fragment of Type 3, flattened round with central perforation, 15 g, diameter 40 mm, height 29 mm, degree of preservation 25%

Table 17. Maidanetske, Trench 111, contextualisation and description of non-pottery ceramic objects.

Find-ID	Feature- ID	Level	Quadrat	Number (n)	Weight (kg)	Cate- gory	Material
1110838	111024	3	H4	1	0.3	Quarrystone	Granite, coarse-grained, red
1111004	111025	4	K21	1	>5	Quarrystone (perhaps millstone fragment)	Granite, coarse-grained
1111006	111025	4	M19	1	>5	Quarrystone	Granite, coarse-grained, red
1111008	111025	4	J18	1	>5	Mill stone fragment (quern, lower)	Granite, coarse-grained
1111010	111025	4	J17	1	>5	Mill stone fragment (quern, lower)	Granite, coarse-grained
1111012	111025	4	J16	1	>5	Quarrystone	Granite, fine-grained, yellowish grey
1111014	111025	4	L16	2	>5	Mill stone fragment (unknown position)	Granite, coarse-grained
1111018	111025	4	I19	1	>5	Quarrystone (perhaps millstone fragment)	Granite, coarse-grained
1111166	111025	4	N7	1	0.1	Quarrystone	Granite, fine-grained, yellowish grey
1111172	111025	4	I18	1	0.02	Mill stone fragment (unknown position)	Unknown

Table 18. Maidanetske, list of quarry stone and groundstone artefacts found in features attributed to the levelling layer below Mega-structure 3.

The filling of Pit 33 consisted mainly of burnt daub, probably from another context, weighing in total about 135 kg (Tab. 19). This burnt daub had been disposed in the pit without any apparent order. The majority of this material (98%!) contained organic temper with cereal chaff, whereas only about 2% showed no visible tempering and only 0.1% had a crumbly yellowish structure. In terms of the number of fragments, almost 75% of the burnt daub was of amorphous shape and gave no indication of the type of architecture. The remaining approximately 400 fragments (corresponding to about 50% of the weight) showed mostly flat surfaces and impressions of split wood planks as architectural features. In contrast, imprints of round timber were much rarer.

Besides burnt daub, the pit contained two bones of large mammals and one of a bovine, as well as 73 ceramic fragments weighing 3.4 kg. From a technological point of view, the small ceramic assemblage showed a usual composition, with about 95% of finer so-called tableware and 5% coarser kitchenware (Tab. 20). A comparatively high average sherd weight of nearly 50 g and a relatively high sherd density of 2.78 kg/m³ indicates that the pit filling represents either primary waste or only slightly relocated secondary waste.

From a morphological point of view, different classes and type groups of vessels were present in the pit (Tab. 21; Fig. 46: 1–2). In terms of the pure number of sherds, closed vessels including bi-conical vessels dominate, followed by conical bowls and pots. However, the minimum number of vessels obtained by measuring the rim, belly and bottom portions tends to show a uniform frequency of the categories identified.



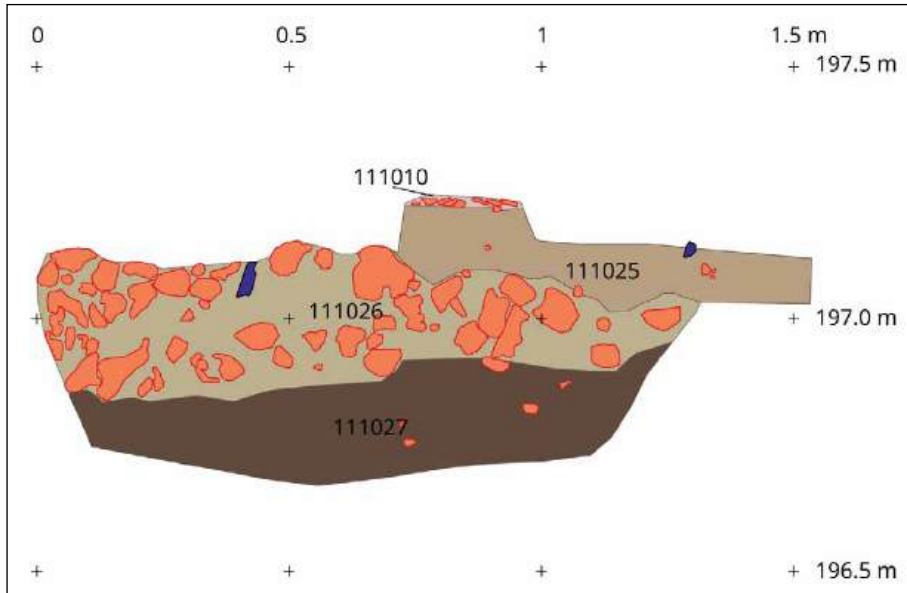


Figure 44 (above). Maidanetske, below the already partially removed central fireplace of Mega-structure 3, the upper edge of Pit 33, filled with burnt daub, is visible.

Figure 45. Maidanetske, profile through Pit 33, the backfill of which is superimposed by the Levelling Layer 111025 and the central fireplace of the Mega-structure 3.

Pit 34

Pit 34 (111/2), situated in Quadrats E–F/8–9, represents one of the larger pits in Trench 111. It was located below the southwestern longitudinal side of the megastructure (Fig. 40). Here, subsidence of the pit filling led to the displacement of wall debris, which seems to be the reason for the emergence of the apse-like extension on the northeastern longitudinal wall of the mega-structure.

		Calculat	tion by nur	nber (n)			Calculat	ion by wei	ight (kg)	
Architectural features	Organic tempered (chaff)	Compact (without chaff)	Crumbly yellow	Total number	Percentage	Organic tempered (chaff)	Compact (without chaff)	Crumbly yellow	Total weight	Percentage
1 Amorphous	1192			1192	73.76	63.0			63.0	47.1
4 Split wood	131	7		138	8.54	21.9	1.4		23.3	17.4
2 Plain surface	134	24		158	9.78	17.5	1.3		18.8	14.1
5 Log wood	67			67	4.15	11.2			11.2	8.3
6 Combination: Split wood + split wood	22			22	1.36	7.9			7.9	5.9
8 Combination: 2x split wood + plain surface	20			20	1.24	7.4			7.4	5.5
3 Two plain surfaces	5			5	0.31	0.9			0.9	0.7
7 Combination: Split wood + plain surface	2			2	0.12	0.6			0.6	0.4
10 Combination: Split wood + log wood	2			2	0.12	0.5			0.5	0.4
Non-classified		7	3	10	0.62		0.2	0.1	0.3	0.2
Percentage	97.5	2.4	0.2			97.7	2.2	0.1		

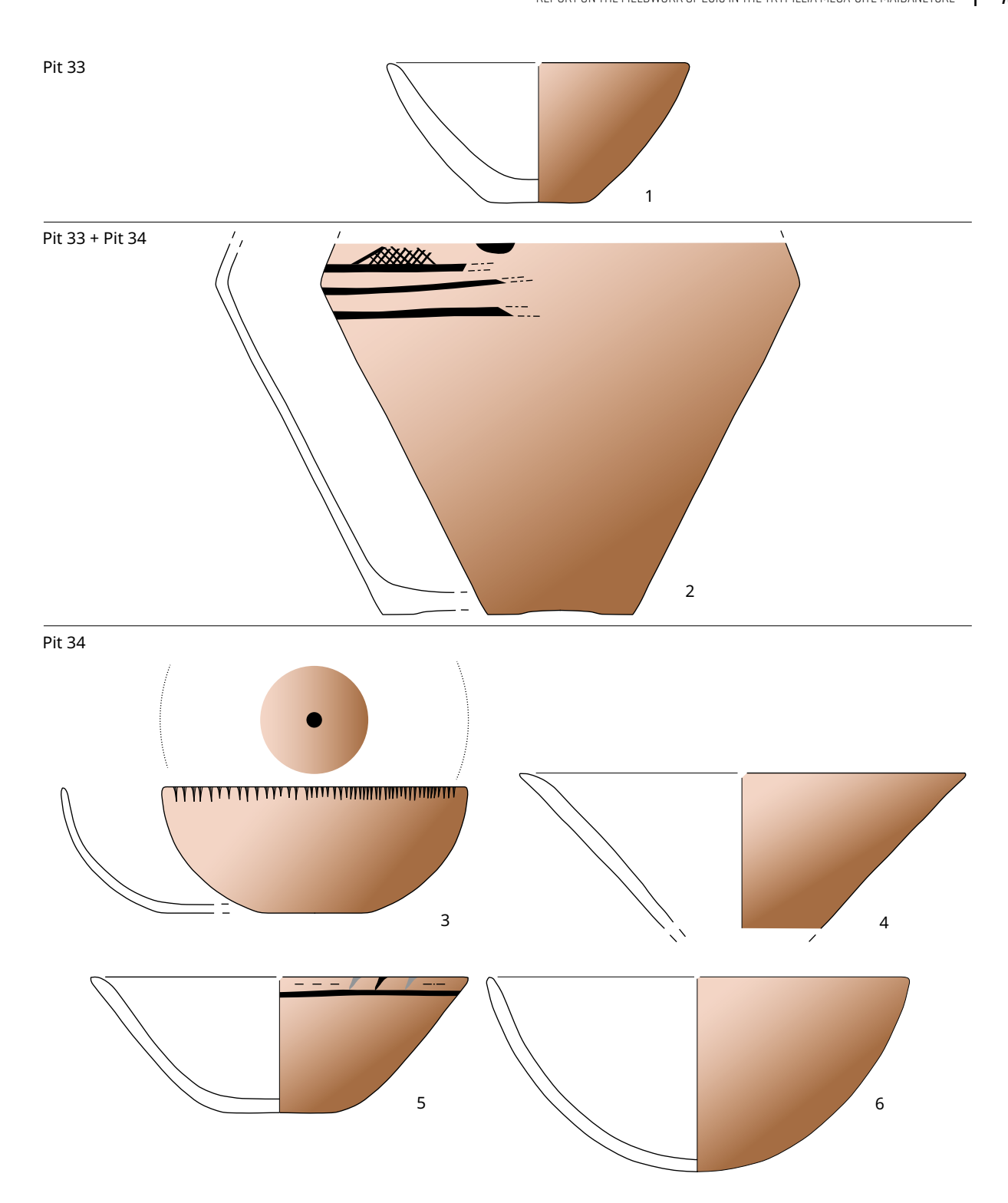
Table 19 (above). Maidanetske, frequency of material categories and architectural features of burnt daub in the filling of Pit 33.

Table 20. Maidanetske, frequency (number, weight) and fragmentation (average sherd weight) of ceramic fabrics in Pit 33.

Fabric	Number (n)	Weight (kg)	Number (%)	Weight (%)	Fragmentation (g)
Kitchenware	4	0.2	5.5	5.7	49
Tableware	69	3.2	94.5	94.3	47
Total	73	3.4			47

Class	Type group	Number (n)	Weight (kg)	Summed rim percentage	Summed belly percentage	Summed bottom percentage	Minimum number of vessels
Bowl	Conical	3	0.3	51		65	1
DOWI	Sphero-conical	2	0.015	8			1
Goblet		1	0.04		25		1
Bi-conical vessel		5	0.5				1
Closed vessel		48	2.2	27	11	100	1
Pot		3	0.095				1
Non-classified		18	0.37	7		42	1
Total		80	3.52				7

Table 21. Maidanetske, frequency of morphological pottery classes and type groups in Pit 33.



As we discovered the pit only during the last day of the excavation, we could not fully document it. Thus, its size and stratigraphic relationships could only be determined roughly. While the pit was clearly located stratigraphically below the floor of the mega-structure, its relationship to the Levelling Layer 111025 remained unclear.

Pit 34 had a diameter of approximately 3 m. While the upper edge of the pit was situated at a level of about 167.20 m and thus about 0.2 m below the floor of the megastructure, the lower edge was located beneath 166.60 m. In addition to almost 10 kg

Figure 46. Maidanetske, ceramic inventory of the Pits 33 and 34: bowls (1, 3–6); biconical or sphero-conical vessel (2). (1), (4)–(6) Scale 1:3; (2)–(3) Scale 1:4.

Species	NISP	Weight (kg)
Bos	153	8.34
Indet.	67	0.28
Large mammal	12	0.10
Cervus elaphus	2	0.31
Unio	1	-
Sus	1	0.03
Helix pomatia	1	-
Total	237	9.07

Table 22. Maidanetske, Trench 111, frequency of animal species in Pit 34 (after Benecke et al.: Chapter 9, this work, Vol. I).

Fabric	Number (n)	Weight (kg)	Number (%)	Weight (%)	Fragmentation (g)
Tableware	207	9.5	82.8	89.0	45.8
Kitchenware	43	1.2	17.2	11.0	27.3
Non-classified	36	2.3			63.2
Total	286	12.9			45.2

Table 23. Maidanetske, frequency (number, weight) and fragmentation (average sherd weight) of ceramic fabrics in Pit 34.

of animal bones, the pit contained a large quantity of pottery fragments (about 13 kg), burnt daub (about 7 kg) and a collection of eight ground stone artefacts (Tab. 14).

Pit 34 contained a large collection of 237 animal bones, highly dominated by cattle bones (Tab. 22; Chapter 9, this work, Vol. I). Since elements of the different meat value classes are represented according to the anatomical composition, from the zoological point of view nothing seems to argue against this being normal domestic waste from slaughter. However, the pit stands out because of its extremely high density of bone finds of more than 2 kg/m³ and the low degree of fragmentation, with an average fragment weight of 67 g. In this respect, the assemblage shows characteristics for which a ritual character may be considered.

Comparable to other pits in Maidanetske, pottery in Pit 34 also shows an increased density (3.4 kg/m³) and low fragmentation (45 g average sherd weight). In total, we recovered almost 13 kg which shows a much better preservation of paintings than the material from the mega-structure and the levelling layer. Depending on the calculation basis, 83–89% are so-called tableware and 11–17% are so-called kitchenware (Tab. 23). Thus, the frequency of the fabrics is within the normal range of variability (Shatilo 2021, 158–168).

According to the quantification of the preserved percentages of rim, belly and base fragments, the ceramic inventory comprises at least 23 vessels and represents a wide range of shapes (Tab. 24; Figs. 46–49). This includes at least six conical and spheroconical bowls (Fig. 46: 3–6, Fig. 47: 1, 3), one of which is decorated with a comet-shaped design scheme (Fig. 47: 1) and another which has a simplified line scheme with central dot and with circumferential ladder band on the periphery (Fig. 47: 3).

Half-open forms are represented by several pots made of different fabrics. There are two tableware pots with short vertical rim and steep shoulder, painted with leaf-shaped design scheme (Fig. 47: 5, 6) and one pot made of kitchenware, decorated with combed decoration groups of round impressions, and plastic applications of animal heads (Fig. 49: 3).

Closed shapes in the inventory include at least one goblet with funnel-shaped rim zone, conical neck, rounded bi-conical belly and leaf-shaped decoration (Fig. 47:

Class	Type group	Number of fragments (n)	Weight (g)	Summed rim percentage	Summed belly percentage	Summed bottom percentage	Minimum number of vessels
Bowl		16	1069	5		132	2
Bowl	Conical	25	1420	185		262	3
Bowl	Sphero-conical	12	237	60.5		65	1
Goblet	Goblet	1	57	26			1
Amphora		9	382	80		100	1
Bi-conical vessel		33	2340	170		100	2
Closed vessel		63	2148	19	31	582	6
Krater		1	55	6			1
Krater-shaped		12	415	37	65	55	1
Container		1	56	6			1
Pot		43	1304	87		8	1
Non-classified		70	3443	210		258	3

7). A krater/krater-shaped vessel has a similar shape, with a handle at the rim and neck. It is painted with a band of hanging triangles at the rim and a segment-shaped shoulder decoration (Fig. 47: 9). In the otherwise undecorated neck area, tree or earshaped signs are depicted. Probably also belonging to the category of krater/krater-shaped vessel is the neck shown in Figure 47: 4, on which two hook and ladder bands are shown under a leaf-shaped decoration on the rim.

Table 24. Maidanetske, frequency of morphological pottery classes and type groups in Pit 34.

Closed forms are additionally represented by one small amphora (Fig. 47: 8) and at least three larger vessels of the category amphora/bi-/sphero-conical vessels (Figs. 48, 49: 1). While the latter vessels show typical developed collar-shaped rims, the former amphora has only a rudimentary ridge-shaped thickened rim. The very simple and ephemeral decoration of this vessel with vertical groups of strokes between circumferential lines gives a very archaic impression. In comparison, the 'segment-shaped' decoration of one of the amphora/bi-/sphero-conical vessels is much more complex (Fig. 48: 3).

Overall, it can be shown that the ceramic inventory of Pit 34 is clearly dominated by closed forms, of which there are at least 15 vessels. In contrast, open serving vessels are represented by at least six specimens and semi-open vessels by three specimens.

In addition, eight possibly modified quarry stones derive from Pit 34 (Tab. 25). A fragment of granite could be part of a millstone; in all other cases the artefact character is not determinable.

Pit 35

The funnel-shaped Pit 35 (111/3) was located under the northwestern narrow end of the mega-structure (I–L/4–7; Fig. 40). While the pit was clearly below the floor level of the mega-structure, the determination of the stratigraphic relation to the underlying layer (Feature 111025) was difficult. The round pit had a diameter of 1.5 m at its upper edge; the pointed pit bottom was located 1.25 m below the floor of the mega-structure (Fig. 50).

The pit contained a small collection of burnt daub with a total weight of 5.7 kg (Tab. 26), which was evenly distributed over all levels. As in other contexts, chaff-tempered material predominates, while fragments without temper are much rarer and the 'crumbly-yellow' variant is present only in one piece. The most common



Figure 47. Maidanetske, ceramic inventory of Pit 34: bowls (1–3); pots (5–6); goblet (7); amphora (8); krater/krater-shaped vessel (4, 9); all made of tableware. (1), (3)–(4), (8)–(9) Scale 1:4; (2), (5)–(7) Scale 1:3.

architectural features are flat surfaces, followed by impressions of split wood planks. The accumulation of fragments with a flat surface and without temper in the upper two levels of the pit indicates that they belong to the rammed earth floor of the mega-structure.

A total of 31 animal bones were recovered from the middle part of the pit fill (between 196.47 m and 197.06 m; Tab. 27). Similar to Pit 34, domestic cattle represent the dominant species, followed by two bones of red deer and one of a sheep or goat. From a zoological perspective, nothing contradicts the assumption that this collection represents normal domestic butchery waste (Chapter 9, this work, Vol. I).

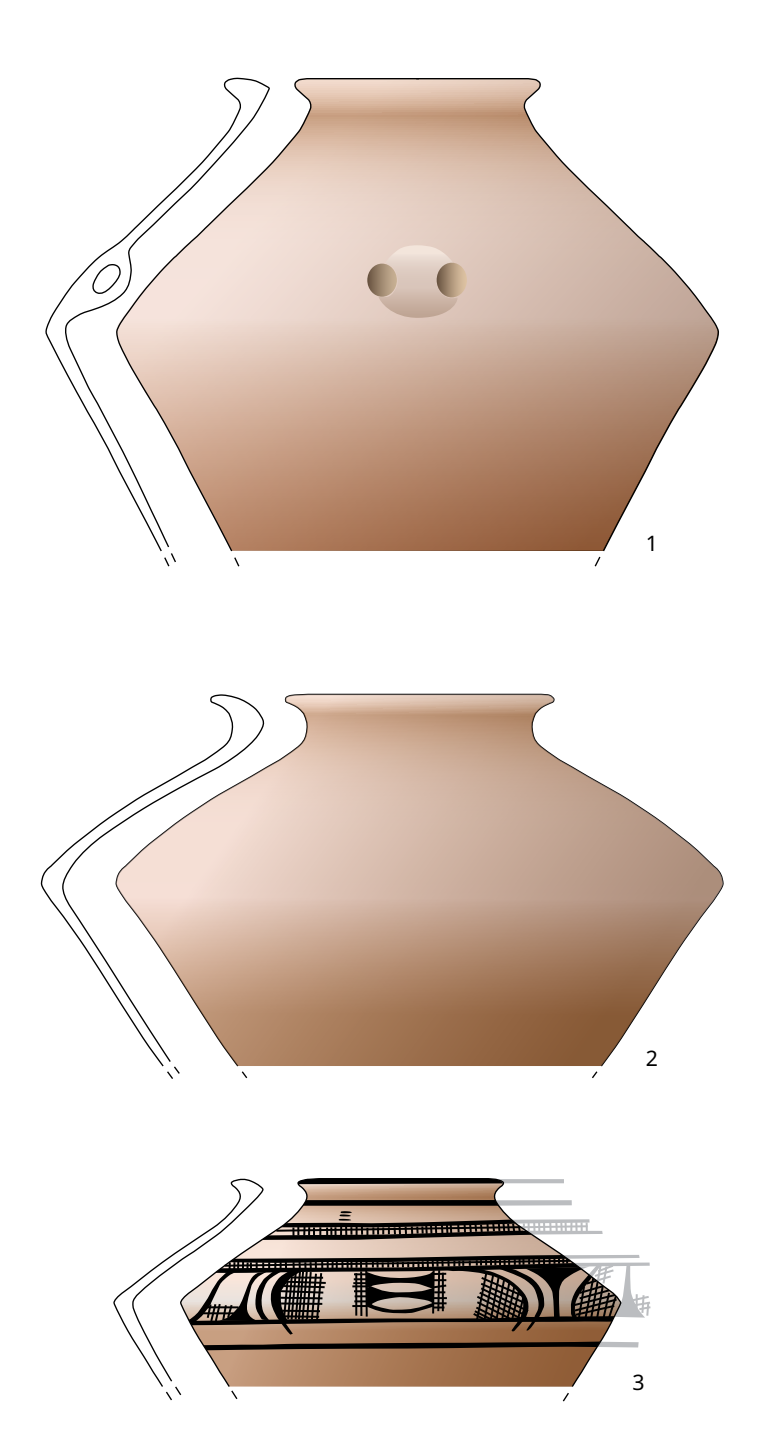


Figure 48. Maidanetske, ceramic inventory of Pit 34: amphora/bi-/sphero-conical vessels (1–3); all made of tableware. Scale 1:4.

Apart from the burnt daub, the animal bones and one flint artefact (Find-ID 1111554, a 6 g point made of dark brown (Volynian?) flint; Fig. 52: 3), the backfilling of the pit comprised a larger ceramic inventory which was distributed over the entire depth of the pit (Fig. 49: 4–7, Figs. 51 and 52). The find density amounted to $3.7~{\rm kg/m^3}$ and was similar to that of neighbouring pits, although with an average sherd weight of $34~{\rm g}$ the degree of fragmentation was slightly higher.

As in the Levelling Layer 111025, the proportion of tableware is relatively low at 76–77% and that of kitchenware is correspondingly high at 22–23% (Tab. 28). The composition of the pottery assembly, with remains of at least 20 vessels including 5 bowls, 1 pot, 2 goblets, 1 jug, and 7 closed vessels, is also similar to that of other contexts in Trench 111 (Tab. 29).

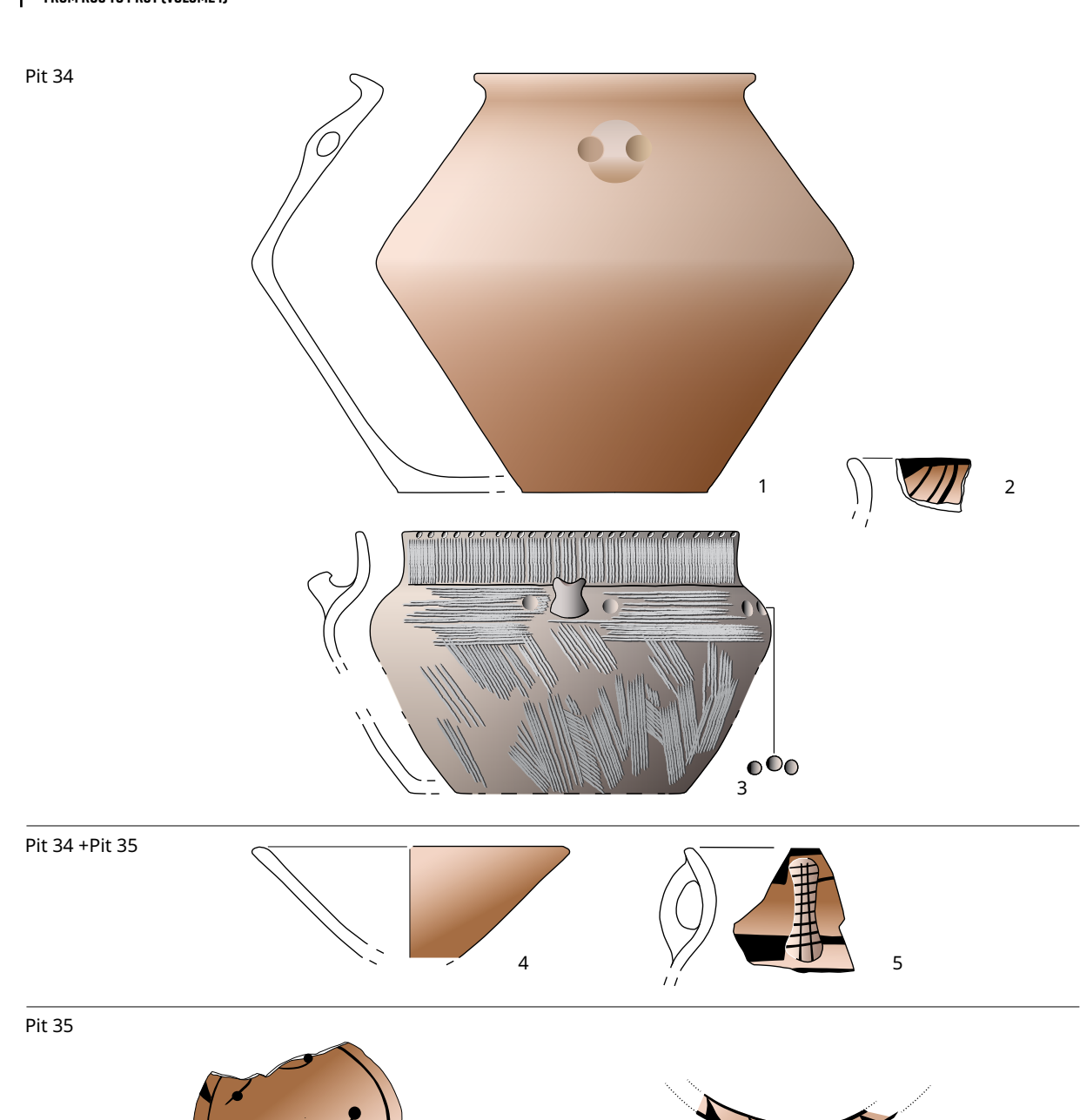


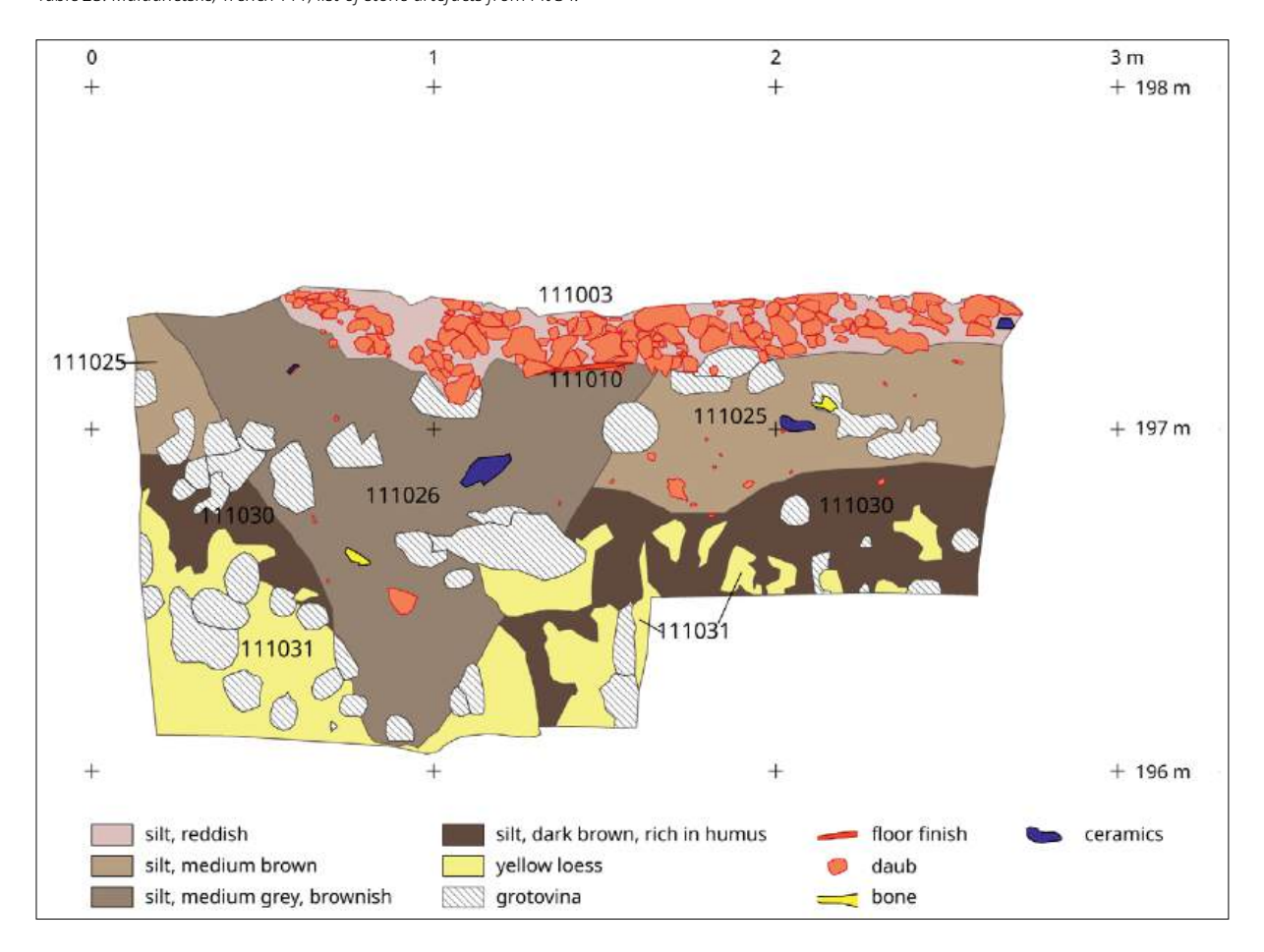
Figure 49. Maidanetske, ceramic inventory of Pits 34 and 35: amphora (1); pot (3); bowls (4, 6–7); goblet (5); made of tableware (1–2, 4–7) and kitchenware (3). Scale 1:4.

The majority of the bowls show open conical shapes, frequently decorated on the rim zone with bands composed of hanging triangles and showing decoration in some places of the comet-shaped scheme and signs (Fig. 49: 6–7, Fig. 51: 5). The bowl in Figure 49: 6 is decorated with a variation of the simplified-line scheme.

Half-open shapes are rare in the inventory and are actually only represented by a kitchenware pot with cattle protomes, round stamps and a perforation at the edge (Fig. 52: 2).

Find-ID	Context description	Category					
4444422	Fortuna 1D 444033 Lovel 4b Overdent F F/O 0	1 quarry stone, 310 g, material not determined (feldspar?)					
1111422	Feature-ID 111033, Level 4b, Quadrat E–F/8–9	1 quarry stone, 528 g, material not determined					
		1 quarry stone, 168 g, coarse granite, yellow, perhaps fragment of a grinding stone					
1111542	Feature-ID 111033, from the profile, Quadrat E6	1 quarry stone, 408 g, material not determined, elongated shape $200 \times 60 \times 26$ mm					
		4 quarry stones, 338 g, material not determined					

Table 25. Maidanetske, Trench 111, list of stone artefacts from Pit 34.



The inventory also includes numerous closed shapes such as fragments of a double-conical cup, with leaf-shaped decoration and bands composed of angled triangles and squares in horizontal zones (Fig. 51: 9). The category of closed forms also includes two pear-shaped vessels, one with a bi-conical shape and the other with volute scheme painting (Fig. 51: 6, 8).

The category of amphora/bi-/sphero-conical vessels includes the rim fragment of an amphora with pairs of knobs on the upper shoulder (Fig. 51: 10) and parts of a sphero-conical vessel with tangent scheme painting and ladder bands (Fig. 52: 1). On the other hand, the classification of the closed vessels in Figure 51: 7 and 11, the first of which has leaf-shaped scheme painting, is unclear.

The only chipped stone artefact from Pit 35 is a triangular arrowhead manufactured from a flake of dark brown Volhynian flint, showing on its base a cursory finishing and remains of cortex (Fig. 52: 3). It was found in the centre of the pit halfway down the pit filling.

Figure 50. Maidanetske, Profile 32 cutting trough Pit 34 below Mega-structure 3.

	Calculation by number (n)					Calculation by weight (g)				
Architectural features	Organic tempered (chaff)	Compact (without chaff)	Crumbly yellow	Total number	Percentage	Organic tempered (chaff)	Compact (without chaff)	Crumbly yellow	Total weight	Percentage
1 Amorphous	83	2		85	76.6	3862	62		3924	71.1
2 Plain surface	7	9		16	14.4	392	208		600	10.9
4 Split wood	5	1		6	5.4	662	80		742	1.4
5 Log wood	2			2	1.8	172			172	3.1
Non-classified		1	1	2	1.8		40	40	80	1.4
Total				109					5518	

Table 26 (above). Maidanetske, Trench 111, frequency of material categories and architectural features of burnt daub in Pit 35.

Table 27. Maidanetske, Trench 111, frequency of animal species in Pit 35 (after Benecke et al.: Chapter 9, this work, Vol. I).

Species	NISP	Weight (g)
Cattle	10	206
Large mammal	3	30
Red deer	2	44
Sheep/goat	1	3
Large garden snail	1	-
Indet.	14	56
Total	31	339

Pits 36 and 37

Further smaller pits or depressions were situated in Quadrats H/16 below the central part (Pit 36 or 111/4) and in E–F/23–25 south-east of the mega-structure (Pit 37 or 111/5; Fig. 40). Pit 36 was discovered only during the final works on the last day of the excavation and could therefore be only partially investigated and only extremely cursorily documented. The dimensions of the pit are therefore largely unclear. The backfill of the pit contained mainly chaff-tempered burnt daub mostly without architectural features (Tab. 30).

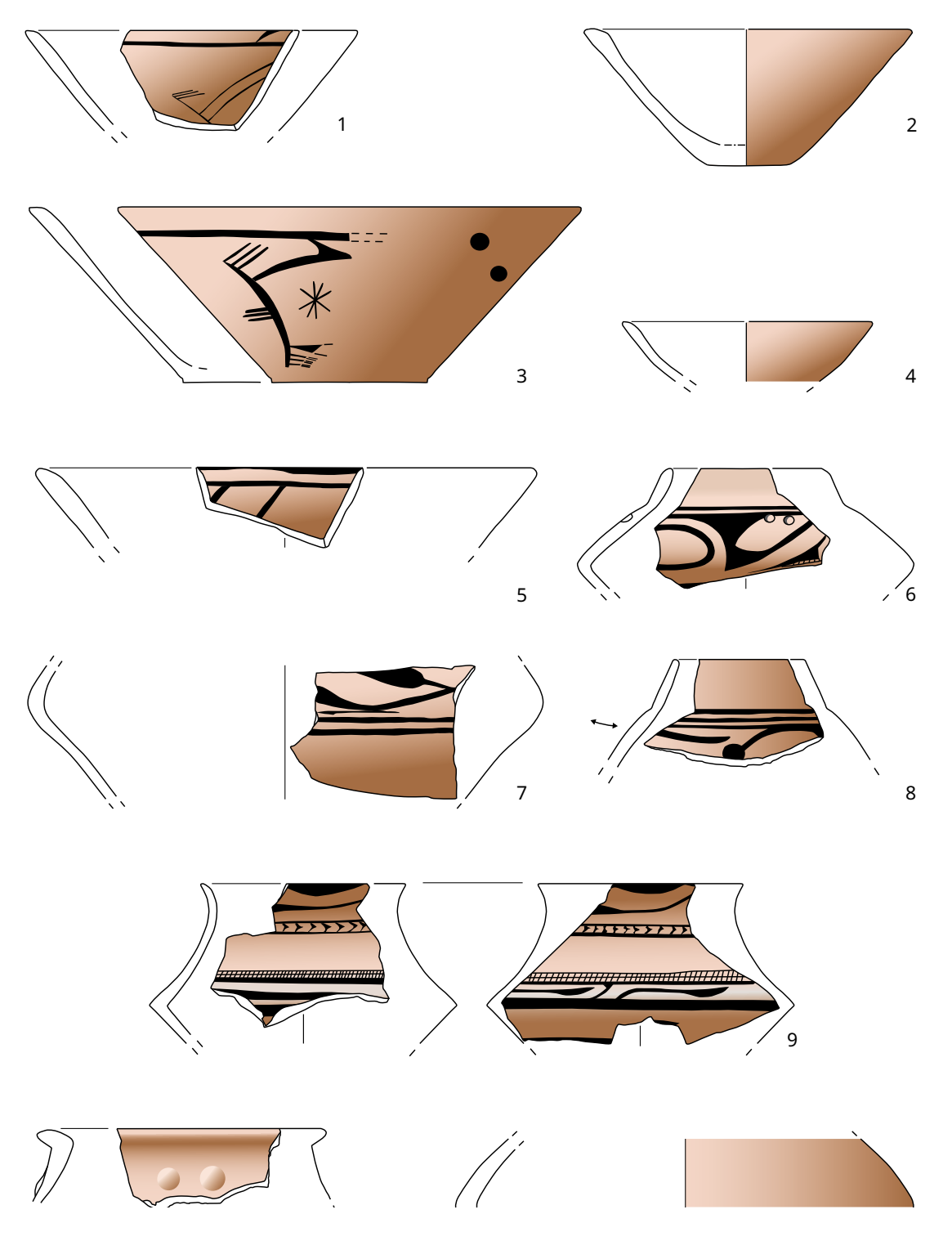
The backfill of Pit 36 contained also a small amount of tableware (Tab. 31) of at least four bowls and closed vessels (Tab. 32). The filling of Pit 37 did not yield any pottery.

Interpretation

Within the investigated area, four of the five pits which presumably belonged to the pre-mega-structure occupation form a row running in a northwest-southeast direction. While the fifth pit (Pit 34) is adjacent, to the southwest, we found no pits northeast of this line.

The distribution of the pits in the excavation area indicates that the supposed older row of houses running within the ring corridor according to the plan of the archaeomagnetic survey would have continued to the northwest. Accordingly, the pits explored in the excavation most probably belong to a pit zone located in the rear area behind houses (Fig. 40). In the pit-free zone to the northeast must have been the location of the associated houses. While to the southeast of the excavation remains of burnt houses are still preserved *in situ*, these were apparently removed in the area of the mega-structure.

As the massive filling of Pit 33 with burnt daub shows, the houses of the earlier phase were at least partly burnt down. The partly find-rich horizon between the



backfill of the pit and the floor of the mega-structure can be explained as a levelling layer to prepare the building ground for the mega-structure. An alternative explanation for the artificial dumping of earth would be the construction of some kind of podium, which may have served to architecturally highlight the building and increase its public visibility (Chapter 5, this work, Vol. I). The finds from this levelling layer, which are characterised by low to moderate fragmentation, might belong to inventories of dwellings that had to make place for the mega-structure or were transported here from the outside.

Figure 51. Maidanetske, ceramic inventory of Pit 35: bowls (1–5); pear-shaped vessels (6, 8); closed vessel (7); goblet (9); amphora (10); all made of tableware. Scale 1:4.

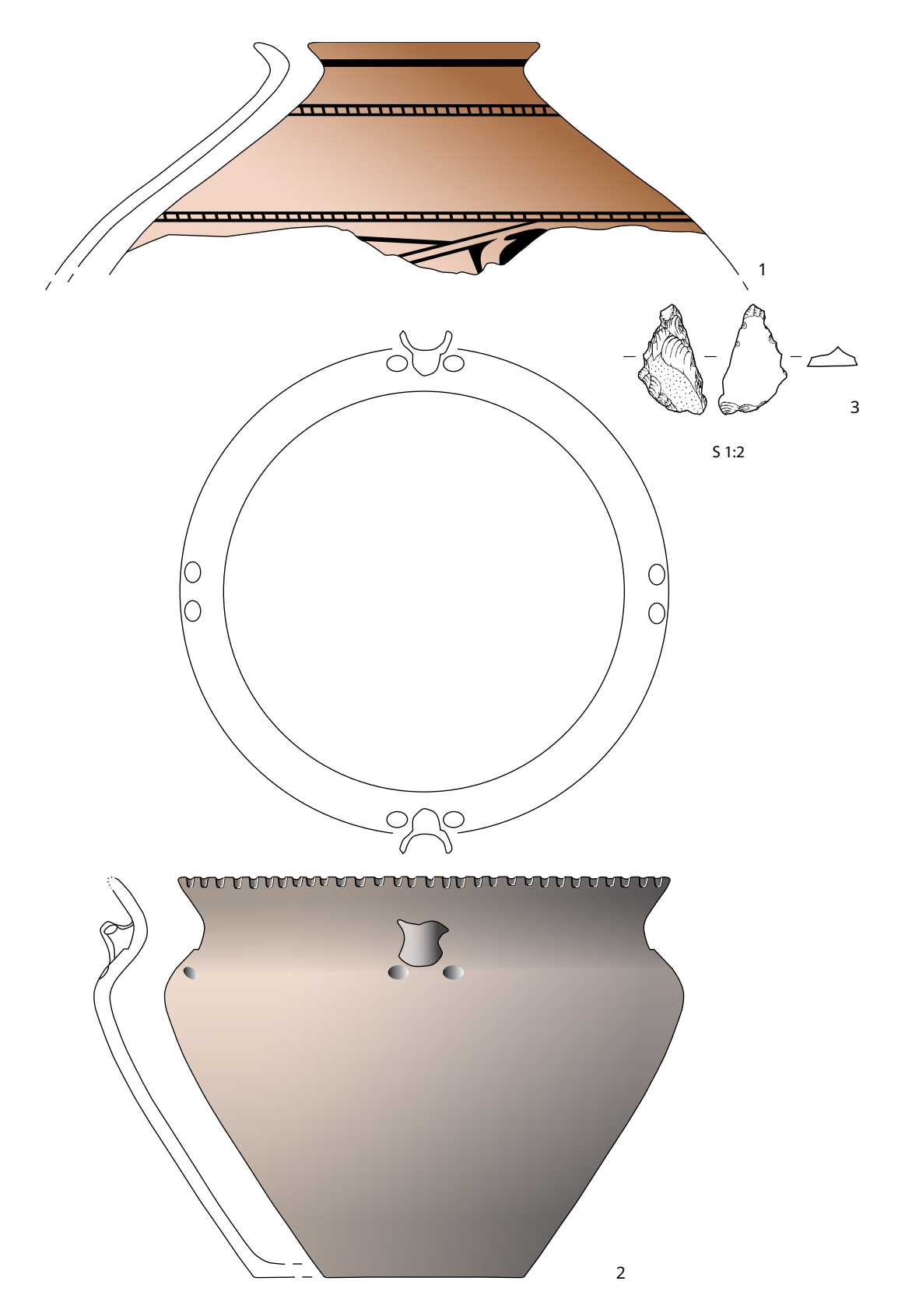


Figure 52. Maidanetske, find inventory of Pit 35: sphero-conical vessel made of tableware (1); pot made of kitchenware (2); chipped stone point (3). Scale 1:3.

Fabric	Number (n)	Weight (kg)	Number (%)	Weight (%)	Fragmentation (g)
Table	197	6.9	75.8	77.3	35
Kitchen	62	2.0	23.8	22.0	32
Indefinite	1	0.1	0.4	0.6	55
Total	260	8.9			34

Table 28. Maidanetske, frequency (number, weight) and fragmentation (average sherd weight) of ceramic fabrics in Pit 35.

Class	Type group	Number (n)	Weight (g)	Summed rim percentage	Summed belly percentage	Summed bottom percentage	Minimum number of vessels
Bowl		10	286			102	2
Bowl	Bowl, conical	27	1280	205		152	3
Bowl	Bowl, sphero-conical	1	12	11			1
Goblet		1	2				1
Goblet	Goblet, goblet	6	92	28	57		1
Goblet	Goblet, jug	1	57	3			1
Amphora		1	51	25			1
Bi-conical vessel		26	1611	100		39	1
Closed vessel		92	2694	91	129	343	4
Four-legged vessel		1	40				1
Pear-shaped vessel		2	110	22			1
Pot		55	1782	50		50	1
Unknown shape		37	861	109	7	71	2

	Ca	lculation	by num	ber (n)	Calculation by weight (kg)			
Architectural features	Organic tempered (chaff)	Compact (without chaff)	Crumbly yellow	Total number	Organic tempered (chaff)	Compact (without chaff)	Crumbly yellow	Total weight
1 Amorphous	31			31	2.9			2.9
2 Plain surface	3	4	2	9	0.7	0.5	2.9	4.1
4 Split wood	3			3	1.2			1.2

Table 29 (above). Maidanetske, frequency of morphological pottery classes and type groups in Pit 35.

Table 30. Maidanetske, Trench 111, frequency of material categories and architectural features in Pit 36.

In view of the partially poor preservation of the painted pottery surfaces and the weak relative chronology so far established for the find inventories, absolute dating is of crucial importance for the clarification of the chronological development of the sequence described.

14C dating

From the various stratigraphic contexts of Trench 111, eleven bone-samples were ¹⁴C dated by accelerator mass spectroscopy at the Poznan Radiocarbon Laboratory (Tab. 33). Pre-mega-structure activities are dated by Poz-87599 to Poz-87605, derived from Pits 33–35 and the levelling layer below the floor of the mega-structure. The phase of use of Mega-structure 3 is represented by two dates from disarticulated

Table 31. Maidanetske, frequency (number, weight) and fragmentation (average sherd weight) of ceramic fabrics in Pit 36.

Fabric	Number (n) Weight (kg)		Number (%)	Weight (%)	Fragmentation (g)	
Table	15	0.6	100	100	38	

Class	Type group	Number (n)	Weight (g)	Summed rim percentage	Summed belly percentage	Summed bottom percentage	Minimum number of vessels
Bowl		4	283	4		85	1
Bowl	Sphero-conical	1	5				1
Closed vessel		9	224	3			1
Goblet	Goblet	1	55		22		1
Total		15	567				4

Table 32. Maidanetske, frequency of morphological pottery classes and type groups in Pit 36.

Laboratory-ID	^и С age (ВСЕ)	(%) N	C (%)	(%)	Find-ID	Feature-ID	Level	Grid x	Grid y	Material	Taxon	Context
Poz-87721	4900 ± 40	0.9	7.0	1.0	1110275	111002	2	F	9	Bone	Bos	Layer above mega-structure
Poz-87609	5055 ± 35	2.5	10.4	5.6	1110085	111002	2	L	5	Bone	Bos	Layer above mega-structure
Poz-87610	5035 ± 35	2.5	10.9	4.4	1110689	111003	3	F	9	Bone	Bus	Wall debris of mega-structure
Poz-87598	4990 ± 35	2.9	11.0	5.9	1110750	111003	3	М	14	Bone	Bos	Wall debris of mega-structure
Poz-87599	5010 ± 35	4.5	14.5	3.0	1111565	111025	4a	J	13	Bone	Bos	Cultural layer below mega-structure
Poz-87600	4970 ± 30	2.9	11.0	2.0	1110981	111025	3	L	9	Bone	Bos	Cultural layer below mega-structure
Poz-87601	5020 ± 35	1.8	9.7	2.4	1111294	111026	4e	K	9	Bone	Bos	Upper edge of Pit 111/1
Poz-87602	4955 ± 30	1.2	7.9	1.1	1111077	111026	4e	K	9	Bone	Bos	Upper edge of Pit 111/1
Poz-87603	4990 ± 35	4.3	13.6	8.2	1111368	111029	4d	J	5	Bone	Bos	Pit 111/3 below mega-structure
Poz-0	>0	0.3	5.7		1111373	111029	4d	K	5	Bone	Bos	Pit 111/3 below mega-structure
Poz-87604	5000 ± 35	2.4	9.5	3.1	1111542	111033	Profile 30	F	6	Bone	Bos	Lower level of Pit 111/2
Poz-87605	5035 ± 35	2.7	10.9	4.2	1111519	111032/33	Profile 30	F	8	Bone	Bos	Lower level of Pit 111/2

Table 33. Maidanetske, list of ¹⁴C dates from Trench 111.

bones which were found inside the wall debris of the mega-structure (Poz-87598, Poz-87610). Post-mega-structure activities are represented by two dates from the layer directly above the wall debris (Poz-87609, Poz-87721).

Overall, the dates fall into a plateau of the calibration curve and the following steep section, covering a long range of about 300 years between 3950 and 3650 BCE. Through application of Bayesian modelling and the use of the function *boundary* with the assumption of two successive occupation phases and several events, the range of dates becomes significantly narrowed, roughly into the 38th century BCE (Fig. 53a). However, the overall probability of this model 1 amounts to only 40% (A_{model}=33.8)

due to largely identical dates from the different phases. Higher overall model probabilities of more than 100% can only be obtained by excluding the potential (too old) outliers Poz-87605, Poz-87609, and Poz-87610 (Fig. 53b). The dating results imply that Mega-structure 3 was constructed during Phase 3 of the site chronology suggested by René Ohlrau (2020a). Consequently, Mega-structure 3 at Maidanetske was built related to the rapid population increase of the 38th century and abandoned at the beginning of Phase 4, related to the start of the population decrease.

Trenches 113-117 - Unbuilt open spaces

In two transects with six trenches in total, the central unbuilt area of the settlement and the ring corridor were sampled (Fig. 1). The transect within the ring corridor included Trenches 113 to 115 and stretched in the north of the settlement over a length of 80 m, approximately 35–75 m east of the road in a north-south direction. The trenches were dug using an excavator.

The transect in the central undeveloped area of Trenches 116–118 run along (Trench 116) or within (Trenches 117 and 118) a forest strip which crosses the settlement in a northeast-southwest direction over a total length of approximately 300 m. Here, the trenches were dug by hand. Trenches 116–118 were each 10–15 m long and 1 m wide. The two outer Trenches 116 and 118 were each located at a distance of about 100 m from the nearest burnt Trypillia houses.

The terrain surface in the area of the ring corridor transect slopes very gently from a level of 203.75 m at the northern end of Trench 113 to 204.3 m at the southern end of Trench 115. Along the transect in the central unbuilt area, the terrain surface slopes gently to the southwest from a level of 201.9 m in Trench 116 to 201.0 m in Trench 118.

Stratigraphically, the same natural sequence of layers was found in all examined trenches, as far down as the corresponding depth was reached (Figs. 54 and 55). Below a humic surface horizon of Chernozem with a thickness of between 0.6–1.0 m, partly differentiable into two sub-layers Axh 1 and Axh 2, a relict browning horizon (rBw) with thicknesses of between 0.35–0.45 m was found. This horizon, a buried forest soil, transitioned into the underlying carbonate-bearing rock (Cc), in this case a weakly altered loess. However, this horizon was reached only in Trenches 117 and 116 (?), where it began below an rBw-Cc transition zone 1.4 m below the terrain surface.

Practically none of the trenches showed direct anthropogenic influence. An exception were small pieces of daub and pottery embedded in the rBw horizon of Trenches 113, 115 and 116, situated closest to the houses. However, this material was extremely fragmented and had probably been relocated several times. In view of the otherwise apparently undisturbed stratigraphic sequences, with no intrusions or anthropogenic deposits, these artefacts might have been deposited due to post-depositional processes.

The archaeological excavations were complemented by various scientific analyses. Soil samples were taken and analysed for macrobotanical remains (charcoal, seeds/fruits), soil properties (pedology, geoarchaeology, and geochemistry), biomarkers and snails. Three samples contained charcoal (Trench 114: 2 samples, Trench 117: 1 sample), eight samples contained snails (Trench 113: 2 samples; Trench 114: 2 samples; Trench 115: 2 samples; Trench 117: 2 samples) and three samples contained botanical macroremains (Trench 115: Cerealia indet.; Trench 117: 2 samples with *Stipa* sp.).

Geoarchaeological investigations show differences in the geochemical signature of the sedimentary sequences both between the settlement and its surroundings and between the ring corridor and the central unbuilt area of the settlement (Chapter 5, this work, Vol. I). Accordingly, we can assume different functions for the different settlement areas, possibly of an agricultural nature in the unbuilt centre of the settlement and rather more domestically-oriented in the ring corridor.

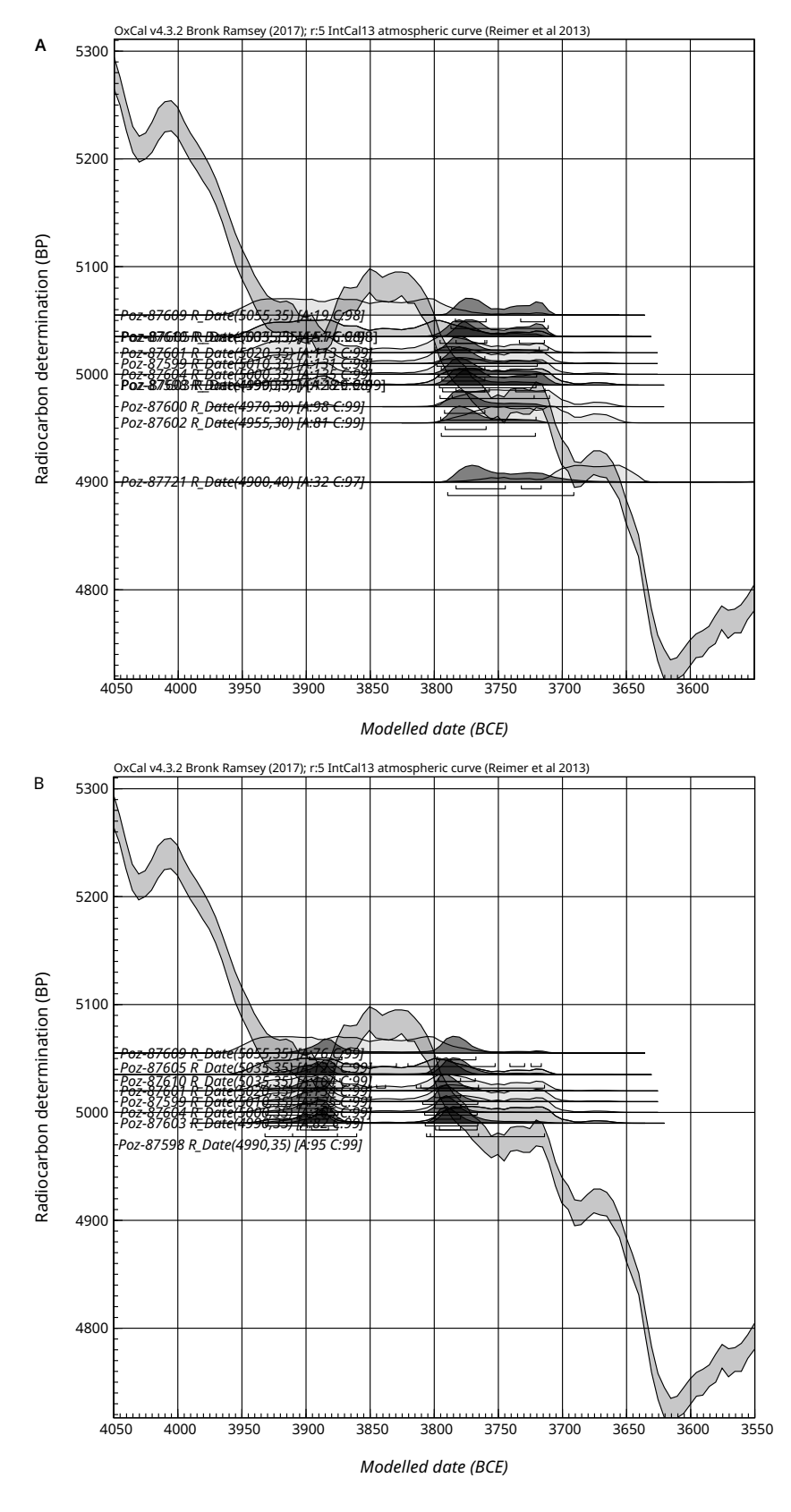


Figure 53. Maidanetske, Bayesian models 1 (a) and 2 (b) of 14 C dates from Trench 111 plotted on the calibration curve.

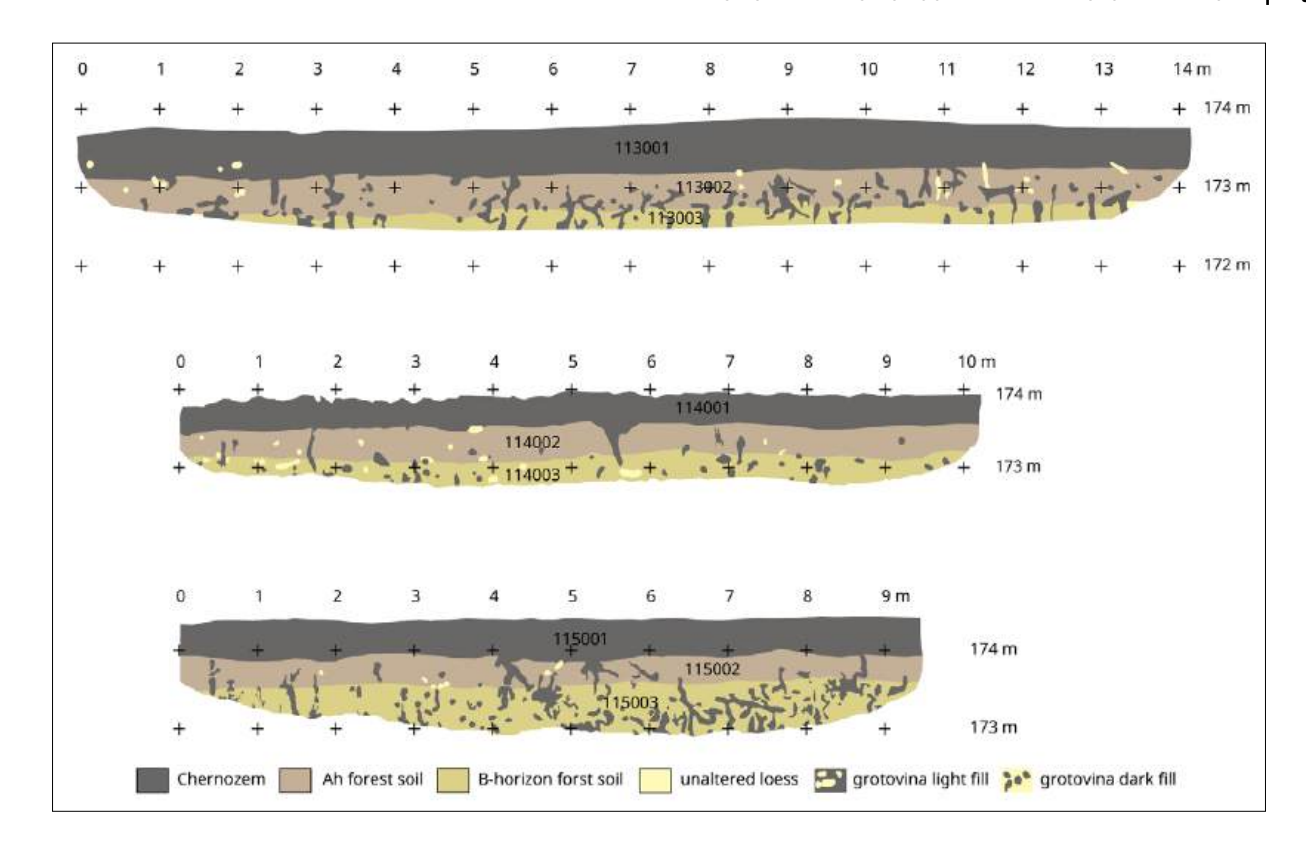


Figure 54. Maidanetske, profiles of the Trenches 113–115.

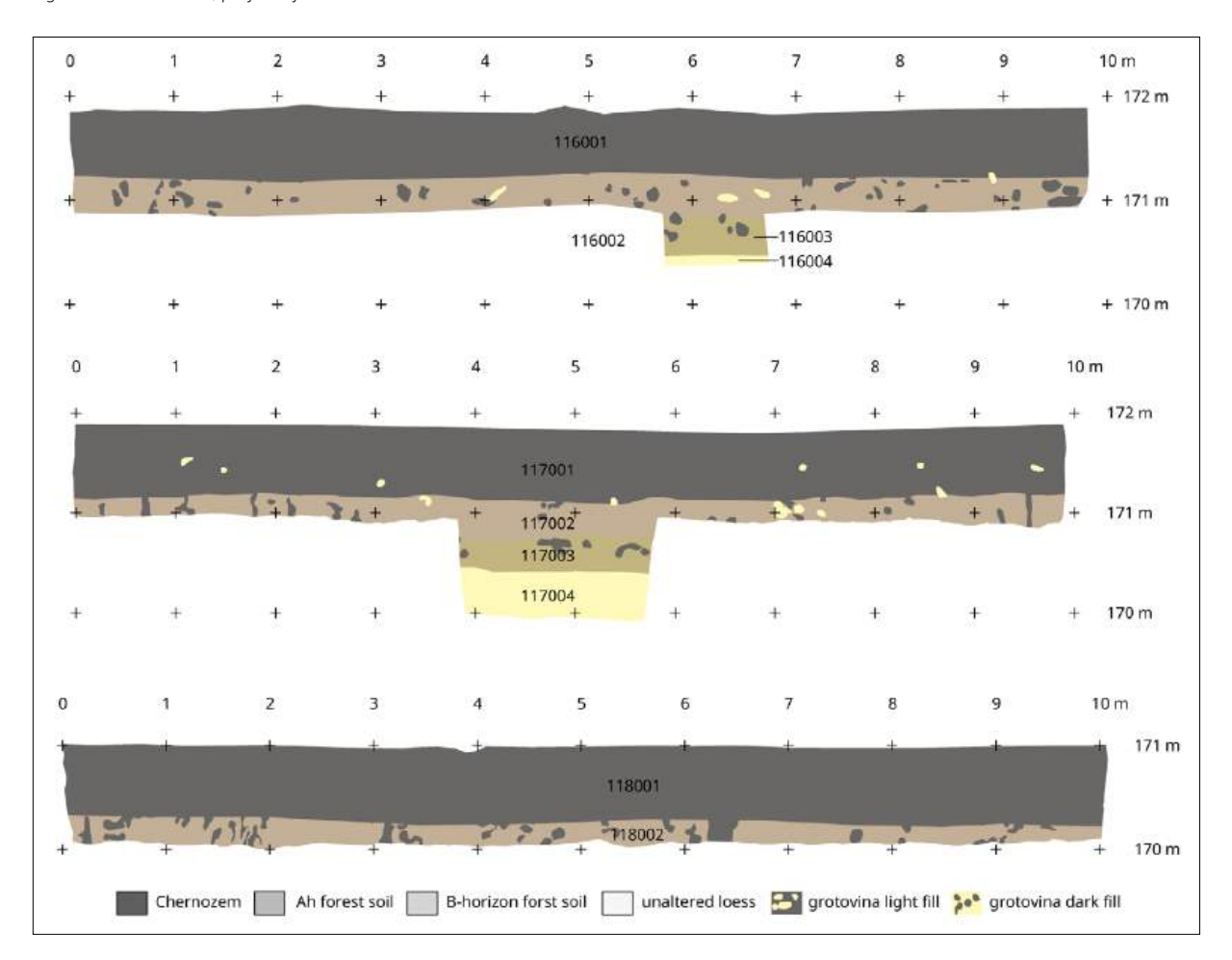


Figure 55. Maidanetske, profiles of the Trenches 116–118.

Discussion

Functional and architectural differentiation within the Maidanetske settlement

In several respects, the fieldwork of 2016 contributes to the functional and architectural differentiation of the mega-site of Maidanetske.

(a) Use of space within the settlement

Through continuation of the archaeomagnetic survey, three new mega-structures were discovered in the northern section of the ring corridor, confirming the predominant placement of such buildings in the ring corridor. Another possible central mega-structure was detected in a rectangular plaza to the east of the settlement, whose size and shape, however, could not be determined due to its proximity to metal objects and a row of trees.

It is hard to overestimate the importance of having found increased phosphate values in open spaces on the site of the settlement, compared to off-site areas. This applies not only to the ring corridor, as the potentially intensively used main street, but equally also to the unbuilt space in the centre of the settlement. The intensive use of the central zone of the settlement, often assumed on the basis of ethnographic analogies (Hale 2020, 127), *e.g.* for the enclosure of cattle or manured gardens, is thus confirmed for the first time.

(b) Architectural differentiation of private dwellings and public mega-structures

In Maidanetske, 82% of the total settlement area has been surveyed by high resolution magnetometry. Among other things, thirteen so-called mega-structures were identified in this plan, which we interpret as communal buildings due to their highly visible location in the public space of the settlement, their specific architecture and their size (Figs. 56 and 57; Tab. 34). Including the excavated Mega-structure 3, seven of these buildings are located within the ring corridor of the settlement. In another five cases they were placed within radial trackways. Lastly, one construction was situated on a rectangular square in the east-northeast part of the settlement. However, only a very small section of this could be recorded. In analogy to integrative architecture in ethnographically investigated non-ranked societies, we consider this decentralised distribution within the settlement as an evidence for the use of these buildings for integrative action by specific sub-groups within the community (Hofmann *et al.* 2019; Ohlrau 2020b). For integrative activities on the level of the whole settlement served likely Mega-structure 1 which is located on a rectangular plaza in the east of the settlement.

In addition to the positioning, the buildings show considerable size differences of between 120 and 580 m² and also a certain degree of architectural variability. In the archaeomagnetic plan of Maidanetske, eleven of thirteen special buildings show an at least partially empty interior surface. Only in the case of Mega-structure 5 is there laminar deposition of daub. In Mega-structures 1, 3, 6 and 9, remains of internal partitions are visible. In eight cases point or pointlike anomalies are visible along the central axis of the structures which most likely represent fireplaces. Thus, in Maidanetske, mega-structures show considerable variability. Besides partly roofed buildings that were investigated at Mega-structure 3, we may also need to consider that some of the mega-structures were completely unroofed and others completely roofed.

Mega-structure-ID	Identified as mega-structure based on size	Identified as mega-structure based on position	Identified as mega-structure based on architecture	Floor area (m²)	Length (m)	Width (m)	Length to width ratio	Type (after Hofmann <i>et al.</i> 2019)	Interpretation Extend of roofing of the interior space		Division in longitudinal direction	Central installation	Position (after Hofmann <i>et al.</i> 2019)
1		Х	Х	>312.0	>26.0	>12.0		?	High-level	Unroofed	?	?	2
2		Х	Х	175.0	17.5	10.0	1.8	2b	Low-level	Unroofed	One part	yes	3
3		Х	Х	155.0	18.0	8.6	2.1	3	Low-level	Partly roofed	Two-part?	yes	3
4		Х	Χ	180.0	18.0	10.0	1.8	2b	Low-level	Unroofed	One part?	yes?	3
5		Х		378.0	27.0	14.0	1.9	5a	Low-level	Completely roofed	?	?	3
6		Х	Х	578.0	34.0	17.0	2.0	2a	Low-level	Unroofed	One/two-part?	?	3
7		Х		391.0	29.0	13.5	2.1	6c	Low-level	Completely roofed	Two-part	?	3
8		Х	Х	334.0	23.0	14.5	1.6	2a	Low-level	Unroofed	One part	yes	3
9			Х	135.0	15.0	9.0	1.7	2b	Low-level	Unroofed	One/two-part?	yes	6
10			Х	162.0	18.0	9.0	2.0	3	Low-level	Unroofed	One/two-part?	yes?	6
11			Х	158.0	17.0	9.3	1.8	3	Low-level	Unroofed	One part	yes	6
12			Х	258.5	23.5	11.0	2.1	2b	Low-level	Unroofed	One part	yes	4
13			Х	122.5	17.5	7.0	2.5	2c	Low-level	Unroofed	One part	?	4

Through the excavation of Mega-structure 3, valuable data were obtained on the architecture and inventory of such a building. Accordingly, the architecture of this building (covering ca. 190 m²) differs substantially from that of the Houses 44 (77.5 m²) and 59 (42 m²). Both dwellings are characterized by massive platforms and indications of two 'storeys' (Fig. 58). Partly standardised arrangements of ovens, fireplaces (so-called altars), podiums, storage bins and workplaces appear often, but not always, to be concentrated on top of the elevated platform (Chernovol 2012; Chernovol 2019). Thus, we consider this upper level as main living floor while the lower one might represent subordinate space, for storage purposes, craft activities or for stabling animals. In contrast, Mega-structure 3 represents a one-storey construction, where all activities took place on one level.

Residential buildings are in most cases completely roofed and have a correspondingly stronger magnetisation in contrast to the mega-structures with their partially or completely open floor plans. Due to the different design, much smaller amounts of daub were used for the construction of a mega-structure (House 44: $1-100 \text{ kg/m}^2$ to Mega-structure 3: $<1-50 \text{ kg/m}^2$; Pickartz *et al.* 2019).

The remains of the internal architecture also differ. While in Megastructure 3 only a fireplace is documented, in each dwelling both a fireplace and an oven are present. The absence of ovens suggests that mega-structures were possibly not or not permanently inhabited. Additionally, within the dwellings a podium and a bin were documented, which were missing in the mega-structure. While the division of the mega-structure into two parts could be seen as a reflection of the division of dwellings into two rooms, the aspect of roofing indicates clear differences: an open activity space which is much larger in size cannot be compared to a roofed and much smaller anteroom of a dwelling.

The inventory of the examined Mega-structure 3 show (contrary to earlier findings in Hofmann *et al.* 2019, Tab. 4) less clear differences compared to the fully investigated Houses 44 and 54. Renewed quantitative analyses reveal that the

Table 34. Maidanetske, list of mega-structures and information regarding the floor area, dimensions, extent of roofing, interior division, furnishing, and position in the settlement.

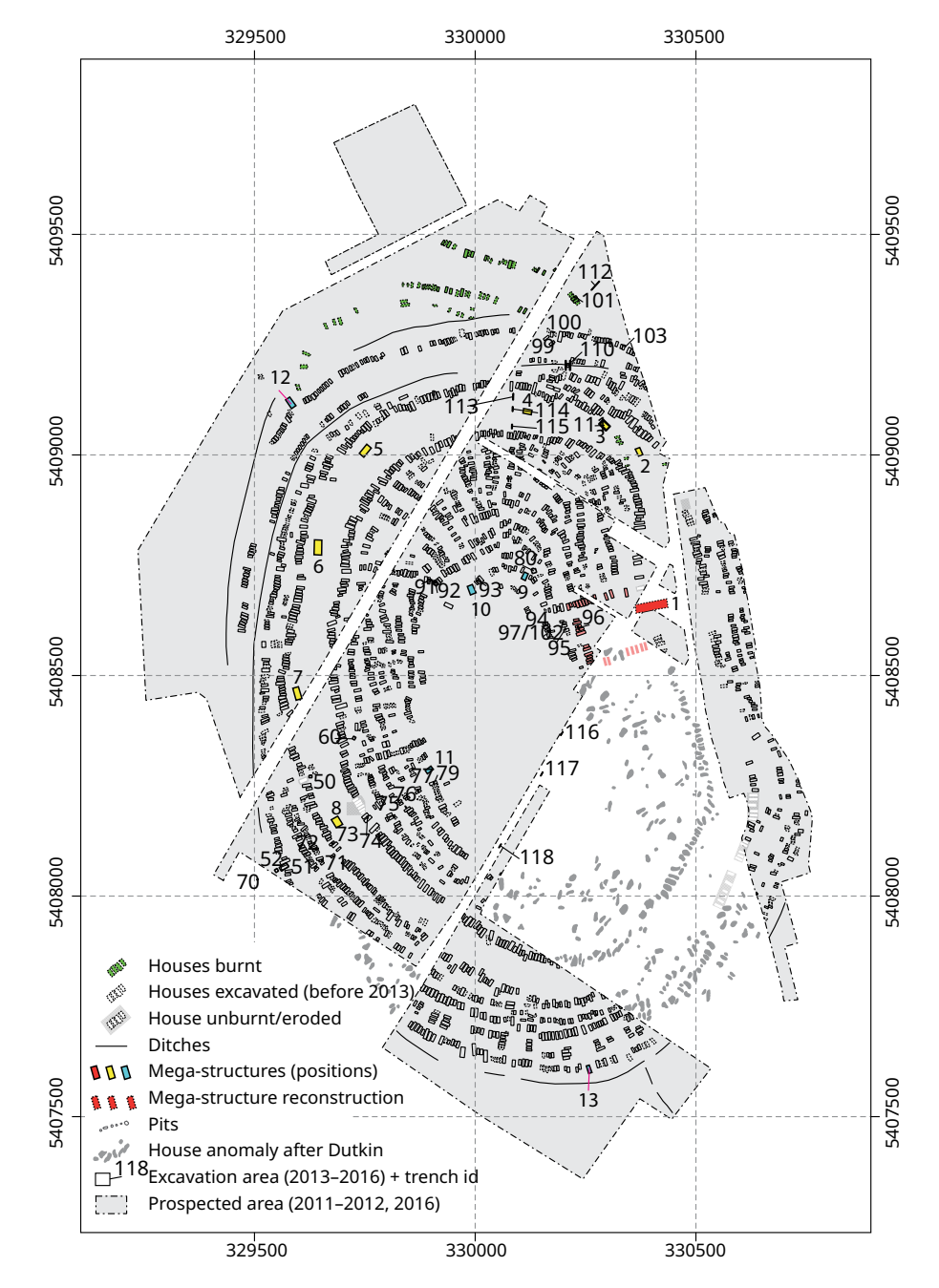


Figure 56. Maidanetske, redrawing of the plan of the archaeomagnetic survey with positions of mega-structures (after Hofmann et al. 2019); green buildings: dwellings of settlement Maidanetske 1a; white buildings: dwellings of settlement Maidanetske 1b; light red buildings: adjacent dwellings of the primary plaza; red buildings: mega-structures at the primary plaza; yellow buildings: mega-structures in the ring-corridor; blue buildings: mega-structures at different positions of radial pathways.

density of pottery and the frequency of vessel categories is remarkably consistent between these three contexts (Tab. 35). The frequency of grinding stones is also very similar, although it is generally difficult to distinguish between specimens that were still in use at the time of the abandonment of a house or mega-structure and those that were used secondarily, *e.g.* as building material. Comparing the inventory of the mega-structure and residential houses, some possible differences concern, among other things, artefacts related to the textile production. While such finds in Mega-structure 3 are represented by at least ten objects, they are very rare in both compared dwellings. Certain differences become also apparent when comparing assemblages of charred botanical macro-remains (Chapter 7, this work, Vol. I). Indeed, the proportions of cereal grains and cereal by-products in houses and Mega-structure 3 are very similar. However, the find concentration of charred botanical macro-remains in houses is somewhat higher than in Mega-structure 3.

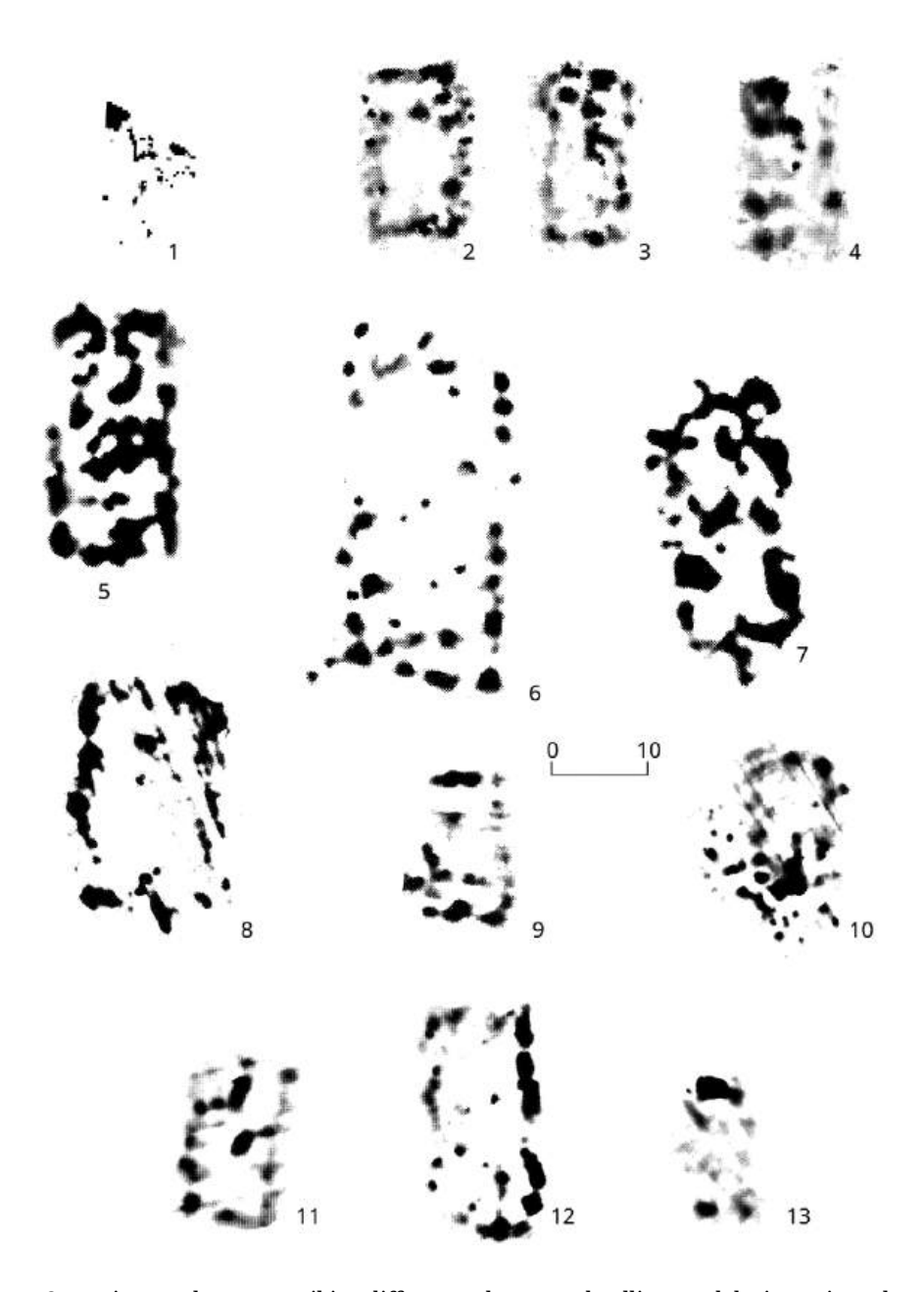


Figure 57. Maidanetske, archaeomagnetic anomalies of Mega-structures 1–13.

Summing up, there are striking differences between dwellings and the investigated Mega-structure concerning architectural design, internal organisation, and to a lesser extent also the kind and intensity of performed activities. Shared aspects of dwellings and mega-structures concern numerous 'domestic' activities which were identified in both types of buildings such as storage, preparation and consumption of food, the milling of grain, the craft production and specific ritual activities, represented by vessel assemblages, animal bones, botanical macro-remains, querns, artefacts for textile production, and anthropomorphic figurines. The absence of ovens suggests that mega-structures were possibly not or not permanently inhabited.

Important for our interpretation of mega-structures is the comparison with integrative buildings in 28 ethnographically documented societies from North America, South America, New Guinea/Oceania, and Africa. In ethnographic situations, a poly-functional character and a frequent use for both ritual and non-ritual activities have consistently been observed (Adler 1989; Adler and Wilshusen 1990). This use can include various aspects such as information sharing, joint decision-making, administrative purposes, body cleansing, stockpiling, or the

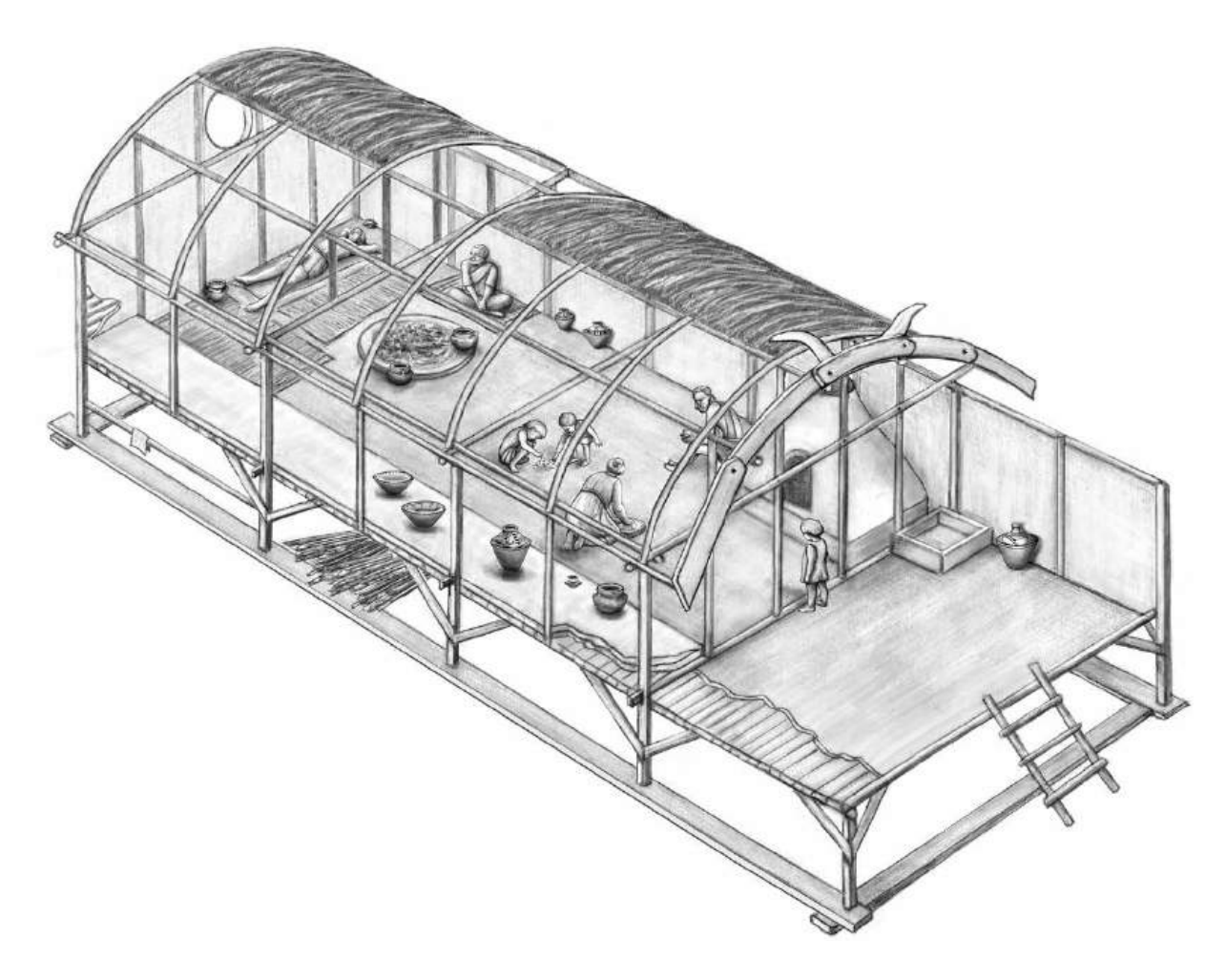


Figure 58. Maidanetske, graphical reconstruction of a Trypillia dwelling based on excavation results from House 44 (cf. Müller et al. 2017), with a raised platform, an anteroom, a main room and numerous details of the inventory and interior (graphic: Susanne Beyer, Kiel).

redistribution of goods. Consequently, performing day-to-day 'domestic' activities in integrative facilities is the normal state rather than the exception.

Thus, we do not consider the various domestic activities which have been proven for the excavated examples from Maidanetske and Nebelivka (Chapman et al. 2014a; Nebbia et al. 2018; Gaydarska 2020) as a reason to question the expected public functions. In contrast, in our opinion, the described wide range of activities associated with Trypillia mega-structures completely prevents the interpretation of these constructions as specialized production or central storage facilities, but rather indicates their communal nature as a place for integrative action. Such integrative actions could include feasting during which certain rituals of consumption were performed to share surplus, to acquire prestige and social power, or to maintain existing inequalities (Dietler 1996; Hofmann et al. 2024). In another context in Maidanetske feasting activities have already been proven connected with the deposition of two cattle skulls and numerous bowls at the bottom of a pit (Müller et al. 2017). Generally, in Trypillia mega-sites we can assume an increased importance of ritual and ceremonial activities that provide a frequently observed mechanism for reducing scalar stress in large human groups (Johnson 1983).

A longer-term perspective on the development and use of mega-structures presented elsewhere could show that these multi-functional buildings probably functioned as institutions in sequential political decision-making processes (Hofmann *et al.* 2019). Indicating a widely distributed participation in political processes and in the collective consumption of surpluses, they probably had a paramount role in the social constitution of Trypillia communities and in the maintenance of social balance (Müller *et al.* 2022; Hofmann *et al.* 2024).

Find category	Interpretation	House 44 (Trench 51)	House 54 (Trench 92)	Mega- structure 3 (Trench 111)
Flint artefacts	Flint production	3 flakes	1 blade	3 debris 1 flake
Anthropomorphic figurines (fragments)	Ritual activities?	3	2	3
Ceramic disk (fragment)	?			1
Spindle whorl		1		1
Loom weight (complete)	Textile production			2
Loom weight (fragment)				8
Whetstone				1
Pounder		1	1	
Rubbing stone				1
Polishing/punching stone			1	
Grinding stone: handstone		2		
Grinding stone: quern, lower	Cereal processing? Construction?	3		1
Grinding stone fragments		6	5	5–6
Quarry stone	Construction?	1	4	21
Stone slab	Construction?		1	1
Amount of pottery*		45.1 kg	60.1 kg	39.0 kg
Pottery density (overall)*	Food handling	0.98 kg/m ³	2.10 kg/m ³	1.83 kg/m³
Pottery density (range)		0->5 kg/m²	0-4.8 kg/m ³	0-4 kg/ m ³
Frequency of bowls: MNI (proportion)	Transport (serving)	20 (26%)	22 (23%)	10 (24%)
Frequency of cups: MNI (proportion)	1 , 3,	20 (26%)	9 (9%)	4 (9.5%)
Frequency of closed and half-closed vessels (except of cups/goblets): MNI (proportion)	Transport (serving) or storage	29 (38%)	60 (62%)	23 (55%)
Frequency of kitchenware vessels: MNI (proportion)	Processing (without heat)	7 (9%)	6 (6%)	4 (9.5%)

(c) On the question of the function of the ditch

With regard to the function of the causewayed enclosure examined in Trench 110, we would like to highlight two aspects in particular:

As is shown by a compilation of the dimensions of ditches during different Trypillia periods, ditches of the Trypillia B2 and C1 periods are characterised by rather small widths and depths (cf. Chapter 17, this work, Vol. II). In accordance with the results of the investigations in Nebelivka (Hale 2020, 127–128), a defensive function for the ditch in Maidanetske is rather unlikely, due to its dimensions and its interruptions. In this respect, alternative interpretations of the ditches of Trypillia mega-sites as perimeter ditches for the symbolic demarcation of 'inside' and 'outside' (Hale 2020, 127–128) or as 'planning devices to mark the settlement area to be built on' (Ohlrau 2020a, 282) seem extremely plausible. The latter interpretation is substantiated by, among other factors, the dating of the ditches in Maidanetske to the early phase of the settlement.

The evidence of causewayed enclosures in Maidanetske and Nebelivka, which are elsewhere distributed mainly in western and central Europe (Fig. 59), highlights the integration of the mega-sites into a very far-reaching communication and exchange network, possibly associated with certain ritual connotations and practices (Klassen 2014). Accordingly, in the process of filling the ditches, certain

Table 35. Maidanetske, comparison of inventories of Mega-structure 3 and Houses 44 and 56. *The ceramic masses and densities refer to both the narrower area of the building and the adjacent waste disposal areas.

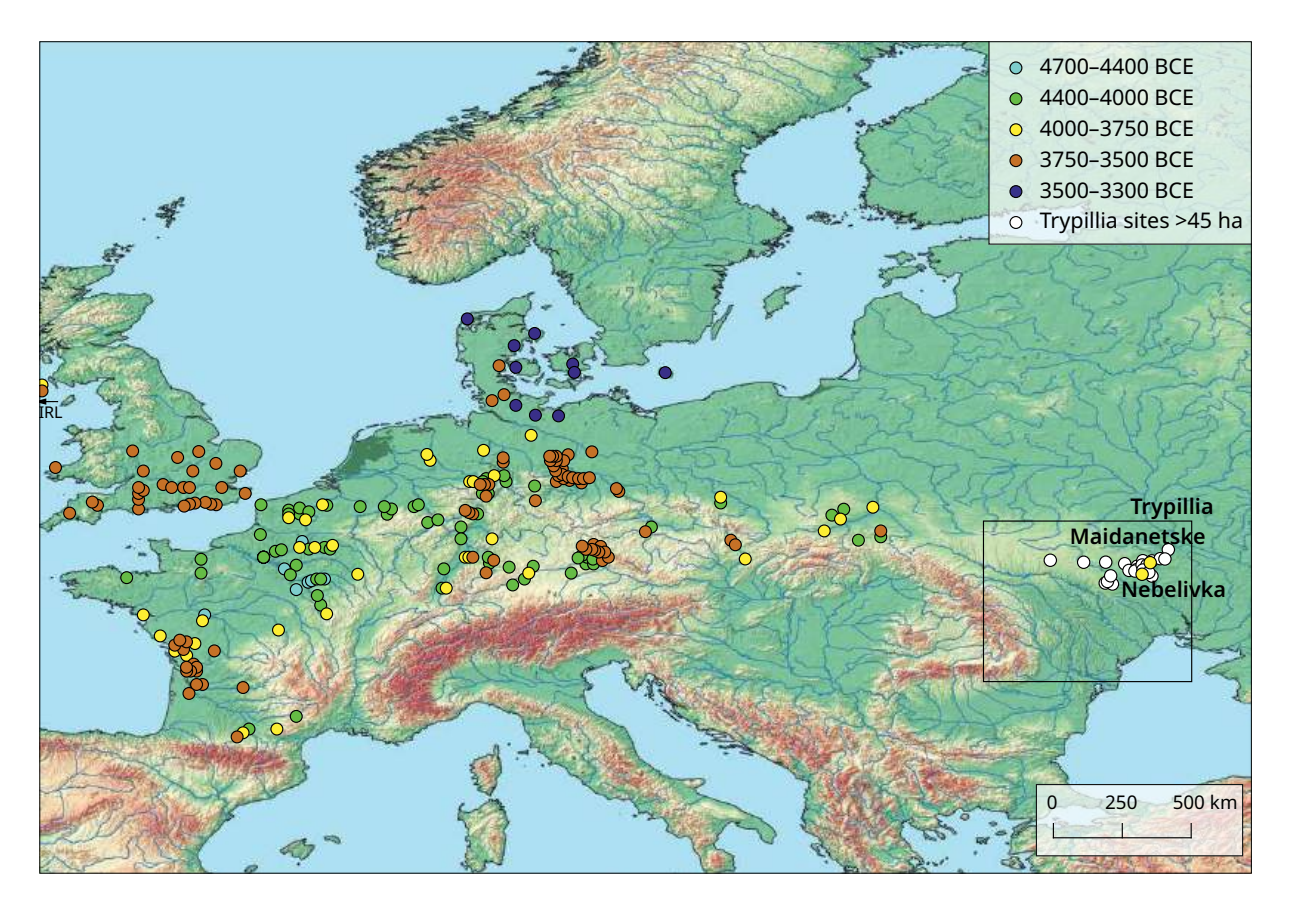


Figure 59. Spatial distribution of so-called causewayed enclosures of the Neolithic and Chalcolithic, often composed of several rows of parallel ditch segments, spread in a longer process from the area of present-day France to the forest-steppe zone of present-day Ukraine and often marking strategic points in an extensive communication and exchange network (extended after Klassen 2014, 214–238, with additions).

ritual activities associated with the deposition of *bucrania* and ceramic vessels also took place in Maidanetske (Ohlrau 2020a, 282).

Internal development of the mega-site of Maidanetske

Regarding the different spatial concepts of the settlements Maidanetske 1a and 1b, our investigations have yielded a stratigraphic sequence of settlement Maidanetske 1a and the Mega-structure 3, probably belonging to settlement Maidanetske 1b. This sequence confirms in principle the sequence that would be assumed from the archaeomagnetic prospection plan based on the fragmentary character of the settlement 1a. The stratigraphic sequence found indicates that the plan of Maidanetske 1a represents the original concept of the settlement, which was modified in the course of the occupation in favour of the new layout of Maidanetske 1b. Our analysis shows that the different concepts possibly only concern the northern part of the site, while the planning in the south seems to be consistent.

Regarding the chronological dimension of the two settlements, it should be emphasised that the remains of settlement Maidanetske 1a found in Trench 111 below the mega-structure certainly do not date only to the beginning of settlement in Maidanetske, but were still in use during Phase 3 in the 38th century. Only shortly afterwards, Mega-structure 3 was built and probably abandoned still in the course of the 38th century BCE. In principle, sample Poz-87542 from House 64 in Trench 101, which also belongs to the Maidanetske 1a plan, dates to the same period (Chapter 19, this work, Vol. II). Unfortunately, only one sample from a hazelnut shell could be dated from this trench, which indicates a considerably longer period of use of this house between roughly 3900 and 3700 BCE (Ohlrau 2020a, 22).

According to our dating, the two different spatial concepts of Maidanetske 1a and 1b thus apparently coexisted for a longer time-span. On the question of this coexistence,

René Ohlrau (2020a, 228) had assumed that perhaps not all residents felt committed to Plan 1b and maintained a competing structure. This indicates an inhomogeneous population of the settlement, as is also assumed on the basis of population growth rates (Ohlrau 2020b) and supports our conclusion regarding the fusion of different local units which attempted to maintain their local organisational structure.

When interpreting this, we must take into account the results obtained by Liudmyla Shatilo (2021, 211–216) for Talianki on intra-site micro-chronology, according to which temporal sequences of houses in Trypillia mega-sites are most likely to be located within house clusters. If we date only one house of a house cluster, we obtain a result that does not represent the entire duration of the house cluster but only a part of its real lifespan.

Under the premise of having recorded particularly late houses of Plan 1a beneath the mega-structure, it is entirely plausible, according to this model, not to assume a simultaneity of the two settlement plans, despite similar ¹⁴C dating. Instead, we could assume an overall earlier age of settlement Maidanetske 1a. While the new layout concept of Maidanetske 1b had already been actively implemented, residents of individual house clusters in the settlement 1a may have continued to follow the original spatial concept for a longer period.

As René Ohlrau (2020a, 212–214) was able to show, the western trench segment of the inner causeway enclosure was already backfilled between 3955 and 3810 BCE (68.2% probability), while the backfilling of the eastern trench segment took much longer. Consequently, we can assume a temporal overlap and possible competition between the two concepts, long before the final abandonment of Maidanetske 1a.

Conclusions

While the Ukrainian-German field excavations of 2013 and 2014 focused primarily on the study of individual households and the chronological and demographic reconstruction of the mega-site Maidanetske, the 2016 field campaign explored different aspects of the intra-site development, the use of space, and characteristics of facilities belonging to the communal infrastructure. Although questions remain, *e.g.* regarding the architecture of the central mega-structure in the east of the settlement, our investigations contribute decisively to the understanding of the social organisation and the changing history of a Trypillia mega-site.

Investigations within the ring corridor and the central unbuilt area of the settlement confirm the long-supposed intensive use of these parts of the settlement. Very important in several respects is the finding that the investigated ditch represents a causewayed enclosure. Accordingly, ditches did not have a primarily fortificatory significance, but rather served other purposes such as the demarcation of the settlement area or as an instrument of settlement planning. Moreover, the specific structure of the ditch indicates the integration of the Maidanetske settlement into an extensive communication network directed towards Western and Central Europe.

The identification and temporal fixation of two competing concepts of settlement planning constitutes an important argument for the hypothesis, that the formation of Trypillia mega-sites was based on the fusion of previously independent communities. In the public space distributed mega-structures perhaps represent focal points of these communities and probably integrative institutions within a decentrally organised

socio-political constitution of mega-sites. The excavation of such a mega-structure demonstrated that these buildings were significantly different from dwellings in architectural terms. The find inventory indicates that a variety of ritual and non-ritual domestic activities were carried out in these buildings, pointing to their multifunctional integrative character in decision-making processes and in the consumption of surplus. Evidence for the existence of a central mega-structure suggests that, similar to ethnographically studied societies, a hierarchical system of high-level integrative buildings for the whole community and different low-level integrative architectures for certain segments of local communities existed in Maidanetske.

Acknowledgements

We would like to express our sincere thanks to the participants in the excavation campaign in Maidanetske from Ukraine, Poland and Germany, without whose dedicated work the field campaign would not have been possible. Many thanks are due to Vladislav Chabanyuk and his team from the State Historical and Cultural Reserve 'Trypillia Culture' Lehedzyne, Cherkasy Oblast, for their manifold support during the fieldwork and the processing of the finds. We would also like to thank the photographer Sara Jagiolla, Kiel, for taking the find photos, and the graphic designer Susanne Beyer, both Kiel, for the wonderful find drawings and graphic reconstructions of the studied architecture. The work was funded by the Deutsche Forschungsgemeinschaft (DFG, German Research Foundation)—Project-ID 290391021—Sonderforschungsbereich 1266.

Supplementary materials

All primary data in this chapter are freely available online under a CC BY 4.0 licence, in the Kiel University research data repository opendata@uni-kiel.de: https://doi.org/10.57892/100-317.

Appendix

Description and contextualisation of the finds in figures.

Figure	Find-ID	Ceramic-ID	Ceramic- Unit-ID	Fabric	Number (n)	Weight (g)	Feature-ID	Level	Quadrat
20: 1	1110213	15437	520	Table: fine white	1	26	111002	2	H20
20: 1	1110581	15438	520	Table: fine white	1	25	111003	3	H20
20: 2	1110532	15282		Table: medium reddish	1	36	111003	3	L14
20: 3	1110927	15439		Table: medium reddish	1	59	111004	3	M10
20: 4	1110839	15355		Table: medium reddish	6	463	111018	3	J22
20: 5	1110729	15359	508	Table: fine white	1	100	111003	3	F14
20: 5	1111577	15360	508	Table: fine white	1	141	111003	Profile	J11
20: 5	1111417	15361	508	Table: fine white	2	84	111029	4d	K5
20: 6	1111597	15320		Table: fine white	2	63	111018	4a	H23
20: 7	1110873	15159	86	Table: fine white	1	80	111003	3	J5
20:7	1110008	15160	86	Table: medium white	1	8	111002	2	К9
20: 8	1111577	16712		Table: medium reddish	1	14	111003	Profile	J11
20: 9	1110043	15156		Table: undifferentiated	1	40	111002	2	L10
20: 10	1110202	15379		Table: fine white	1	26	111002	2	G6
20: 11	1110405	15433	518	Table: medium reddish	1	23	111002	2	L21
20: 11	1110610	15432	518	Table: medium reddish	1	53	111003	3	
20: 12	1110531	15371		Table: medium reddish	2	133	111003	3	L11
20: 13	1110561	16771		Table: fine white			111003	3	H5
20: 14	1110903	16110		Table: fine white	1	8	111020	3	N20
20: 15	1110927	15852	532	Table: medium reddish	5	67	111004	3	M10
20: 15	1110975	15458	532	Table: fine white	3	63	111012	3	M5
20: 16	1110584	16402		Table: medium white	1	25	111003	3	F16
20: 17	1110957	15428		Table: medium reddish	1	89	111004	3	M8
21: 1	1110049?						111002	2	M12
21: 2	1110555	16507		Table: medium reddish	1	15	111003	3	L9
21:3	1110940	15388		Table: medium reddish	1	76	111018	3	M22
21: 4	1110395	15397		Table: medium reddish	2	40	111002	2	L19
21: 4	1111161	15398		Table: medium reddish	2	47	111025	4	L19
21:5	1110781	15829		Table: medium reddish	12	846	111018	3	G22

Figure	Find-ID	Ceramic-ID	Ceramic- Unit-ID	Fabric	Number (n)	Weight (g)	Feature-ID	Level	Quadrat
21:6	1110781	15819	530	Table: medium reddish	14	490	111018	3	G22
21:6	1110782	15805	530	Table: medium reddish	70	2344	111018	3	G22
21: 6	1111597	15487	530	Table: medium reddish	8	230	111018	4a	H23
21: 7	1110297	16410		Table: low secondary fired	1	12	111002	2	08
21: 8	1110782	15791		Table: medium reddish	18	429	111018	3	G22
21: 8	1110781	15823		Table: medium reddish	1	23	111018	3	G22
21: 9	1110869	15369	509	Table: medium reddish	1	71	111002	2	M12
21: 9	1110052	15368	509	Table: medium reddish	1	47	111009	3	M11
21: 10	1110781	15829		Table: medium reddish	12	846	111018	3	G22
22: 1	1110613	15759		Table: fine white	12	1213	111003	3	M-024-25
22: 2	1110781	15819	530	Table: medium reddish	14	490	111018	3	G22
22: 2	1110782	15805	530	Table: medium reddish	70	2344	111018	3	G22
22: 2	1111597	15487	530	Table: medium reddish	8	230	111018	4a	H22
23: 1	1110353	15380	511	Table: medium reddish	1	126	111002	2	M17
23: 1	1110354	15382	511	Indefinite: uncleaned	1	55	111029	4b	L5
23: 2	1110395	15612		Table: medium reddish	1	2	111002	2	L19
23: 3	1110921	15892		Indefinite: reduced	1	18	111020	3	H10
23: 4	1110725	16433		Kitchen: strongly secondary fired	1	43	111017	3	F18
23: 5	1110966	16079		Kitchen: coarse, orange	1	16	111020	3	J21
23: 6	1110966	15456		Kitchen: coarse, grey brown	9	71	111020	3	J21
23: 7	1110110	16325		Kitchen: coarse, grey brown	1	68	111002	2	I10
24: 1	1110274			Whetstone	1	220	111002	2	Ј7
24: 2	1110611			Ceramic disk	1	40	111003	3	J21
24: 3	1111572			Loom weight	1	120	111003	3	J21
24: 4	1110331			Spindle whorl	1	11	111002	2	F6
24: 5	1110576			Loom weight	1	63	111003	3	G21
24: 6	1119995	15166		Table: fine white	1	194	Surface find		
24: 7	1119994	15167		Table: medium red	1	164	Surface find		
41: 1	1110896	15903	548	Kitchen: coarse, grey brown	8	1260	111025	3	K20
41: 2	1111083	16035		Kitchen: coarse, grey brown	29	1642	111025	4	L16-17

Figure	Find-ID	Ceramic-ID	Ceramic- Unit-ID	Fabric	Number (n)	Weight (g)	Feature-ID	Level	Quadrat
41: 3	1111089	15179	91	Kitchen: coarse, orange	15	358	111025	4	Н8
42: 1	1111253	15384		Table: medium reddish	1	50	111025	4	L7
42: 2	1111139	15377		Table: undifferentiated	2	217	111025	4	L7
42: 3	1111139	15378		Table: medium reddish	1	47	111025	4	L7
42: 4	1111085	15161		Table: fine white	19	616	111024	4	L5
42: 5	1111098	15174	89	Table: medium red	4	356	111025	4	G8
42: 6	1111216	15683		Kitchen: coarse, grey brown	1	37	111025	4	L10
42: 7	1111309	16188		Table: medium white	1	43	111025	4a	L5
42: 8	1111395	16469		Table: fine white	1	16	111024	4b	F7
42: 9	1111232	16372		Table: medium reddish	1	21	111024	4	J5
42: 10	1111230			Not Trypillia?			111024	4	K5
42: 11	1111230			Not Trypillia?			111024	4	K5
43: 1	1111277	15318		Table: fine reddish	1	42	111024	4c	K5
43: 2	1111361	16067		Table: medium reddish	1	56	111024	4a	E7
43: 3	1111309	15317		Table: medium reddish	1	42	111025	4a	L5
43: 4	1111237	19023		No entry			111023	4b	K9
43: 4	1111550	19024		No entry			111029	Profile	J6
43: 5	1111257	15250		Table: medium reddish	1	48	111024	4	K5
43: 6	1111257	15294		Table: fine white	1	20	111024	4	K5
43: 7	1111563	16111		Table: fine reddish	1	17	111025	Profile	J10-14
43: 8	1111091	15363		Table: medium reddish	9	445	111025	4	G8
43: 9	1111284	15362		Table: fine white	8	300	111024	4	N12
43: 10	1111230	15164		Table: fine white	1	120	111024	4	K5
43: 11	1111049	15434		Table: undifferentiated	1	40	111025	4	M18
43: 12	1111253	15372		Table: fine reddish	3	89	111024	4c	L7
43: 13	1111230	15385		Table: medium reddish	1	77	111024	4	K5
43: 13	1111253	15384		Table: medium reddish	2	100	111025	4c	L7
46: 1	1111299	15356	507	Table: medium reddish	2	258	111026	4e	K10
46: 1	1111422	15357	507	Table: medium reddish	1	200	111033	4b	E-F8-9
46: 2	1111421	15181	92	Table: medium white	13	1500	111026	4h	J-K10
46: 2	1111513	15185	92	Table: medium white	3	100	111026	?	J10
46: 2	1111519	15183	92	Table: medium white	1	140	111033	Profile	E8
46: 3	1111422	15162		Table: medium red	9	217	111033	4b	E-F8-9

Figure	Find-ID	Ceramic-ID	Ceramic- Unit-ID	Fabric	Number (n)	Weight (g)	Feature-ID	Level	Quadrat
46: 4	1111519	15323		Table: fine reddish	2	135	111033	Profile	E8
46: 5	1111519	15165		Table: medium white	6	458	111033	Profile	E8
46: 6	1111395	15344	506	Table: fine white	7	193	111024	4b	F7
46: 6	1111519	15345	506	Table: fine white	1	21	111033	Profile	E8
47: 1	1111422	15168	87	Table: medium red	1	100	111033	4b	E-F8-9
47: 1	1111519	15169	87	Table: medium red	1	48	111033	Profile	E8
47: 2	1111541	16228		Table: fine white	1	9	111032	Profile	E6
47: 3	1111519	15187	93	Table: medium red	1	60	111033	Profile	E8
47: 3	1111541	15186	93	Table: medium red	5	200	111032	Profile	E6
47: 3	1110566	15188	93	Table: medium red	1	32	111003	3	G7
47: 4	1111422	16339		Table: medium reddish	1	56	111033	4b	E-F8-9
47: 5	1111422	15394		Table: medium reddish	2	138	111033	4b	E-F8-9
47: 6	1111422	16336		Table: medium reddish	1	71	111033	4b	E-F8-9
47: 7	1111519	15386		Table: fine white	1	57	111033	Profile	E8
47: 8	1111422	15176	90	Table: medium white	9	382	111033	4b	E-F8-9
47: 8	1110566	15177	90	Table: medium white	1	10	111003	3	G7
47: 8	1111519	15178	90	Table: medium white	1	16	111033	Profile	E8
47: 9	1111541	16317	545	Table: medium reddish	11	400	111032	Profile	E6
47: 9	1111542	16318	545	Table: medium reddish	3	40	111033	Profile	E6
47: 9	1111519	16319	545	Table: medium reddish	1	6	111033	Profile	E8
48: 1	1111422	15198	96	Table: fine white	15	1000	111033	4b	E-F8-9
48: 1	1111519	15199	96	Table: fine white	12	680	111033	Profile	E8
48: 2	1111518	15189	94	Table: fine red	8	340	111033	Profile	E8
48: 2	1111519	15191	94	Table: fine red	9	390	111033	Profile	E8
48: 2	1111422	15190	94	Table: fine red	2	150	111033	4b	E-F8-9
48: 3	1111541	15375	510	Table: fine reddish	4	148	111032	Profile	E6
48: 3	1111543	15376	510	Table: fine reddish	1	50	111033	Profile	E6
49: 1	1111361	15196	95	Table: medium red	2	250	111024	4a	E7
49: 1	1111395	15197	95	Table: medium red	2	250	111024	4b	F7
49: 1	1111422	15193	95	Table: medium red	3	338	111033	4b	E-F8-9
49: 1	1111519	15192	95	Table: medium red	9	1000	111033	Profile	E8
49: 1	1111541	15194	95	Table: medium red	2	200	111032	Profile	E6
49: 1	1111542	15195	95	Table: medium red	5	300	111033	Profile	E6
49: 2	1111422	16049		Table: medium reddish	3	56	111033	4b	E-F8-9
49: 3	1111422	15881	535	Kitchen: coarse, grey brown	27	719	111033	4b	E-F8-9

Figure	Find-ID	Ceramic-1D	Ceramic- Unit-ID	Fabric	Number (n)	Weight (g)	Feature-ID	Level	Quadrat
49: 4	1111419	15242	98	Table: fine white	1	66	111029	4b	K6-7
49: 4	1111541	15249	98	Table: fine white	1	44	111032	Profile	E6
49: 5	1111419	15396		Table: medium reddish	1	57	111029	4b	K6-7
49: 6	1111139	15172	88	Table: medium red	1	10	111025	4	L7
49: 6	1111267	15173	88	Table: medium red	1	10	111025	4	I7
49: 6	1111351	15170	88	Table: medium red	2	100	111029	4b	L5
49: 6	1111505	15171	88	Table: medium red	1	14	111029	Profile	K-5-6
49: 7	1111350	15157		Table: medium white	2	248	111029	4b	L5
51: 1	1111359	15335	503	Table: medium reddish	1	40	111029	4d	K6
51: 1	1111421	15337	503	Table: medium reddish	1	26	111026	4h	J-K10
51: 2	1111418	15326	99	Table: fine white	1	50	111029	4c	K6-7
51: 2	1111489	15324	99	Table: fine white	2	79	111029	Profile	K7
51: 2	1111553	15327	99	Table: fine white	1	50	111029	Profile	K6
51:3	1111553	15163		Table: medium reddish	2	175	111029	Profile	K6
51: 4	1111418	15232	97	Table: fine reddish	1	40	111029	4c	K6-7
51: 4	1111505	15233	97	Table: fine reddish	1	42	111029	Profile	K5-6
51: 5	1111505	15743		Table: medium reddish	1	90	111029	Profile	K5-6
51: 6, 8	1111309	15436	519	Table: fine white	1	10	111025	4a	L5
51: 6, 8	1111505	15435	519	Table: fine white	1	110	111029	Profile	K5-6
51: 7	1111505	15743		Table: medium reddish	1	90	111029	Profile	K5-6
51: 9	1111253	15422	516	Table: fine white	3	133	111025	4c	L7
51: 9	1111274	15407	516	Table: medium reddish	2	20	111025	4c	L7
51: 9	1111312	15408	516	Table: medium reddish	1	10	111029	4c	J5
51: 9	1111362	15406	516	Table: fine white	1	17	111029	4b	L5
51: 10	1111505	15431		Table: fine reddish	1	70	111029	Profile	K5-6
51: 11	1111230	15613	522	Table: medium reddish	1	42	111024	4	K5
51: 11	1111282	15444	522	Table: fine reddish	1	20	111024	4c	K5
51: 11	1111474	15443	522	Table: fine reddish	7	380	111029	Profile	J5
51: 11	1111552	15445	522	Table: fine reddish	3	200	111029	Profile	J6
52: 1	1111282	15882		Table: medium reddish	1	516	111024	4c	K5
52: 1	1111474	15786		Table: medium reddish	1	50	111029	Profile	J5
52: 2	1111372	15893		Kitchen: coarse, grey brown	47	1485	111029	4d	K6
52: 3	1111554			Flint	1	6	111029	Profile	K6

References

- Adler, M.A., 1989. Ritual Facilities and Social integration in Nonranked Societies. *In*: W.D. Lipe and M. Hegmon, eds. *The Architecture of Social Integration in Prehistoric Pueblos*. Occasional Papers of the Crow Canyon Archaeological Center 1. Cortez/Colorado: Crow Canyon Archaeological Center, 35–52.
- Adler, M.A. and Wilshusen, R.H., 1990. Large-scale integrative facilities in tribal societies: cross-cultural and southwestern US examples. *World Archaeology*, 22 (2), 133–146. Available from: https://doi.org/10.1080/00438243.1990.9980136
- Anderson, P.C. and M'hamdi, M., 2014. Harvesting of the Wild Grass Alfa (*Stipa tenacissima* L.) by Pulling in the High Tunisian Steppe: an Unusual Method. *In:* A. van Gijn, J.C. Whittaker and P.C. Anderson, eds. *Exploring and Explaining Diversity in Agricultural Technology.* Early Agricultural Remnants and Technical Heritage (EARTH): 8,000 Years of Resilience and Innovation 2. Oxford, Havertown/Pennsylvania: Oxbow Books, 98–132.
- Brandtstätter, L., 2017. *Tripolje-Keramik aus Maidanteske (Ukraine): Auswertung der Grabungskampagne 2013*. [Unpublished Master thesis. Institute of Prehistoric and Protohistoric Archaeology, Kiel University, Germany].
- Bronk Ramsey, C., 2009. Bayesian Analysis of Radiocarbon Dates. *Radiocarbon*, 51 (1), 337–360. Available from: https://doi.org/10.1017/S0033822200033865
- Caswell, E., Arbeiter, S., Ovchinnikov, E., Gaydarska, B., Nebbia, M. and Chapman, J., 2020. Pottery. *In:* B. Gaydarska, ed. *Early Urbanism in Europe. The Trypillia Megasites of the Ukrainian Forest-Steppe*. Warsaw, Berlin: De Gruyter, 266–326. Available from: https://doi.org/10.1515/9783110664959-009
- Chapman, J., Videiko, M.Y., Gaydarska, B., Burdo, N. and Hale, D., 2014a. Architectural differentiation on a Trypillia mega-site: preliminary report on the excavation of a mega-structure at Nebelivka, Ukraine. *Journal of Neolithic Archaeology*, 16, 135–156. Available from: https://doi.org/10.12766/jna.2014.4
- Chapman, J., Videiko, M.Y., Hale, D., Gaydarska, B., Burdo, N., Rassmann, K., Mischka, C., Müller, J., Korvin-Piotrovskiy, A.G. and Kruts, V., 2014b. The Second Phase of the Trypillia Mega-Site Methodological Revolution: A New Research Agenda. *European Journal of Archaeology*, 17 (3), 369–406. Available from: https://doi.org/10.1179/1461957114Y.0000000062
- Chernovol, D., 2012. Houses of the Tomashovskaya Local Group. *In:* F. Menotti and A.G. Korvin-Piotrovskiy, eds. *The Tripolye Culture Giant-Settlements in Ukraine.* Formation, Development and Decline. Oxford, Oakville: Oxbow Books, 182–209. Available from: https://doi.org/10.2307/j.ctvh1dvmn.13
- Chernovol 2019: Черновол, Д., 2019. *Інтер'єр споруд Трипільскої култьури*. Автореферат дисертації на здобуття наукового ступеня кандидата історичних наук. [Summary of the unpublished PhD thesis. Національна академія наук України].
- Dal Corso, M., Hamer, W., Hofmann, R., Ohlrau, R., Shatilo, L., Knitter, D., Dreibrodt, S., Saggau, P., Duttmann, R., Feeser, I., Knapp, H., Benecke, N., Videiko, M., Müller, J. and Kirleis, W., 2019. Modelling landscape transformation at the Chalcolithic Tripolye mega-site of Maidanetske (Ukraine): Wood demand and availability. *The Holocene*, 29 (10), 1622–1636. Available from: https://doi.org/10.1177/0959683619857229
- Dannath, Y., Heske, I. and Kirleis, W., 2019. Ein weiter Blick in die Landschaft. Entdeckungen an einem Standort der Stichbandkeramik. *Archäologie in Niedersachsen*, 22, 50–54.
- Dietler, M., 1996. Feasts and commensal politics in the political economy. Food, Power and Status in Prehistoric Europe. *In:* P. Wiessner and W. Schiefenhövel, eds. *Food and the Status Quest: An Interdisciplinary Perspective*. Oxford: Berghahn Publishers, 87–125.

- Gaydarska, B., ed., 2020. *Early Urbanism in Europe. The Trypillia Megasites of the Ukrainian Forest-Steppe*. Warsaw, Berlin: De Gruyter. Available from: https://doi.org/10.1515/9783110664959
- Gaydarska, B., Nebbia, M., Chapman, J., Caswell, E., Arbeiter, S., Ovchinnikov, E., Gaskevych, D., Lazăr, C., Ignat, T., Boyce, A., Dolan, A., Newton, J., Kiosak, D., Belenko, M., Craig, O.E., Robson, H.K., von Tersch, M., Lucquin, A., Tóth, Z., Choyke, A., Orton, D., Nottingham, J., Rainsford-Betts, G., Hosking, K., Millard, A. and Pashkevych, G., 2020. The finds. *In*: B. Gaydarska, ed. *Early Urbanism in Europe. The Trypillia Megasites of the Ukrainian Forest-Steppe*. Warsaw, Berlin: De Gruyter, 265–414. Available from: https://doi.org/10.1515/9783110664959-009
- Hale, D., 2020. Geophysical Investigations and the Nebelivka Site Plan. *In:* B. Gaydarska, ed. *Early Urbanism in Europe. The Trypillia Megasites of the Ukrainian Forest-Steppe.* Warsaw, Berlin: De Gruyter, 122–148. Available from: https://doi.org/10.1515/9783110664959-008
- Hofmann, R., 2013. Okolište 2 Spätneolithische Keramik und Siedlungsentwicklung in Zentralbosnien, Neolithikum und Chalkolithikum in Zentralbosnien. Universitätsforschungen zur prähistorischen Archäologie 243 (Neolithikum und Chalkolithikum in Zentralbosnien 2). Bonn: Dr. Rudolf Habelt.
- Hofmann, R., Kujundžić-Vejzagić, Z., Müller, J., Müller-Scheeßel, N. and Rassmann, K., 2006. Prospektionen und Ausgrabungen in Okolište (Bosnien-Herzegowina): Siedlungsarchäologische Studien zum zentralbosnischen Spätneolithikum (5300-4500 v. Chr.). Bericht der Römisch-Germanischen Kommission, 87, 41–212.
- Hofmann, R., Shatilo, M., Ohlrau, R., Dal Corso, M., Dreibrodt, S., Videiko, M., Rassmann, K., Kirleis, W. and Müller, J., 2018. Tripolye Strategy and Results of an ongoing Ukrainian-European Project. *Vita Antiqua*, 10, 146–154. Available from: https://doi.org/10.37098/2519-4542-2018-1-10-146-154.
- Hofmann, R., Müller, J., Shatilo, L., Videiko, M., Ohlrau, R., Rud, V., Burdo, N., Dal Corso, M., Dreibrodt, S. and Kirleis, W., 2019. Governing Tripolye: Integrative architecture in Tripolye settlements. *PLoS ONE*, 14 (9), e0222243. Available from: https://doi.org/10.1371/journal.pone.0222243
- Hofmann, R., Müller, J., Kirleis, W., Terna, S., Rud, V., Terna, A., Dal Corso, M. and Schlütz, F., 2023. Database of the Kiel CRC 1266 sub-project D1 'Population Agglomerations at Trypillia-Cucuteni Mega-sites'. [Dataset, status as of 06.10.2023] https://doi.org/10.57892/100-317
- Hofmann, R., Müller-Scheeßel, N. and Müller, J., 2024. Trypillia mega-sites: a social levelling concept? *Antiquity*, 98 (398), 380–400. Available from: https://doi.org/10.15184/aqy.2024.18
- Johnson, G.A., 1983. Decision-Making Organization and Pastoral Nomad Camp Size. *Human Ecology*, 11, 175–199. Available from: https://doi.org/10.1007/BF00891742
- Klassen, L., 2014. *Along the Road. Aspects of Causewayed Enclosures in South Scandinavia and Beyond.* East Jutland Museum Publicatios. Aarhus: Aarhus University Press. Available from: https://doi.org/10.2307/jj.608320
- Körber-Grohne, U., 1987. Federgras-Grannen (Stipa Pennata L. s. str.) als Vorrat in einer mittelneolithischen Grube in Schöningen, Landkreis Helmstedt. *Archäologisches Korrespondenzblatt*, 17 (4), 463–466.
- Korvin-Piotrovskiy *et al.* 2016: Корвін-Піотровський, О.Г., Пічкур, Є.В., Чабанюк, В.В. and Шатіло, Л.О., 2016. Черкаська область. Роботи Трипільської експедиції. *Археологічні дослідження в Україні*, 2015, 201–203.
- Kruts et al. 2005: Круц, В.А., Корвин-Пиотровский, А.Г., Рыжов, С.Н., Бузян, Г.Н., Овчинников, Э.В., Черновол, Д.К. and Чабанюк, В.В., eds., 2005. Исследование поселений-гигантов трипольской культуры в 2002-2004 гг. Киев: Институт археологии НАН Украины.
- Müller, J. and Videiko, M., 2016. Maidanetske: New Facts of a Mega-Site *In*: J. Müller, K. Rassmann and M. Videiko, eds. *Trypillia Mega-Sites and European Prehisto-*

- ry 4100-3400 BCE. Themes in Contemporary Archaeology 2. London, New York: Routledge, 71–93. Available from: https://doi.org/10.4324/9781315630731
- Müller, J., Hofmann, R., Kirleis, W., Dreibrodt, S., Ohlrau, R., Brandtstätter, L., Dal Corso, M., Out, W., Rassmann, K., Burdo, N. and Videiko, M., eds., 2017. *Maidanetske 2013. New excavations at a Trypillia mega-site / Майданецьке 2013. Нові розкопки великого Трипільського поселення*. Studien zur Archäologie in Ostmitteleuropa 16. Bonn: Dr. Rudolf Habelt.
- Müller, J., Hofmann, R. and Shatilo, M., 2022. Tripolye Mega-Sites: "Collective Computational Abilities" of Prehistoric Proto-Urban Societies? *Journal of Social Computing*, 3 (1), 75–90. Available from: https://doi.org/10.23919/JSC.2021.0034
- Nebbia, M., Gaydarska, B., Millard, A. and Chapman, J., 2018. The making of chalcolithic assembly places: Trypillia megasites as materialized consensus among equal strangers? *World Archaeology*, 50 (1), 41–61. Available from: https://doi.org/10.1080/00438243.2018.1474133
- Ohlrau, R., 2015. Trypillia Großsiedlungen: Geomagnetische Prospektion und architektursoziologische Perspektiven. *Journal of Neolithic Archaeology*, 17, 17–100. Available from: https://doi.org/10.12766/jna.2015.3
- Ohlrau, R., 2020a. *Maidanets'ke: Development and decline of a Trypillia mega-site in Central Ukraine*. Scales of Transformation in Prehistoric and Archaic Societies 7. Leiden: Sidestone Press. Available from: https://doi.org/10.59641/h0912kt
- Ohlrau, R., 2020b. Modelling Trypillia 'mega-site' populations. *In*: M. Dębiec and T. Saile, eds. *A Planitiebus usque ad montes: Studia Archaeologica Andreae Pelisiak vitae anno sexagesimo quinto oblata*. Rzeszów: Zimowit, 399–413.
- Ovchynnykov 2014: Овчинников, Е.В., 2014. *Трипільська культура Канівського Подніпров'я*. Київ: Видавець Олег Філюк.
- Pickartz, N., Hofmann, R., Dreibrodt, S., Rassmann, K., Shatilo, L., Ohlrau, R., Wilken, D. and Rabbel, W., 2019. Deciphering archeological contexts from the magnetic map: Determination of daub distribution and mass of Chalcolithic house remains. *The Holocene*, 29 (10), 1637–1652. Available from: https://doi.org/10.1177/0959683619857238
- Pickartz, N., Rabbel, W., Rassmann, K., Hofmann, R., Ohlrau, R., Thorwart, M., Wilken, D., Wunderlich, T., Videiko, M. and Müller, J., 2022. Inverse Filtering of Magnetic Prospection Data—A Gateway to the Social Structure of Cucuteni–Tripolye Settlements? *Remote Sensing*, 14 (3), 484. Available from: https://doi.org/10.3390/rs14030484
- Rassamakin, Y., 2012. Absolute Chronology of Ukrainian Tripolian Settlements. *In:* F. Menotti and A.G. Korvin-Piotrovskiy, eds. *The Tripolye Culture giant-settlements in Ukraine: Formation, development and decline.* Oxford, Oakville: Oxbow Books, 19–69. Available from: https://doi.org/10.2307/j.ctvh1dvmn.7
- Rassmann, K., Ohlrau, R., Hofmann, R., Mischka, C., Burdo, N., Videjko, M.Y. and Müller, J., 2014. High precision Tripolye settlement plans, demographic estimations and settlement organization. *Journal of Neolithic Archaeology*, 16, 96–134. Available from: https://doi.org/10.12766/jna.2014.3
- Reimer, P.J., Austin, W.E.N., Bard, E., Bayliss, A., Blackwell, P.G., Bronk Ramsey, C., Butzin, M., Cheng, H., Edwards, R.L., Friedrich, M., Grootes, P.M., Guilderson, T.P., Hajdas, I., Heaton, T.J., Hogg, A.G., Hughen, K.A., Kromer, B., Manning, S.W.,

- Muscheler, R., Palmer, J.G., Pearson, C., van der Plicht, J., Reimer, R.W., Richards, D.A., Scott, E.M., Southon, J.R., Turney, C.S.M., Wacker, L., Adolphi, F., Büntgen, U., Capano, M., Fahrni, S.M., Fogtmann-Schulz, A., Friedrich, R., Köhler, P., Kudsk, S., Miyake, F., Olsen, J., Reinig, F., Sakamoto, M., Sookdeo, A. and Talamo, S., 2020. The IntCal20 Northern Hemisphere Radiocarbon Age Calibration Curve (0–55 cal kBP). *Radiocarbon*, 62 (4), 725–757. Available from: https://doi.org/10.1017/RDC.2020.41
- Rice, P.M., 1987. *Pottery Analysis. A Sourcebook*. Chicago, London: The University of Chicago Press.
- Rivera Núñez, D., Matilla Séiquer, G., Obón, C. and Alcaraz Ariza, F., 2012. *Plants and Humans in the Near East and the Caucasus: Ancient and Traditional Uses of Plants as Food and Medicine, a Diachronic Ethnobotanical Review*. Vol. 2: *The Plants: Angiosperms*. Murcia: Ediciones de la Universidad de Murcia.
- Ryzhov 1999: Рижов, С.М., 1999. *Кераміка Поселень Трипільської Культури Бу- со-Дніпровського Межиріччя Як Історичне Джерело*. [Unpublished PhD thesis. Національна Академія Наук України].
- Ryzhov, S.N., 2012. Tripolian Pottery of the Giant-settlements: Characteristics and Typology. *In:* F. Menotti and A.G. Korvin-Piotrovskiy, eds. *The Tripolye Culture giant-settlements in Ukraine: Formation, development and decline.* Oxford, Oakville: Oxbow Books, 139–168. Available from: https://doi.org/10.2307/j.ctvh1dvmn.11
- Shatilo, L., 2021. *Tripolye Typo-chronology: Mega and Smaller Sites in the Sinyukha River Basin.* Scales of Transformation in Prehistoric and Archaic Societies 12. Leiden: Sidestone Press. Available from: https://doi.org/10.59641/m5457py
- Shmaglij and Videiko 2005: Шмаглий, Н.М. and Видейко, Ю.М., 2005. *Майданец-кое-трипольский протогород*. Киев: Институт археологии НАН Украины.
- Sommer, U., 1991. Zur Entstehung archäologischer Fundvergesellschaftungen: Versuch einer archäologischen Taphonomie. *In:* Mattheusser, E., author. *Die geographische Ausrichtung bandkeramischer Häuser*. Studien zur Siedlungsarchäologie 1 (Universitätsforschungen zur prähistorischen Archäologie 6). Bonn: Dr. Rudolf Habelt, 51–193.
- Videiko 2020: Відейко, М.Ю., 2020. Дослідження пізньотрипільського поселенн я Вільховець. *Археологія і давня історія України*, 34, 68–79. Available from: https://doi.org/10.37445/adiu.2020.01.05
- Videiko et al. 2013: Видейко, М., Чапмен, Д., Гейдарская, Б., Бурдо, Н., Овчинни-ков, Э., Пашкевич, Г. and Шевченко, Н., 2013. Исследования мегаструктуры на поселении трипольской культуры у с. Небелевка в 2012 году. *Tyragetia, serie nouă*, 7 [22] (1), 97–124. Available from: https://ibn.idsi.md/sites/default/files/j_nr_file/Tyragetia_1_2013.pdf#page=98
- Wotzka, H.-P., 1997. Keramikformen und -funktionen: Wider die systematische Trivialisierung kulturspezifischer Zusammenhänge. *Archäologische Informationen*, 20 (2), 269–299.

3. Geophysical Investigations at Maidanetske

Natalie Pickartz, Tina Wunderlich, Erica Corradini, Knut Rassmann, Dennis Wilken, Wolfgang Rabbel

Abstract

In this chapter we report the results of electric resistivity tomography (ERT), electromagnetic induction (EMI) and ground-penetrating radar (GPR) measurements carried out at the site of Maidanetske in addition to previously conducted magnetic prospection. The aim of this field campaign, which was performed in September 2017, was to test the applicability of these methods on the remains of the burnt houses at Maidanetske. The tests showed that GPR cannot resolve these structures. Also, the apparent conductivity measured with EMI does not show any anomalies that are similar to those in the magnetic map. However, the In-phase component, which is sensitive to the magnetic susceptibility, shows the anomalies of the house remains. Moreover, the cross-section of some house remains are visible in an ERT-profile. Therefore, ERT has to be regarded as the most promising non-destructive prospection method for determining the depth and thickness of the layer containing burnt houses in loess environment such as that found in Maidanetske. In future surveys it should be combined with minimal invasive direct-push conductivity soundings or shallow drillings for further validating and constraining the depths of the settlement layer.

Introduction

Magnetic measurements have been successfully conducted at Maidanetske since the 1970s (Dudkin 1978; Rassmann et al. 2016). They have yielded a map with the locations of house remains, pits and kilns as well as estimates of their size based on the magnetic anomalies However, due to the inherent ambiguity of magnetic data, the geometry of a magnetic source body and its magnetic material properties cannot be resolved uniquely from the magnetic data alone (e.g. Li and Oldenburg 1996). Complementary additional depth-sensitive geophysical measurements can reduce this non-uniqueness. However, not all geophysical methods are capable to detect a specific structure. It depends on the subsurface conditions whether or not a structure is detectable with a specific measurement setup. Several factors play a role, mainly material property contrasts, but also depth and thickness of the structure, as well as their ratio, the roughness of the surface and coupling of the device and also the distance between the transmitter and receiver in case of EMI.

The anomalies of the majority of the building remains are clearly visible in the magnetic map since they consist of a layer of burnt clay, *i.e.* daub (*e.g.* Müller *et al.* 2017). The archaeological structures are embedded in Chernozem and Loess (Müller *et al.* 2017). We aimed to add additional geophysical data to the existing magnetic map to resolve the geometry of the magnetic anomalies. Therefore, we tested electromagnetic induction (EMI), electrical resistivity tomography (ERT) and ground-penetrating radar (GPR) measurements on different objects in Maidanetske during a field campaign in September 2017 and report the results in this chapter.

For these types of measurements loess turned out to be a challenging environment, because it strongly absorbs the electromagnetic waves of the GPR. Moreover, due to ploughing, GPR shows a rough surface on top and rough interfaces internally, scattering the remaining non-absorbed radar waves. The GPR measurements conducted with a 200 MHZ antenna and a GSSI unit were not able to record reflections from the expected structures. Therefore, the measurements are not shown here. As to the electric measurements, the loess apparently shows only small contrasts between burnt and unburnt fractions in electric conductivity. For the EMI measurements we used a CMD Mini Explorer by GF Instruments but none of the expected structures could be found in the apparent conductivity maps. However, the map of the so-called In-phase EMI component, which is sensitive to the magnetic susceptibility, does show the expected structures. An addition one ERT-profile, measured with the RESECS device by Geoserve, shows the cross-section of house remains.

In the following chapter, we present these results in detail. The chapter is structured as follows: first, we briefly introduce the methods EMI and ERT; next, we present the results and discuss them; finally, we draw a conclusion.

Methods

Electromagnetic induction

Electromagnetic induction (EMI) devices consist of a transmitter and one or several receiver coils. The transmitter coil emits a 'primary' oscillating electromagnetic field. Oscillating eddy currents are induced in the soil that depend on the electrical conductivity distribution of the subsurface. These generate a 'secondary' electromagnetic field recorded at the receiver coils together with the primary field. EMI devices measure the 'apparent electrical conductivity' of the soil, which is the so-called Out-of-Phase component and the In-Phase component, which is a function of the magnetic susceptibility. The sounding depth depends on signal frequency and transmitter-receiver distance.

We used a CMD Mini-Explorer by GF Instruments. The device consists of one transmitter and three receiver coils. The planes of the coils can be oriented horizontally (horizontal coplanar – HCP) or vertically (vertical coplanar – VCP) modes. The distance between the transmitter and receivers are 0.32 m, 0.71 m and 1.18 m leading to theoretical effective sounding depths of 0.25 m, 0.5 m and 0.9 m in VCP mode and 0.5 m, 1.0 m and 1.8 m in HCP mode for a homogeneous half-space. Further details on the method and the device can be found in *e.g.* Bonsall *et al.* (2013).

The measurements were performed with 10 Hz sampling frequency using VCP and HCP configuration. The areas were covered in zig-zag mode with a spacing of 0.5 m between parallel profiles.

Data processing included a coordinate shift based on the Mini-Explorer coil configuration, assigning the measurement values to the centre point of each coil pair. Regarding the data as time series based on the sample timing of 10 Hz, a bandpass filter was applied to the raw data to remove noise with high spatial frequencies (above 0.05 1/samples) due to movement of the device while walking, as well as possible drift effects occurring as low frequency signals (below 0.002 1/samples). After this, the data of all six measurement parameters was gridded and linearly interpolated to maps of 0.25 m grid spacing. These maps were then spatially filtered by a 2D Gaussian image filter with a half width of 0.5 m.

Electric resistivity tomography

The principle of an electric resistivity tomography is as follows: electric current is sent into the ground by two current electrodes and the resulting difference in the electric potential is measured between a second pair of electrodes, the potential electrodes. From this, the apparent resistivity can be calculated as the ratio of potential difference and applied current, multiplied by a geometrical factor. The geometrical factor contains the distances of the electrodes as well as their arrangement. A larger distance between the electrodes results in a higher depth of investigation.

To perform an electric resistivity tomography, a larger number of electrodes are placed equidistantly along a profile. Then the measurement device uses for each measurement a set of four electrodes and moves through all possible electrode combinations, resulting in a so-called pseudosection of apparent resistivities. The measured apparent resistivities correspond to a mean value for the subsurface volume that was penetrated by the applied current. So-called inversion calculations determine a subsurface model of resistivity values that is in agreement with the measurements and resemble the true resistivity distribution. Nevertheless, this process is also non-unique and several subsurface models can be found to explain the measured values equally well.

We used the RESECS device by Geoserve with 0.5 m electrode spacing using the dipole-dipole configuration. The inversion calculations were performed with the software BERT (Günther et al. 2006).

Results

Figure 1 shows the magnetic map of the site with the measurement locations of EMI and ERT. The magnetic map is discussed in detail by Rassmann et al. (2016) and Ohlrau (2020). A method for quantitative interpretation of the magnetic measurements has been presented by Pickartz et al. (2019). The dominant features in the magnetic map are the anomalies of more than 2500 burnt remains of houses. Besides these, there is another type of building found in the settlement: the so-called mega-structures. These differ in their floor-plan, placement inside the settlement and function from the residential houses. In this chapter, we present the measurements at one megastructure and a group of houses.

EMI

We present two areas measured with EMI. For each area, we present the result of one measurement configuration with a figure in comparison to the magnetic map. In addition, we list in a qualitative manner how well the other configurations are in accordance with the magnetic map.

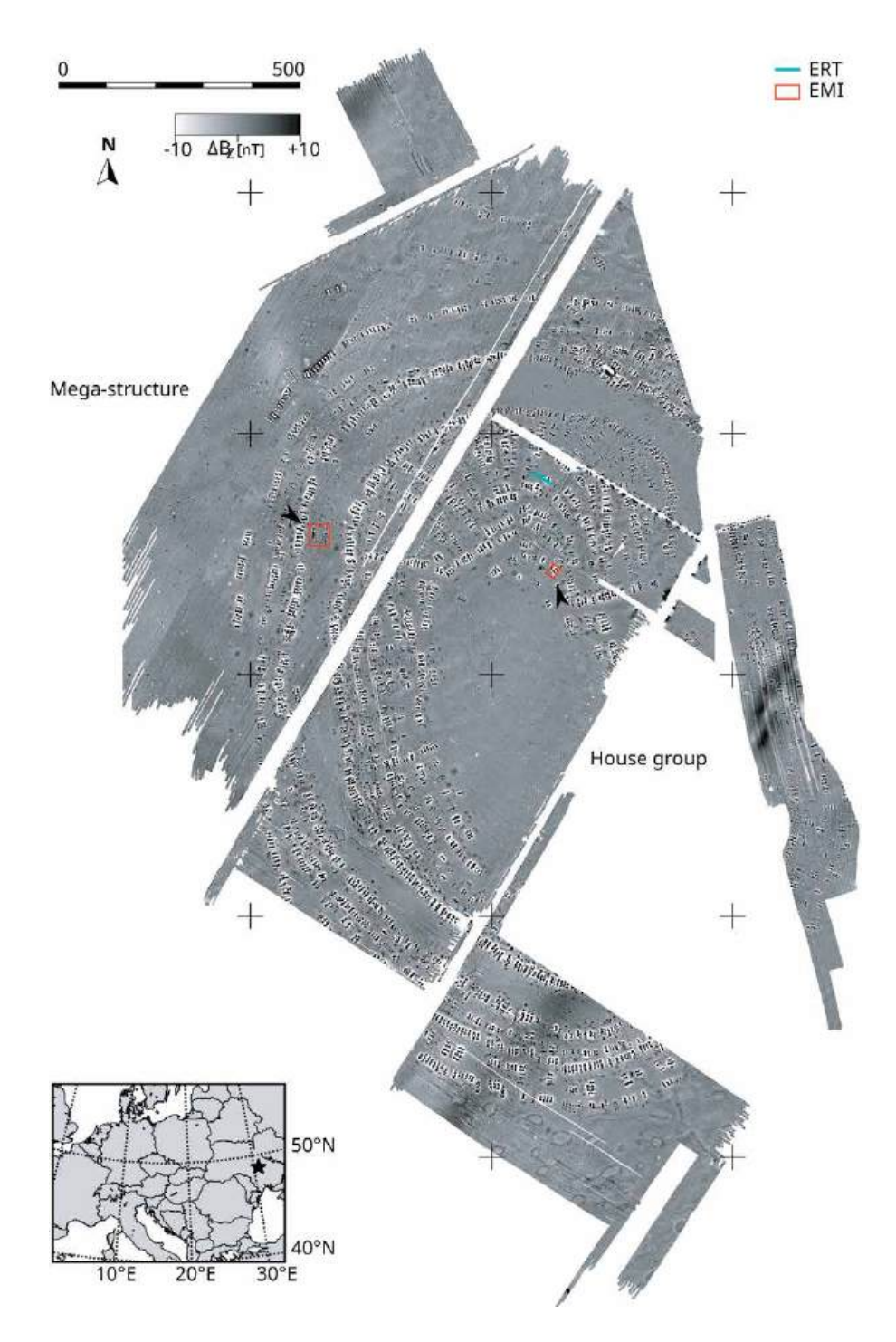
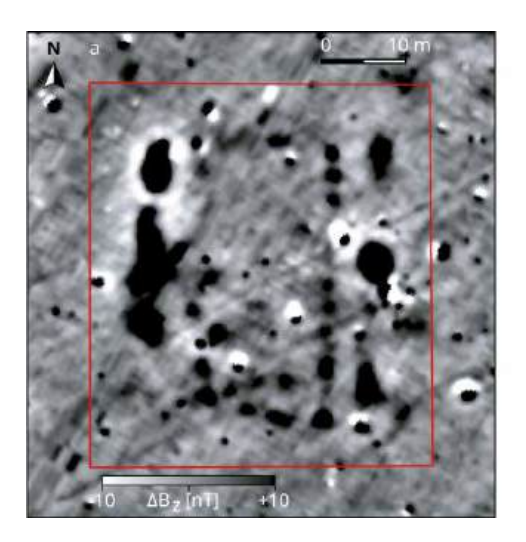


Figure 1. Magnetic map of the site Maidanetske with the location of the areas measured with EMI (red boxes) and the ERT profile (blue line). The insert shows the location of the site in Ukraine.

Mega-structure

Figure 2 shows the comparison of (a) the magnetic map and (b) the In-Phase component (HCP, largest coil separation). The course of the outer walls of the mega-structure is indicated by an apposition of small positive magnetic anomalies. The building was approximately 16 m wide and 35 m long. Outside the building, along the long axis, more positive anomalies of larger scale are visible. Possibly these originate from pits that have been filled with daub. The comparison with the In-Phase values shows that predominantly the anomaly in the northwestern corner of the area is visible as low



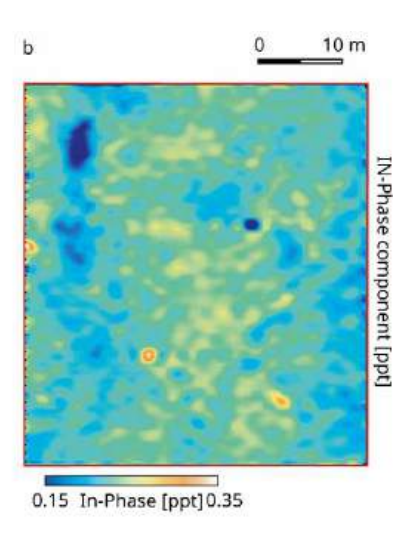


Figure 2. Comparison of
(a) the magnetic map and
(b) the EMI measurements
at a mega-structure in the
western part of the settlement.
The EMI measurements
show the In-Phase values of
HCP configuration with the
intermediate coil separation.

values. Moreover, this anomaly elongates southwards. However, other structures in analogy to the magnetic anomalies cannot be clearly identified.

The images of the apparent conductivity values show streaky patterns parallel to the traces of ploughing. The traces of ploughing are also visible in the In-Phase values of the smallest coil separation. The In-Phase values of the intermediate coil separation yield a similar image as shown in Figure 2b.

House group

The comparison of the magnetic map and the In-Phase component measured in VCP configuration (intermediate coil separation) are shown in Figure 3. The magnetic map shows the anomalies of three buildings. The two eastern ones have a stronger magnetic anomaly than the western one. Moreover, the orientation of the two eastern houses is rotated by approx. 125°. In the In-Phase measurements, the anomalies of the two houses are visible as decreased values. Also, the western building is visible, however the anomaly is not as distinct as for the two other buildings.

Again, in the apparent conductivity maps no anomalies that correspond to the anomalies in the magnetic map are visible. The map of In-Phase values of the largest coil separation is similar to that of the intermediate coil separation, and that of the smallest coil separation shows the expected anomalies also, but with less contrast.

Additionally, for this area measurements in HCP configuration were performed. Also for this configuration, no corresponding anomalies are visible in the apparent conductivity maps. The In-Phase maps of the HCP configuration show the anomalies of the two eastern buildings: for the two smaller coil separations by decreased values and for the largest coil separation by increased values.

ERT

Figure 4 shows in the upper part the magnetic map with the anomalies of three houses and an unclassified anomaly at the western end. The house in the east has the strongest magnetic anomaly out of the three. The electric profile is indicated by a blue line and cuts across the houses approximately in the middle of their long side. The bottom part of Figure 4 shows the distribution of the resistivity along this profile. The inversion results indicate a three-layer structure consisting of a low resistive top layer, a second layer with increased resistivity values and a layer with low resistivity on the bottom. The top layer has a thickness of approx. 0.5 m and resistivity values lower than 30 Ω m. The second layer extends from about 0.5 m to 1 m in depth with a resistivity values higher than 30 Ω m. Between profile

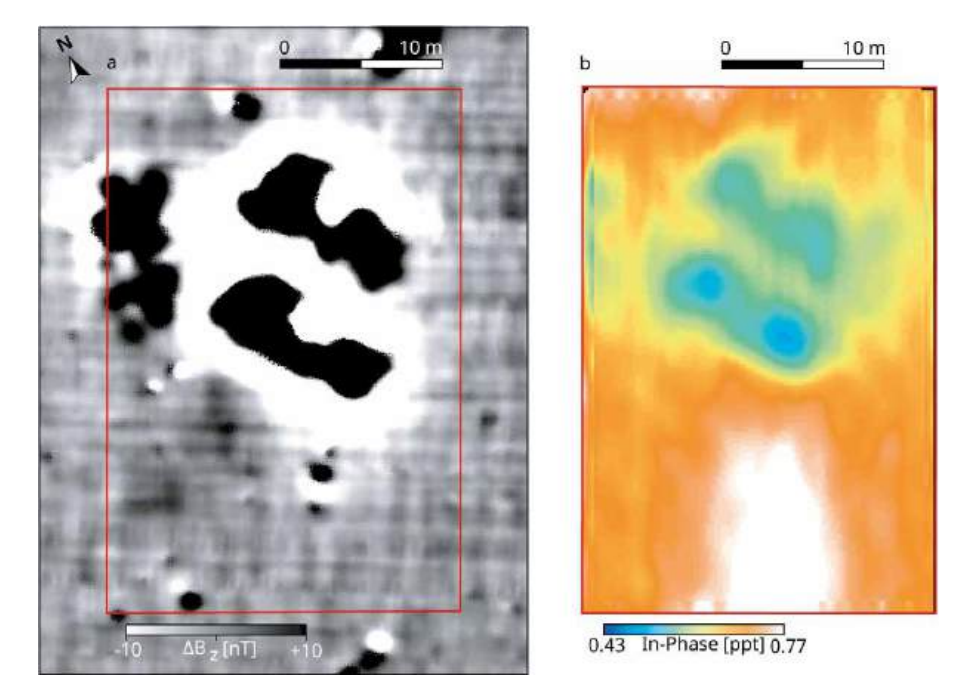


Figure 3. Comparison of
(a) the magnetic map and
(b) the EMI measurements of
three houses in the eastern
part of the settlement. The
EMI measurements show
the In-Phase values of VCP
configuration with the
intermediate coil separation.

metres 10 to 15 lies a high resistive body with a resistivity up to 50 Ω m. Its vertical extension is slightly increased as it nearly reaches the surface and extends up to 1.2 m in depth. In the bottom layer the resistivity decreases again below 30 Ω m. The comparison of the magnetic map and the ERT profile indicates that the highly resistive body corresponds to the remains of the easternmost house. The magnetic anomaly of the two houses in the centre of the profile have a smaller amplitude. They cannot be identified as resistive structures in the ERT profile. However, there are variations of the resistivity throughout the whole second layer.

Discussion

This study aimed to complement the magnetic map with measurements that provide information about the depth extension and geometry of known archaeological structures. This aim has been partly achieved. We were able to find corresponding anomalies to the magnetic ones in ERT measurements and the In-Phase component of EMI measurements. However, compared to the magnetic map, GPR and EMI conductivity mapping were not able to image these archaeological structures in a satisfactory way.

The ERT profile (Fig. 4) shows that the subsurface is a good electrical conductor. As GPR signals are attenuated in good conducting media, this explains the lack of success of the GPR measurements. Another adverse factor for the GPR measurements was the roughness of the surface. The fields were ploughed and the rough surface leads to a bad coupling between the antenna and the subsurface. Consequently, only a fraction of the signal is transmitted into the subsurface.

The comparison of the ERT profile and the magnetic map suggests that house remains with a strong magnetic anomaly can be located with ERT and those with a less strong magnetic anomaly cannot. This can be explained as follows: The strength of the magnetic anomaly is correlated with the mass and volume of daub in the subsurface: the more daub the stronger the magnetic anomaly. Daub is more compact and less porous than the surrounding soil. Therefore, the daub contains less moisture than the soil around. Since a decrease of the moisture content leads to an increase of the electric resistivity of the soil, volumes containing more daub mass

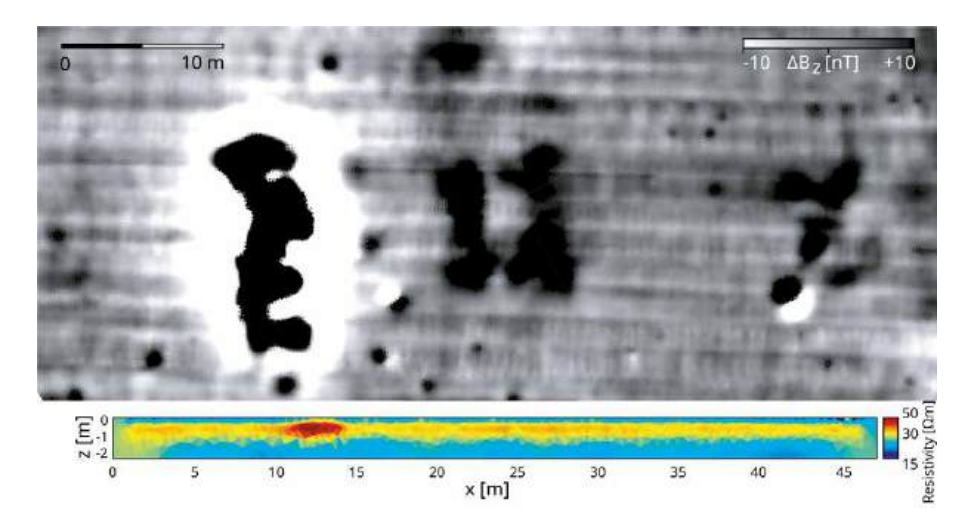


Figure 4. Comparison of magnetic map (top) and ERT profile (bottom). The location of the ERT profile is indicated by the blue line (top). It crosses the remains of three houses. The cross-section of the easternmost house is visible as a high resistive body between 10 m and 15 m in the ERT profile.

than the surrounding show up as a high resistivity anomaly in ERT. This explanation can be supported by additional measurements with similar magnetic signatures or validated by ground-truthing in excavations or corings.

The ERT profile yields an estimate of the depth extension for the easternmost building remains. They start close to the surface, probably directly beneath the ploughing layer at about 30 cm depth and extend to 1.2 m depth. However, since the inversion process is not unique, the depth extension might also be under- or overestimated. This is caused by a loss in resolution with increasing target depth inherent in ERT measurements. Therefore, a combination of ERT profile or areal measurements with minimal invasive direct-push conductivity soundings or shallow drillings appears to be a promising approach for the future.

In addition, the comparison of the magnetic maps and the In-Phase maps show that the structures with a strong magnetic anomaly yield an anomaly in the In-Phase map, too. However, since the structures are visible in all three depth slices, no additional information of the depth extend can be derived.

Conclusion

The rough surface and the conductivity at the site yield challenging conditions for GPR and EMI surveys. Consequently, the GPR measurements did not yield any additional information. Also, the EMI measurements did not contribute depth information of the known structures, since no anomalies are visible in the apparent conductivity distribution and the anomalies in the In-Phase extend over the complete depth range. In contrast, the ERT measurements show that the archaeological structures are located in the uppermost metre under the surface. For further constraining the depth end thickness of the settlement layer, ERT profiling or areal measurements should be combined with minimal invasive direct-push conductivity soundings or shallow drillings in future campaigns.

Acknowledgements

We would like to thank Diana Panning, Lara and Maximilian Lowe for their assistance with the field measurements.

References

- Bonsall, J., Fry, R., Gaffney, C., Armit, I., Beck, A. and Gaffney, V., 2013. Assessment of the CMD Mini-Explorer, a New Low-frequency Multi-coil Electromagnetic Device, for Archaeological Investigations. *Archaeological Prospection*, 20 (3), 219–231. Available from: https://doi.org/10.1002/arp.1458
- Dudkin 1978: Дудкин, В.П., 1978. Геофизическая разведка крупных трипольских поселений. *In*: В.Ф. Генинг, ed. Использование методов естественных наук в археологии. Киев: Издательство "Наукова думка", 35–45.
- Günther, T., Rücker, C. and Spitzer, K., 2006. Three-dimensional modelling and inversion of dc resistivity data incorporating topography II. Inversion. *Geophysical Journal International*, 166 (2), 506–517. Available from: https://doi.org/10.1111/j.1365-246X.2006.03011.x
- Li, Y. and Oldenburg, D.W., 1996. 3-D inversion of magnetic data. *Geophysics*, 61 (2), 394–408. Available from: https://doi.org/10.1190/1.1443968
- Müller, J., Hofmann, R., Kirleis, W., Dreibrodt, S., Ohlrau, R., Brandtstätter, L., Dal Corso, M., Out, W., Rassmann, K., Burdo, N. and Videiko, M., eds., 2017. *Maidanetske 2013. New excavations at a Trypillia mega-site* / Майданецьке *2013.* Нові розкопки великого Трипільського поселення. Studien zur Archäologie in Ostmitteleuropa 16. Bonn: Dr. Rudolf Habelt.
- Ohlrau, R., 2020. *Maidanets'ke: Development and decline of a Trypillia mega-site in Central Ukraine*. Scales of Transformation in Prehistoric and Archaic Societies 7. Leiden: Sidestone Press. Available from: https://doi.org/10.59641/h0912kt
- Pickartz, N., Hofmann, R., Dreibrodt, S., Rassmann, K., Shatilo, L., Ohlrau, R., Wilken, D. and Rabbel, W., 2019. Deciphering archeological contexts from the magnetic map: Determination of daub distribution and mass of Chalcolithic house remains. *The Holocene*, 29 (10), 1637–1652. Available from: https://doi.org/10.1177/0959683619857238
- Rassmann, K., Korvin-Piotrovskiy, A., Videiko, M. and Müller, J., 2016. The new Challenge for Site Plans and Geophysics: Revealing the Settlement Structure of Giant Settlements by Means of Geomagnetic Survey. *In*: J. Müller, K. Rassmann and M. Videiko, eds. *Trypillia Mega-Sites and European Prehistory 4100-3400 BCE*. Themes in Contemporary Archaeology 2. London, New York: Routledge, 29–54. Available from: https://doi.org/10.4324/9781315630731

4. Geoarchaeological analyses on daub pieces from Maidanetske - A treatise on reconstructing burning temperatures of houses and daub processing

Stefan Dreibrodt, Sarah Martini, Robert Hofmann, Marta Dal Corso, Wiebke Kirleis, Johannes Müller

Abstract

44 pieces of daub from the giant Chalcolithic settlement site of Maidanetske, central Ukraine have been analyzed to infer about the burning process of the buildings and on daub processing. A comparison of the data with a large experimental burning experiment has revealed that the investigated domestic house was burnt at higher temperatures (750-850°C) than the communal building of a mega-structure (650-750°C). This could reflect different burning regimes, associated with varying amounts of fuel or different burning processes in general. The chemical composition of the studied daub pieces compared with the local soil imply a loss of clay during the processing in a presumably liquid phase, and an enhancement of phosphorus explainable by the addition of dung to the daub matrix.

Introduction

The analysis of burnt material from archaeological excavations has been carried out to infer about aspects of technology (architecture, ceramic/ metal processing), ancient environments (wood use and availability, cereal imprints) or ideology (ritual burning) to give some examples. The applied approaches varied between archaeological documentation and classification of the burnt material, added by varying analytical techniques. The latter comprise of color measurements (Munsell Scale, colour spectroscometry), neutron activation methods (NAA), XRay fluorescene (XRF), XRay diffractometry (XRD), Fourier transformed infrared analysis (FTIR), the characterization of the magnetic properties of the burnt material, or micromorphological studies (e.g. Peters et al. 2001; Maki et al. 2006; Berna et al. 2007; Nodarou et al. 2008; Mentzer 2014; Forget et al. 2015; Jordanova et al. 2019).

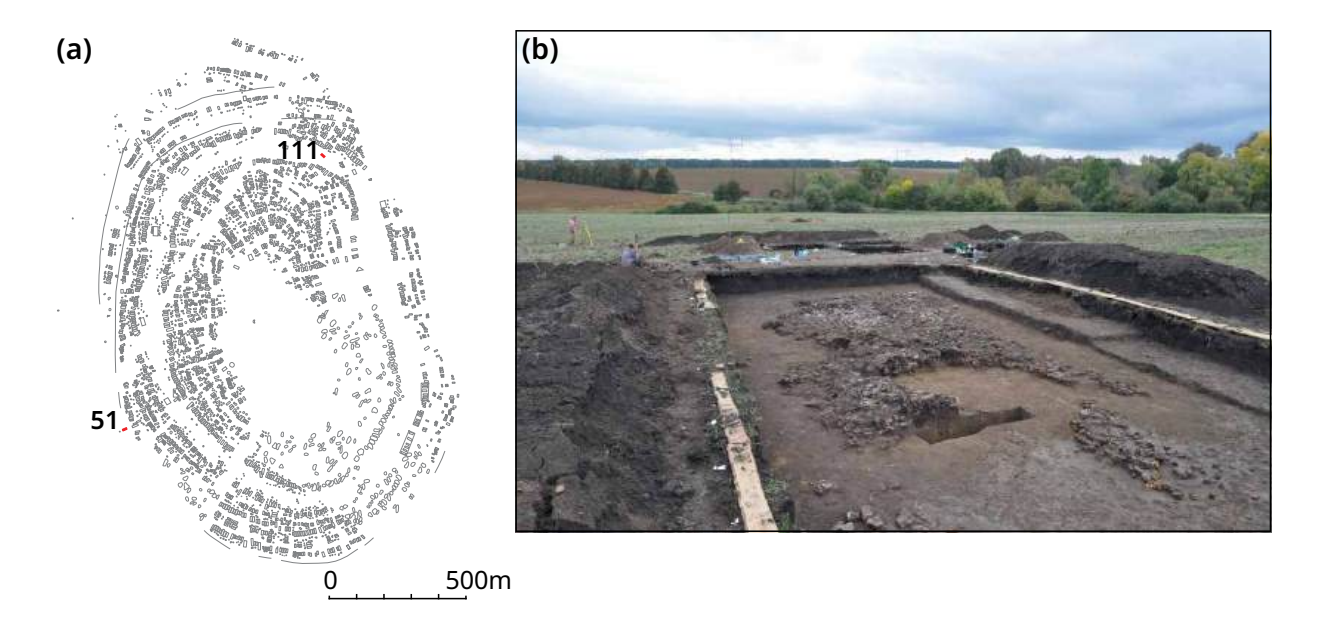


Figure 1. (a) location of the house remains sampled for daub analysis; (b) photograph of the archaeological record, note the dense daub layer in House 44 (Trench 51).

With increased numbers of magnetic maps from archaeological sites, attempts to infer about feature layout and daub masses based on magnetic signatures emerged (Pickartz *et al.* 2019). Additionally, burning experiments are carried out occasionally, to put the analytical data into a controlled context (*e.g.* Bankoff and Winter 1979; Stevanović 1997; Cotiguă 2009; Korvin-Piotrovskiy *et al.* 2012; Burdo *et al.* 2013). In the face of numerous burnt house remains from Neolithic and Chalcolithic sites across Eastern Europe, the question of intentional or unintentional burning has been highly debated among archaeologists during the past decades (*e.g.* Stevanović 1997; Cotiguă 2009; Lichter 2016).

In the presented study, we combined a multi-proxy analytical approach to infer about fire conditions and daub processing at two burnt houses of the Chalcolithic Giant settlement Maidanetske, central Ukraine.

Materials and methods

Site

The investigated giant Trypillia C1 Chalcolithic settlement site of Maidenetske (Müller et al. 2016; Müller et al. 2017; Hofmann et al. 2019) is located at in the district of Talne, central Ukraine (48°48'N, 30°38'E; Fig. 1). Archaeological sites of this type are unique because of their extremely large dimensions. At Maidanetske, on an area of 200 ha approximately 3000 houses arranged in a series of oval structures around an unbuilt central space were inhabited approximately from 3990 to 3640 BCE (e.g. Müller et al. 2016; Ohlrau 2020; Pickartz et al. 2019). Surveys of the many potshards present on the recent surface, magnetic surveys, excavations and exhaustive dating campaigns revealed that about 1500 houses were inhabited contemporaneously by probably 10,000 people (Ohlrau 2020; Pickartz et al. 2019). The climate in the region is humid continental (Dfb) today, with hot summers and cold, wet winters. The potential natural vegetation of the region belongs to the climate sensitive foreststeppe transition zone. Where there is no agricultural land use, deciduous forests are present in the landscape today. A mosaic of loess-covered plateaus dissected by small valleys characterizes the recent topography. The surface soils are classified as particularly thick Chernozems in the research area (Atlas of Soils of the Ukrainian SSR: Krupskovo and Polupana 1979).

Sampling

44 samples of daub from one domestic building (28) and one communal building (16) were taken in the field (Fig. 1) and documented according to their macroscopic properties and find situation (Tab. 1). According to macroscopical properties (discrete layering, colours, inclusions), the daub pieces were cut into subsamples. To produce synthetic daub pieces (bricklets) and study their properties reflecting different burning conditions, loess material from the site was taken (Profile 52). As organic temper, einkorn straw and chaff obtained at the archaeobotanical garden at AÖZA Albersdorf has been added.

Methods

For selected daub pieces, their density was estimated in a simple approach dividing their dry weight by the amount of water the daub pieces replaced (as a volume estimate).

Laboratory analysis was carried out after careful disintegration of the daub pieces (subsampled according to visible layering) with mortar and pestle on the air-dried <2 mm fraction.

The RGB-colours of the samples were determined in three replicates on a Voltcraft Plus RGB-2000 Colour Analyser set to display in a 10-bit RGB colour space (e.g. Rabenhorst et al. 2014; Sanmartín et al. 2014). Since RGB colours are internally highly correlated, these data were converted into Light Intensity, Hue, and Colour Saturation according to Viscarra Rossel et al. (2006).

The volume specific magnetic susceptibility was measured on three replicates of weighed 10 ml- samples using a Bartington MS2B susceptibility meter (resolution 2*10-6 SI, measuring range 1-9999*10-5 SI, systematic error 10%). Measurements were carried out at low (0.465 kHz) and high (4.65 kHz) frequency. A 1% Fe3O4 (magnetite) sample was measured regularly and the samples susceptibility values were calibrated using this standard before the mass specific susceptibility values were calculated. Mass specific magnetic susceptibility and frequency dependent magnetic susceptibility (Dearing 1999; Clark 1996) were calculated based on the weights of the 10 ml samples and the differences of low and high frequency susceptibilities. The total elemental contents of the samples were measured on a p-ed-xrf device (NITON XL3t 900-series) of Thermo Scientific Analysers. For p-ed-xrf measurements, first, the <2 mm fraction was ground in an Agate mill and placed in a plastic tube covered by a 4 µm thick film. These were then measured in a leadmantled measurement chamber with He-flotation using the 'mining, Cu/Zn' settings for 300 s with the p-ed-xrf device. As the device has the ability to not just record quantitative elemental concentrations, but also reports measurement errors, all elements with >10% error were discarded from further analysis. The adjustment of the measurement conditions was carried out according to instructions given in previous papers (Lubos et al. 2016; Martini et al. 2019), that included a calibration of the p-ed-xrf measurements on a wd-xrf data set (Dreibrodt et al. 2017). As loess from Maidanetske and organic temper material from the archaeobotanical garden at AÖZA Albersdorf were used in an extensive burning experiment, the elemental content of components was measured with the p-ed-xrf, too. The loess was prepared in the same manner as described above. The organic temper material was burnt to ash at 550°C (2 h), the elemental contents were measured on the ash and converted into values of 105°C dry biomass. Since it was found to deliver an additional value, sensitive to the burning process in previous investigations (e.g. Khamnueva et al. 2018; Out et al. 2021) the content of dithionite soluble iron (Fed) was measured. This was carried out in a cold digestion process of the daub material (<2 mm) according to Blakemore et al. (1987) and the iron in the supernatant was measured on an Atomic Absorption Spectrometer. The mineral assemblage of daub pieces

sample number	find_id	material description	modification	Square	feature-id	level	remarks
1	51293		2013-16: 6 foamed clay	L-N/12-13	51004	4	
2	51366		2013-14: 7 without surfaces or imprints	J18	51003	4a	
3	51371		2013-16: 6 foamed clay	J13	51003	4a	
4	51372		2013-16: 6 foamed clay	K11	51003	4a	
5	51373		2013-14: 7 without surfaces or imprints	K11	51003	4a	
6	51373B		2013-14: 7 without surfaces or imprints	K11	51003	4a	
7	51378		2013-16: 6 foamed clay	L11	51003	4a	
8	51379		2013-14: 7 without surfaces or imprints	L11	51003	4a	
9	51386		2013-14: 7 without surfaces or imprints	L15	51003	4a	
10	51387		2013-14: 7 without surfaces or imprints	L16	51003	4a	
11	51390	organic tempered (chaff)	2016: 06 combination Splitwood + Splitwood	K15	51003	4a	
12	51391		2013-14: 7 without surfaces or imprints	I17	51003	4a	
13	51392		2013-14: 7 without surfaces or imprints	I17	51003	4a	
14	51393		2013-14: 7 without surfaces or imprints	I14	51003	4a	
15	51394		2013-14: 7 without surfaces or imprints	I13	51003	4a	
16	51395		2013-14: 7 without surfaces or imprints	H13	51003	4a	
17	51396		2013-16: 6 foamed clay	H13	51003	4a	
18	51400		2013-14: 7 without surfaces or imprints	H10	51003	4a	
19	51402		2013-14: 7 without surfaces or imprints	K15	51003	4a	
20	51409		2013-14: 7 without surfaces or imprints	J13	51009	4b	
21	51413		2013-14: 7 without surfaces or imprints	I12	51009	4b	
22	51416		2013-14: 7 without surfaces or imprints	I15	51009	4b	
23	51613		2013-14: 7 without surfaces or imprints	J17	51017	4b	
24	51613B		2013-14: 7 without surfaces or imprints	J17	51017	4b	
25	51615		Rounded edge of the podium	K15	51017	4b	
26	51617		burned daub with imprints	K11	51011	4b	
27	51620	compact (without chaff)	2016: 03 two plain surfaces	I12	51009	4b	
28	53391	2 samples from house	17, no further information				
29	1110515	organic tempered (chaff)	2016: 04 split wood	K22	111023		
30	1110517	organic tempered (chaff)	2016: 01 amorphous	M16	111019		
31	1110519	compact (without chaff)	2016: 02 plain surface	M16	111010		
32	1110634A	organic tempered (chaff)	2016: 02 plain surface	G6	111003		
33	1110634B	organic tempered (chaff)	2016: 02 plain surface	G6	111003		
34	1110636	compact (without chaff)	2016: 02 plain surface	G6	111010		
35	1110642	organic tempered (chaff)	2016: 07 Combination Splitwood + Plain Surface	M19	111019		
36	1110644	organic tempered (chaff)	2016: 01 amorph	G20	111020		

Table 1. Archaeological classification of the sampled daub pieces.

sample number	find_id	material description	modification	Square	feature-id	level	remarks
37	1110646	organic tempered (chaff)	2016: 02 plain surface	J10	111003		
38	1110648	compact (without chaff)	2016: 02 plain surface	J10	111010		
39	1111525	organic tempered (chaff)	2016: 02 plain surface	J13	111010		
40	1111526	compact (without chaff)	2016: 02 plain surface	J13	111025		
41	1111535A	organic tempered (chaff)	2016: 02 plain surface	F17	111017		Upper layer "a" oxidising crumbly light yellow material (7-10 mm thick)
42	1111535B	organic tempered (chaff)	2016: 02 plain surface	F17	111017		Lower layer "b" oxidised light orange to light red. Partly the material is bubbly slagged. Underside likely passive even [?]
43	1111574	organic tempered (chaff)	2016: 03 two plain surfaces	N6	111010		
44	1111575	compact (without chaff)	2016: 02 plain surface	N6	111010		

was determined in ground powder samples using conventional xrd measurements (Siemens diffractometer, Cu- α radiation, 2 Theta 4–90°, step size 0.02, 1 s per step). Identification of mineral assemblages was carried out using d-spacings given in mineralogy textbooks (*e.g.* Brindley and Brown 1980).

Table 1, continued.

Results

Daub experiment

Procedure

Prior to the daub experiment the components used were analysed to characterize their geochemical composition. The elemental composition of the loess is given in Chapter 5 (this work, Vol. I). The elemental composition of the studied cereal composition considered as reference for prehistoric organic temper material shows a certain variability. This might be related to different growing conditions (soils, seasonal weather) and differences in harvest stages. The highest concentrations in P are visible in the grains. Additional elements interesting for phytolith research as silica are found higher concentrated in the chaff and straw. Manuring effected the concentrations of nutritional elements. The chaff and straw of einkorn from the archaeobotanical garden Albersdorf were used as organic temper in the daub experiment.

Bricklets of daub were produced as following. A large sample of loess that originated from the base of exposure 52 was dried for 2 days at 40°C. Afterwards, the loess was sieved through a 2 mm mesh to remove stones and to homogenize the material. Chaff and straw of einkorn cultivated at archaeobotanical garden Albersdorf were used as organic temper material. The straw has been cut into pieces of c. 0.5 cm and was dried together with the husks at 40°C for two days prior to the experiment. The mass of daub material was mixed in a volumetric ratio of one to three (organic temper: mineral matter). Straw and chaff were added in a volumetric amount of one to one. About 480 ml of tab water were added while the mixing process to come out with a plastic mass of daub. After thorough mixing to ensure a high degree of homogeneity, the plastic daub mass was rolled into the form of a

Figure 2. Selected photographs of daub analysis: (a) Bricklets after cutting the mineral-organic daub mass; (b) After burning and cooling in a desiccator; (c) example of one archaeological daub piece, indicating its sub-sampling (center) and measured values of mass specific magnetic susceptibility (left) and colours (right).







Location	Taxon	Taxon Component	Treatment	Elemental content ash [ppm] (value, SD)									
				Zn	Fe	Mn	Ca	К	Р	Si			
Albersdorf	Einkorn	grain	n.s.	1636, 23	1523, 47	887, 52	12692, 368	126425, 678	72521, 234	8504, 145			
		straw*	n.s.	957, 27	12713, 201	3721, 129	110313, 1263	224852, 1319	30339, 151	261814, 869			
		chaff*	n.s.	260, 12	3837, 84	b.d.l. 36969, 460		31379, 325	11536, 120	585776, 1758			
		grain	n.m.	1533, 23	1187, 43	1029, 55	7881, 355	130403, 716	69707, 264	3262, 159			
		chaff	n.m.	1079, 34	8373, 186	2555, 130	64623, 1077	214028, 1581	28622, 211	541395, 1368			
Tuningen		chaff	n.s.	352, 86	3491, 96	b.d.l.	37520, 572	74480, 644	16234, 414	657760, 1667			
Nice		straw	n.s.	b.d.l.	3541, 113	b.d.l.	54208, 663	99656, 713	7494, 91	580385, 1423			
Albersdorf	Emmer	chaff	m.	1129, 48	6101, 221	4541, 229	89636, 1875	444759, 3300	81333, 422	410784, 968			
Albersdorf	Barley	grain	m.	847, 16	1083, 38	b.d.l.	11006, 349	99656, 639	61141, 234	3178, 149			
		grain	n.m.	629, 12	723, 30	b.d.l.	6395, 272	99072, 524	49881, 187	1508, 117			
		chaff	m.	1309, 623	6898, 177	2383, 132	95709, 1571	362148, 2207	50441, 265	319251, 879			
		chaff	n.m.	1087, 423	3541, 113	1448, 100	38173, 930	291127, 1839	41430, 243	453503, 1046			

Table 2. P-ed-xrf elemental contents measured in the ash (2h at 550°C) of cereal components, * used in the bricklet experiment as organic temper material, Treatments n.s. not specified, n.m. not manured, m. manured).

c. 1 cm thick plate. 130 bricklet pieces of approximate size of 4 cm * 1.5 cm * 1 cm (x, y, z) were cut with a knife and dried at 40° C for one week.

After the drying process, replicates of the bricklets were burnt in a muffle furnace under different conditions (Tab. 4). Temperatures, duration of burning, and oxygen access were varied in the experiment. The latter was carried out by covering the bricklets by alumina foil during the burning process. All bricklets were dried at 105°C overnight before burning, and cooled to room temperature after burning in a desiccator. The latter resulted in a comparable, limited oxygen access during the cooling process, considered to result in a similar re-oxidation of magnetite to hematite (e.g. Le Borgne 1955; Le Borgne 1960), also realistic for field conditions of cooling of the collapsed burnt houses. Each variant of burnt bricklets comprised of at least three replicates.

				LOI 550 SD			Element	tal conten	t biomass	[ppm] (105	°C dry)	
Location	Taxon	Component	Treatment	(%)	(n=3)	Zn	Fe	Mn	Ca	К	Р	Si
Albersdorf	Einkorn	grain	n.s.	92.35	0.87	125	116	68	971	9669	5546	650
		straw*	n.s.	97.65	0.37	22	299	88	2596	5292	714	6162
		chaff*	n.s.	84.08	0.72	41	611	b.d.l.	5884	4994	1836	93232
		grain	n.m.	88.34	n.d.	179	138	120	919	15209	8130	381
		chaff	n.m.	96.69	0.11	36	277	84	2136	7076	946	17899
Tuningen		chaff	n.s.	91.41	0.21	30	300	b.d.l.	3223	6398	1395	56505
Nice		straw	n.s.	90.2	0.12	b.d.l.	247	b.d.l.	5313	9767	734	56878
Albersdorf	Emmer	chaff	m.	95.92	0.25	46	249	185	3653	18126	3315	16742
Albersdorf	Barley	grain	m.	86.53	0.92	114	146	b.d.l.	1482	15665	8233	428
		grain	n.m.	87.55	n.d.	78	90	b.d.l.	795	12332	6209	188
		chaff	m.	96.24	0.15	49	259	90	3600	13623	1897	12010
		chaff	n.m.	95.6	0.16	48	156	64	1678	12799	1821	19938

Table 3. Calculations of biomass elemental components (105°C dry) based on LOI550 values of the samples, * used in the bricklet experiment as organic temper material, Treatments n.s. not specified, n.m. not manured, n.d. not determined).

Exposition time (min)	550°C		650°C		750°C		850°C		940°C	
	OX	red	OX	red	OX	red	ОХ	red	OX	red
30	Analysis: Determination of colours (RGB), magnetic susceptibility, dithionite-citrate extractable iron, XRD									
60										
120										
240										

Table 4. Overview of the different treatments and analyses on experimental daub (bricklets).

Results of the daub experiment

Figure 3 gives main results of the experimental burning. The complete set of results is given in Appendix 1. Figure 3a shows that the bricklets expose significant changes in colour as a result of exposure to different temperatures for different times and under different burning conditions. For the sake of readability, bricklets burnt under limited/ unlimited oxygen access are addressed to have been burnt under reducing/oxidizing conditions in the following, although we cannot amount the difference in oxygen access. Considering only the bricklets burnt under oxidizing conditions, the most important changes occurred in the green and blue spectra, whereas the reflectance in red stays at a similar level in all burning variants. Considering the bricklets burnt under reducing conditions, a rapid shift to lower reflectance values (darker) is visible for the samples burnt at 550°C and partly 650°C. This trend disappears or even inverses at temperatures >850°C, when the whole set of bricklets show similar colours. The duration of burning has no (oxidizing) or slight (reducing) unidirectional influence on the change of colours. The latter slight trend towards brighter colours after longer heating duration might indicate the collapse of the alumina foil used to cover the bricklets (visible in the 550°C timeline). Thus, the most pronounced changes in colour are observed under limited oxygen access and lower temperatures.

Figure 3b gives the result of dithionite soluble iron (Fed) standardized against the total iron content of the samples. Compared to the loess material, there is an overall

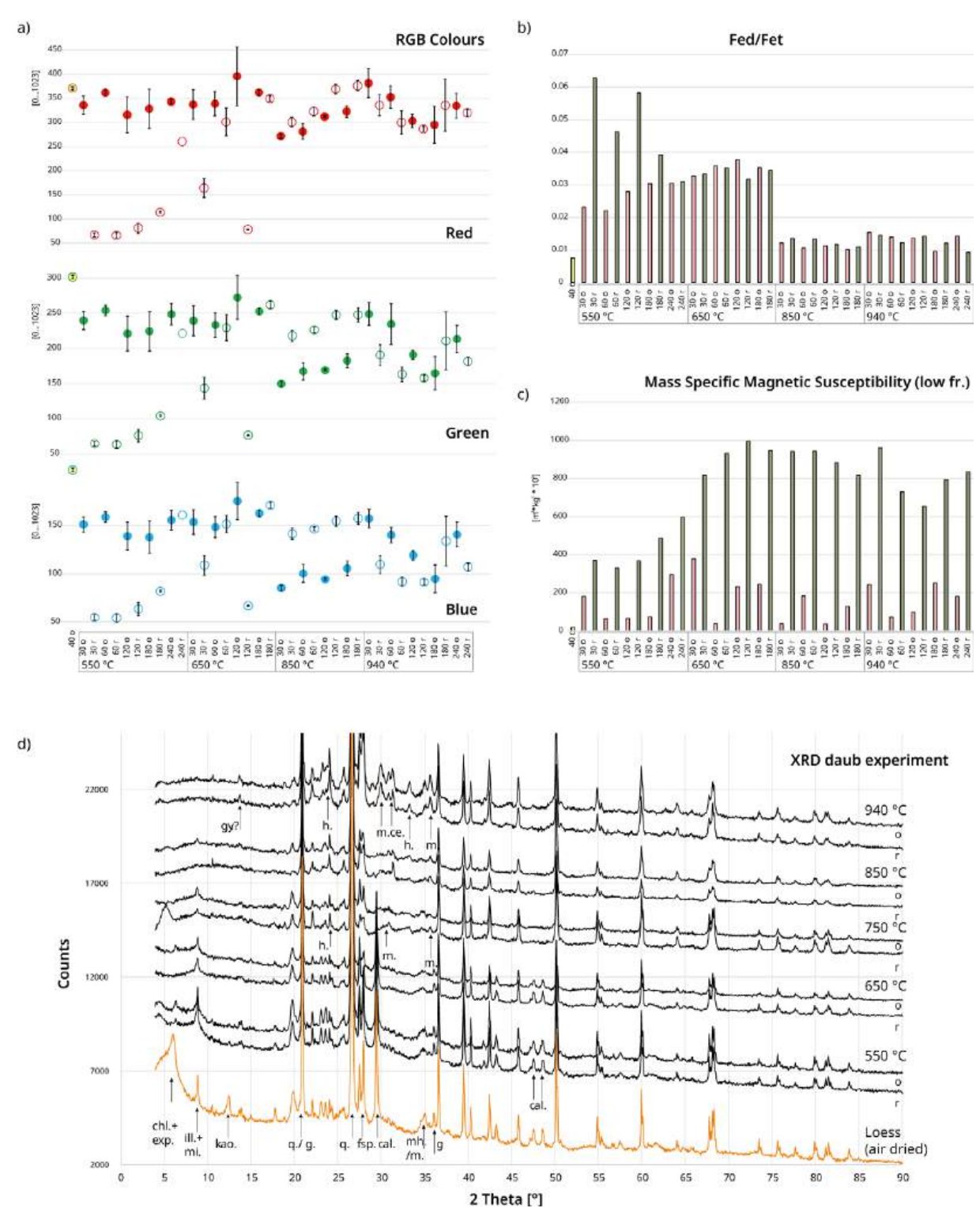


Figure 3. Results of geophysical and geochemical properties of the burning experiment. At the left side, unburnt bricklet values are given (a-c);
(a) RGB colours [0...1023], red, green, blue from top to bottom (oxidized burning-filled circles, reduce burning- open circles);
(b) Fed normalized against the total iron content (oxidized burning - red bars, reduce burning - brown bars);
(c) mass specific magnetic susceptibility (low frequency) (oxidized burning: red bars, reduce burning: brown bars);
(d) xr-diffractograms of the loess and bricklets burnt under oxidizing/ reducing condition for 120 min: chl. + exp. = chlorite + expandable clay minerals; ill. + m. = illite and muscovite; kao. = kaolinite; q. = quartz; g. = goethite; fsp. = feldspars; cal. = calcite; mh. = maghemite; m. = magnetite; h. = hematite; ce. = clinoenstatite; gy. = gypsum.

increase of Fed. At 550°C, a considerable difference between the reducing and oxidizing variants is visible. While the oxidizing samples rise in value with longer duration, the reducing lower. This is probably reflecting the more reducing conditions during the burning process, leading to higher amounts of meta-stable magnetite. The general increase is reflecting the transformation of sedimentary iron compounds (goethite, maghemite) into meta-stable forms ('meta-stable magnetite', hematite) by heating in the presence of organic material (*e.g.* Le Borgne 1955; Le Borgne 1960; Tite and Mullins 1971; Clark 1996). In the 650°C series, all variants reach similar, high values. By the change to 850°C, the values of Fed are all lower and stay at low level after heating to 940°C, too. The most pronounced step in dithionite soluble iron between 650°C and 850°C indicates the transformation of meta-stable iron components ('meta-stable magnetite') into other forms of minerals (magnetite, hematite).

Figure 3c shows the change in mass specific susceptibility as a result of different burning conditions. All bricklets show higher magnetic susceptibility after heating. There are great differences between the bricklets burnt under oxidizing and reducing conditions. After each temperature and duration of burning, the bricklet burnt under reducing conditions show considerably higher values than their oxidizing counterparts do. The absolute values are the lowest at 550°C, and reach high values at temperatures >650°C. At 550°C, a clear trend to increasing magnetic susceptibility values is visible with increasing duration of heating. The bricklets burnt under oxidizing conditions show a certain variability in all variants. A major change (increase) in magnetic susceptibility occurred under reducing conditions between 550°C and 650°C. That points towards magnetite formation during the burning process of organic material under limited oxygen access. Once the organic material has been oxidized completely (temperatures >550°C), no more magnetite (either 'meta-stable' below 850°C or stable above 850°C) is forming and thus magnetic susceptibility is not rising further. The relatively stable (high) magnetic susceptibility values of the bricklets burnt under reduced conditions at temperatures >650°C seen together with the clear decrease in dithionite soluble iron between 650°C and 850°C indicates a complete transformation of the 'meta-stable magnetite' into stable magnetite under the applied experimental conditions.

Figure 3d gives changes in mineral assemblage associated to different burning temperatures. Only samples exposed to heating for 120 min were measured, and a burning variant at 750°C was added. At the base, the loess used as mineral material for the bricklet production is shown. There, a mixture of quartz, feldspars calcite and some clay minerals (chlorite/ expandable clays, illite, kaolinite) and iron oxides (maghemite, magnetite, goethite) are present. After heating at 550°C, the kaolinite has disappeared and the chlorite/expandable clays are largely reduced. At 650°C, the chlorite/ expandable clays have disappeared, and by 750°C small peaks of hematite and magnetite start to form, while in the same steps the calcite peaks disappear and the illite peaks weaken. At 850°C the illite has disappeared, hematite has grown and perhaps some clinoenstatite started to form. By 940°C hematite, clinoenstatite and magnetite form clearly detectable peaks. The changes of the mineral assemblage occur earlier under reduced conditions. The reflectance of increase in magnetite is visible (see the ratio between magnetite and hematite peaks) but less pronounced than in magnetic properties. A very small increase of magnetite (perhaps in the per Mille dimension) leads to an immense increase in magnetic susceptibility, but the xrd method is considered to be sensitive to changes of the mineral assemblage rather in the percentage dimension.

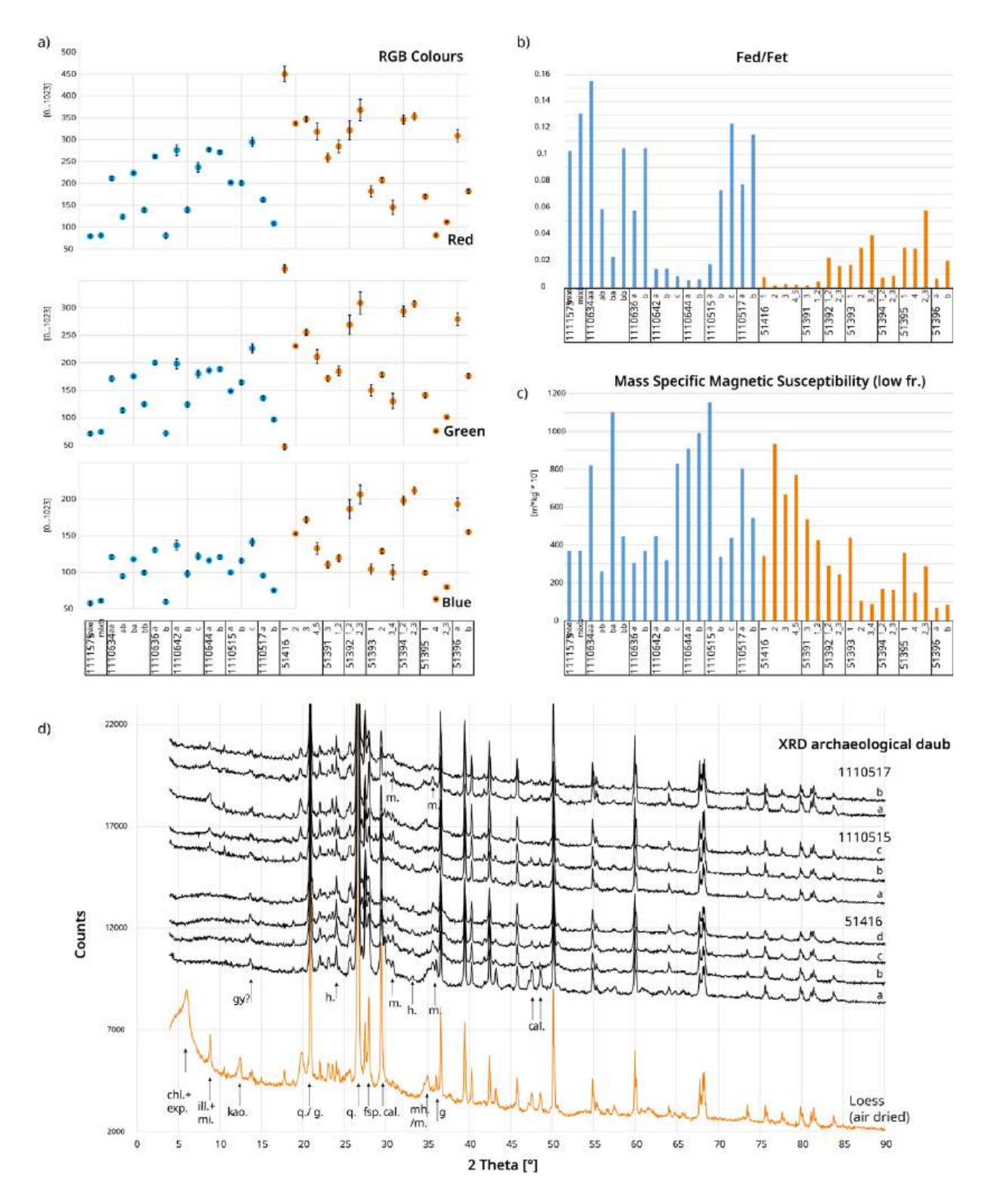


Figure 4. Results of geophysical and geochemical properties of the archaeological daub (communal building 3 – blue bars, domestic building 44 – orange bars);

- (a) RGB colours [0...1023], red, green, blue from top to bottom;
- (b) Fed normalized against the total iron content;
- (c) mass specific magnetic susceptibility (low frequency);
- (d) xr-diffractograms of the loess and selected daub pieces: chl. + exp. = chlorite + expandable clay minerals; ill. + m. = illite and muscovite; kao. = kaolinite; q. = quartz; g. = goethite; fsp. = feldspars; cal. = calcite; mh. = maghemite; m. = magnetite; h. = hematite; ce. = clinoenstatite; gy. = gypsum.

Results of archaeological daub analysis

Additionally, to the geochemical and geophysical analysis, for selected archaeological daub samples, their density has been estimated using their dry weight and volume estimations based on their water replacement (Appendix 2). The mean density of the daub pieces from Maidanetske equals 1.97 g*cm⁻³ (SD 0.303, n=33). There are no significant differences between daub pieces from the communal building and daub pieces from the domestic house.

Geochemical and geophysical data of 14 daub pieces (seven from communal building 3 and domestic house 44) are given in Figure 4. The complete data set can be found in Appendix 2.

Figure 4a shows that the daub pieces exposed significantly different colours. An internal variability is also visible within sub-samples from the daub pieces. In the examples selected for the figure, the daub pieces from the communal building are darker than the ones from the domestic house. Compared to the bricklet experiment these darker communal building daub pieces are in similar range than the reducing variants of the lower temperatures (550–650°C).

Figure 4b gives the result of dithionite soluble iron (Fed) standardised against the total iron content of the samples. This standardisation eliminates possible influences of total iron on the amount extractable by the dithionite digestion. Except of two pieces, the daub from the communal building shows higher values of dithionite extractable iron compared to the daub pieces from the domestic house. The observed maximum values in the daub are considerably higher than the ones observed in the bricklet experiment, indicating a possible influence of postdepositional (pedogenic) processes providing a surplus of dithionite soluble iron. Apart from this shift to higher maximum values, the higher amounts of dithionite soluble iron parallels the observation of similarity of the communal building daub with bricklets burnt under reducing condition at lower temperatures (550–650°C). Within single daub pieces, a similar variability of dithionite soluble iron as in the colours is visible.

Figure 4c shows the mass specific susceptibility values of the archaeological daub pieces. The selected daub pieces from the communal building show higher low frequency mass specific susceptibilities than the selected pieces from the domestic house. The susceptibility values from the communal building are all in the range observed for the reduced variants in the bricklet experiment. The displayed samples from the domestic house show different values, much of them with lower susceptibilities.

Figure 4d compares the mineral assemblages of the loess and selected daub pieces. The general similarity of the overall main mineral spectrum indicates that prehistoric settlers used the local loess for daub production. All displayed daub pieces are free from kaolinite what implies burning temperatures >550°C. In the pieces from the communal building (1110517, 1110515), some illite/ muscovite survived the burning process, indicating temperatures <850°C. No illite/ muscovite is present in the sample from the domestic building (51416), where also hematite and magnetite are more clearly present. This indicates that the piece 5416 was exposed to higher temperatures. In addition to the aforementioned minerals, some calcite (not all sub-samples) and gypsum are present. Considering their instability at higher temperatures and their occurrence in the regional soils, a postdepositional (pedogenic) origin of these minerals is probable. While the whole data set (RGB colours, dithionite soluble iron, mass specific susceptibility, mineral assemblage) is used to infer about burning conditions of the analysed houses in a canonical correspondence analysis, calcite and gypsum occurrences in the daub pieces are disregarded in this statistic analysis.

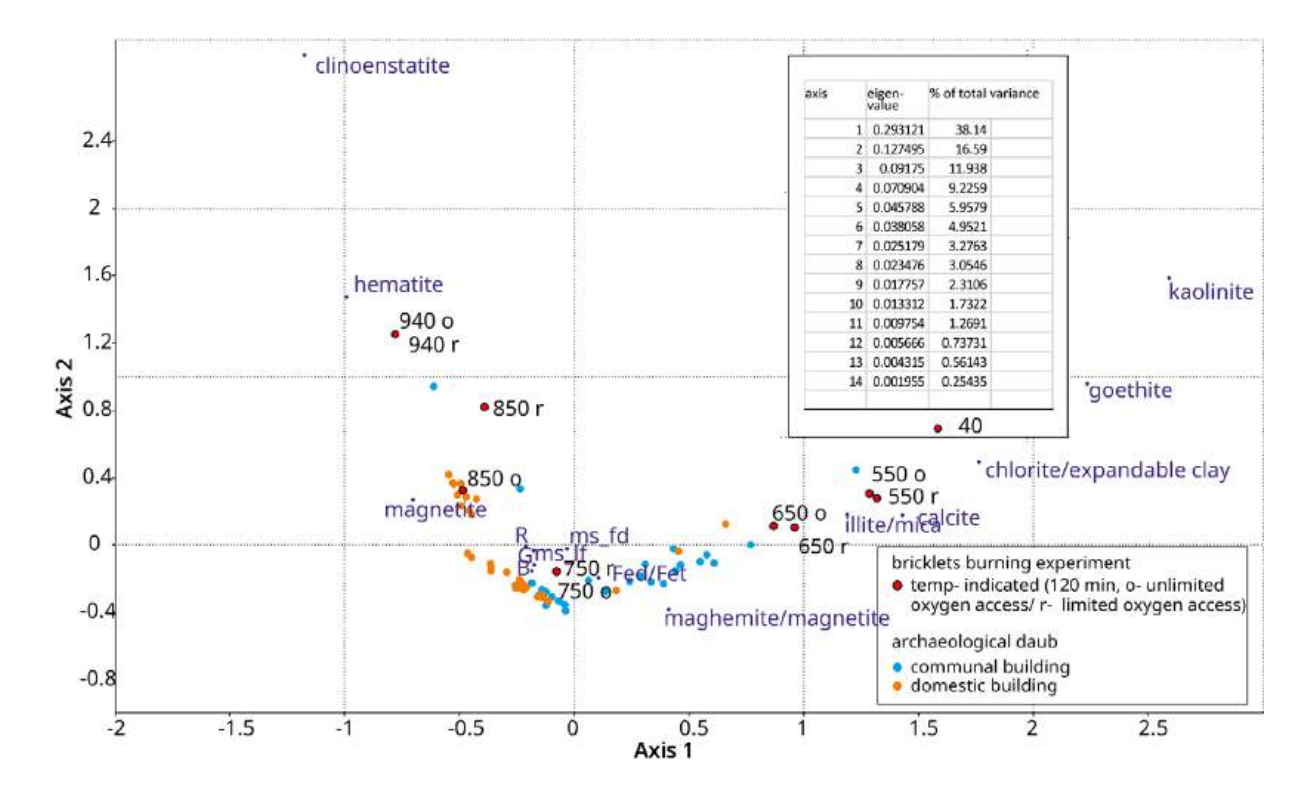


Figure 5. Joint CA plot
(axis 1 and 2) of the results of
the burning experiment (120 min
modes) and the archaeological
daub pieces. Considering
the displayed variability of
the bricklets reflects burning
conditions, archaeological daub
pieces were probably exposed to
similar burning conditions.

Discussion and Interpretation

Daub and fire temperatures

A joint Correspondence Analysis (CA) has been carried out with the results (Fig. 5). There is a clear reflection of the burning temperatures by the clustering of the bricklets within the CA plot, mainly determined by the change of the mineral assemblage. This puts the archaeological daub pieces, assumable produced with the same material (loess from the site), into temperature ranges of between 550°C and 850°C. Furthermore, a difference is visible between the daub from the domestic house (51) burnt at higher temperatures (750°– 850°C), and the communal building (111) burnt at lower temperatures (650°–750°C).

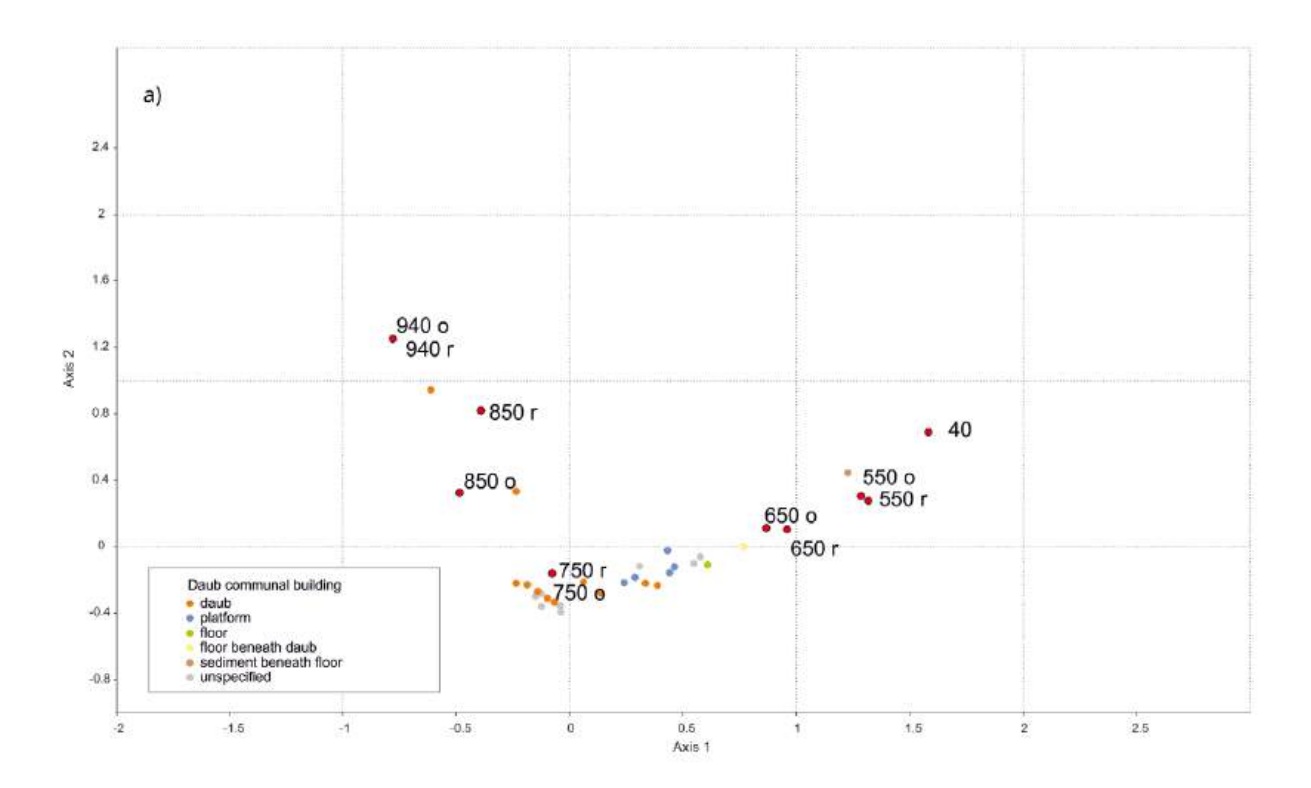
Viewing the results of the CA separately indicating the investigated part of the burnt houses (Fig. 6) backs the results of temperature reconstruction. House parts considered to originate from house floors expose lower temperatures in both buildings. Daub pieces referred to origin form the wall expose rather higher temperatures.

The observed difference between the communal building and the domestic building indicate that these buildings burned down differently. This could reflect differences for fuel available during the fire and/or different burning processes. Whereas the former brings in the question if the compared buildings had a different shape/ architecture, the latter questions an assumed joint process of 'burning down the houses' in the same manner and thus, as a reflection of standardized ritual behaviour.

Daub processing

Some considerations on daub processing based on the geochemical composition of the studied soils and daub pieces are outlined in the following.

Figure 7 shows comparisons of the composition of the daub and the loess from Maidanetske. There are significant differences in the elements considered to reflect



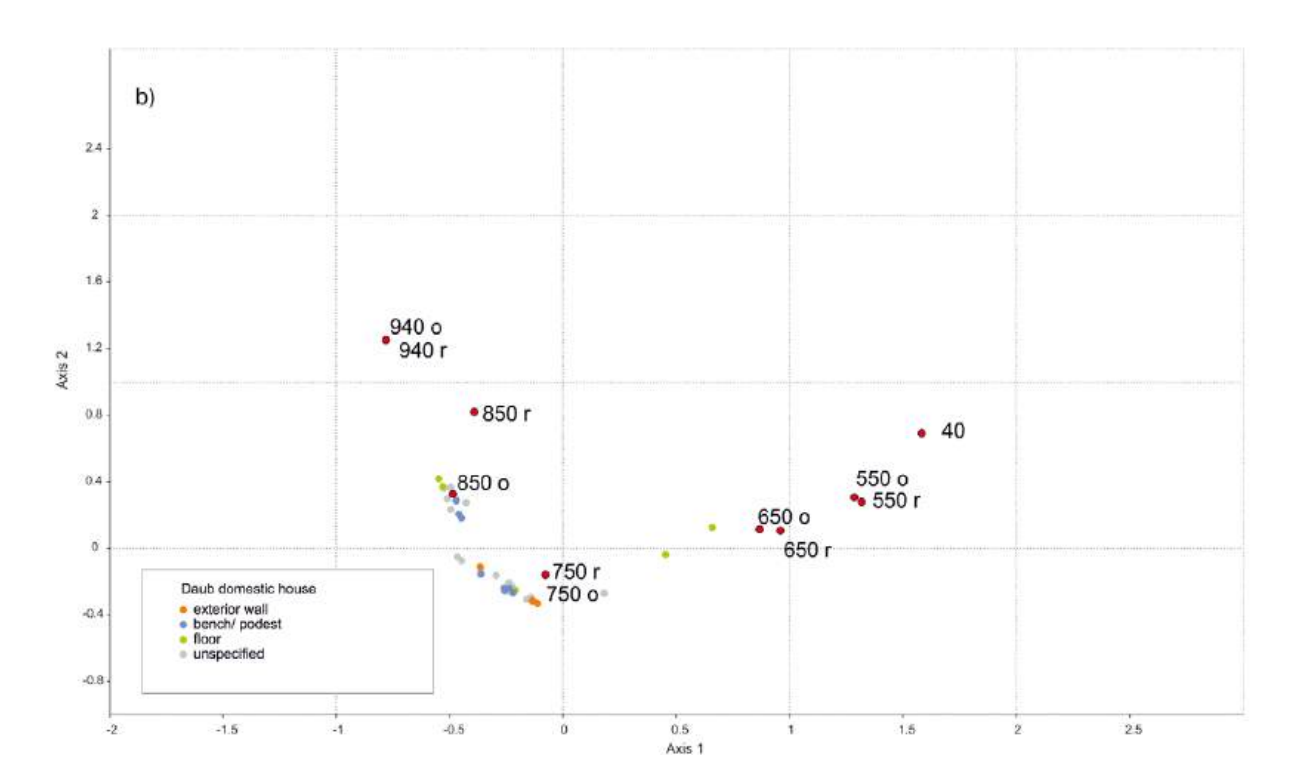
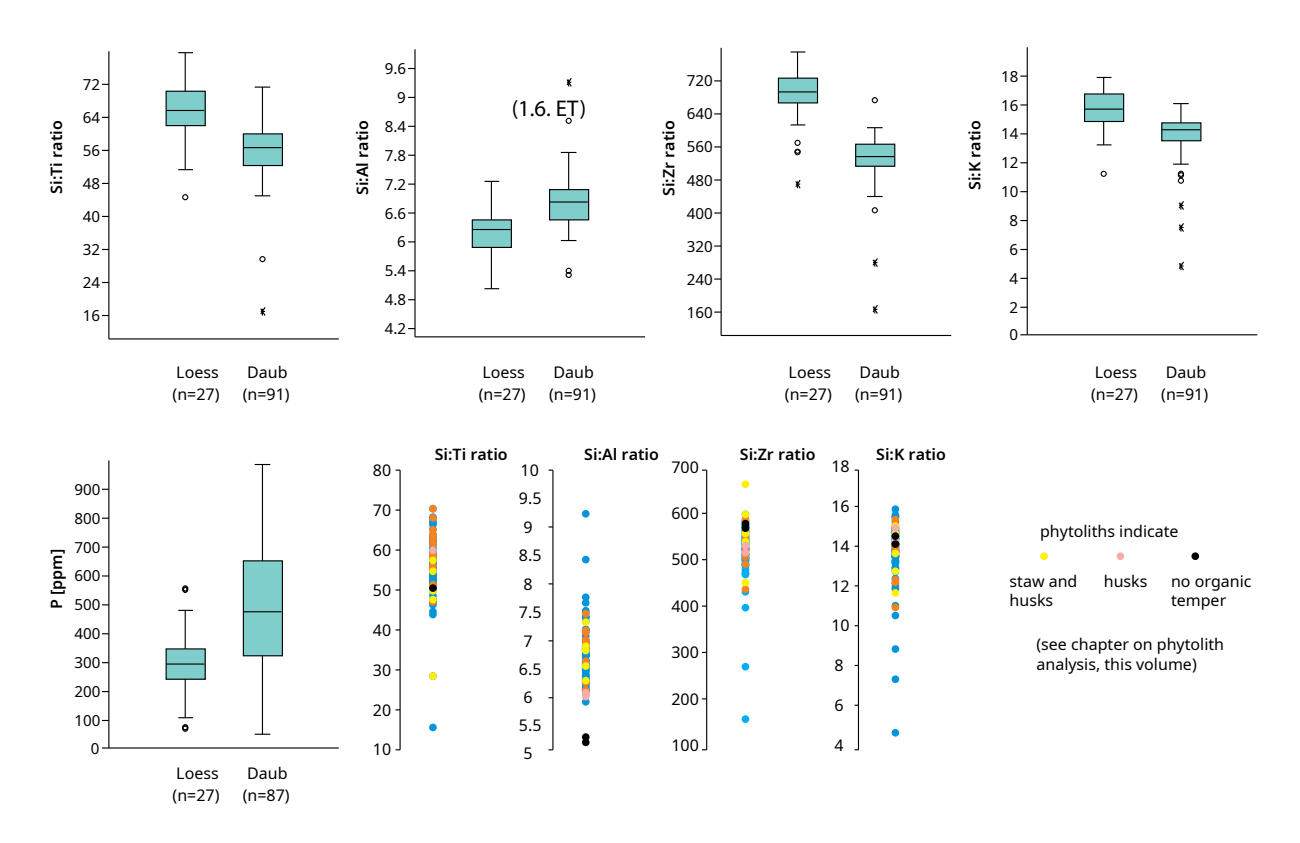


Figure 6. CA plots (axis 1 and 2) for (a) the communal building and (b) the domestic house separately, investigated parts of the house interior are indicated.



	Density	Р	Si	Р	Si	
Material	g*cm ⁻³ (SD, n)	ppm ((SD, n)	mg*	cm ⁻³	
Loess	1.34 (0.09, 9)	145 (76, 27)	281723 (23292, 27)	0.19	378.2	P difference Daub- Loess: 0.74 mg*cm
Daub	1.97 (0.30, 33)	447 (242, 91)	242776 (32211, 91)	0.93	478.3	equals addition of 5.48 g Einkorn pe 1 g Loess
Einkorn*	0.12 (0.04, 8)	1125 (483, 5)	46135 (34771, 5)	0.13	5.54	leaves a gap in Si of 69.8 mg*cm ⁻³ or ca. 70 %

Figure 7 (top). Comparison of boxplots of mean values of mineral elemental contents of daub and loess (upper part), phosphorus (lower left), and the components of organic temper in the daub identified via phytolith analysis (lower right).

Table 5 (bottom). Calculation of phosphorus and silica contents in the daub compared to the loess and organic temper.

*mean values for Einkorn chaff and straw from the garden plot in the Archaeological-Ecological Centre Albersdorf, AÖZA (105 °C dried overnight).

the mineral components. In the boxplots comparing mean values of elemental ratios, Ti, Zr, and K are enriched in the daub relative to Si, the opposite is true for Al (upper part of the figure). Phosphorous is found to be enriched in the daub compared to the loess (lower left). The organic compartments detected in the daub in the form of phytoliths are displayed in the lower right part of the figure.

The enrichment of elements considered to reflect minerals as zirconium (Zr) or rutile, anatase, ilmenite (Ti) is more pronounced than the enrichment in K, present in feldspars, but also clay minerals of the illite/ mica group. This observation points towards the same direction as the depletion in Al. Together, they indicate a considerable depletion of clay minerals (the main source of Al on earth surface) in the daub compared to the loess. This could be explained by the loss of clay during a daub procedure in a liquid phase. During the mixing of mineral and organic components to produce the plastic daub mass, the clay becomes easily dispersed in the liquid phase, and is lost, when the daub is put onto walls or earthen installations (platforms *etc.*). Apart from Ti, Zr, and K, also Si is probably enriched as a result of the clay flotation, since its main source mineral quartz is present in large amounts in the loess and has a high density.

The enrichment of the daub in phosphorus could be considered further by integrating the elemental contents of the organic temper. The content of Si and

P of straw and chaff of einkorn (archaeobotanical garden at Albersdorf) given in Table 2 were used in the following to estimate if the amount of phosphorus added by plant temper could explain the P surplus of the daub at the site. Because of the very different densities of the compared components, the conversion of weight related elemental contents [ppm] into volume related [g*cm-3] is necessary (Tab. 5).

Considering the outcome of the estimation it becomes clear, that the addition of cereal material as organic temper is not able to explain the P enrichment observed in the archaeological daub. Non-realistic high amounts of organic material would have to be added (about 5.5 g per one gram of loess), and a considerable lag in the silica content would result from that mixture. Whereas this is exemplified based on the einkorn chaff and straw from Albersdorf, it would also account for emmer or barley, mainly because of the given P/Si ratios in the organic remains. Thus, while the surplus Si in the daub compared to the loess is probably reflecting partly the addition of the phytolith rich organic material and partly the enrichment of quartz (Si) via the processing (see above), an additional source must exist for the phosphorous. This is very probably the addition of animal manure (excrements, urine) to the daub mass, known from archaeoethnological work.

References

- Bankoff, H.A. and Winter, F.A., 1979. A house-burning in Serbia: What do burned remains tell an archaeologist? *Archaeology*, 32 (5), 8–14.
- Berna, F., Behar, A., Shahack-Gross, R., Berg, J., Boaretto, E., Gilboa, A., Sharon, I., Shalev, S., Shilstein, S., Yahalom-Mack, N., Zorn, J.R. and Weiner, S., 2007. Sediments exposed to high temperatures: reconstructing pyrotechnological processes in Late Bronze and Iron Age Strata at Tel Dor (Israel). *Journal of Archaeological Science*, 34 (3), 358–373. Available from: https://doi.org/10.1016/j. jas.2006.05.011
- Blakemore, L.C., Searle, P.L. and Daly, B.K., 1987. Methods for chemical analysis of soil. *New Zealand Soil Bureau Scientific Report*, 80. Available from: https://doi.org/10.7931/DL1-SBSR-80
- Brindley, G.W. and Brown, G., 1980. *Crystal Structures of Clay Minerals and their X-Ray Identification*. Mineralogical Society of Great Britain and Ireland 5. London: Mineralogical Society.
- Burdo, N., Videiko, M., Chapman, J. and Gaydarska, B., 2013. Houses in the Archaeology of the Tripillia-Cucuteni-Groups. *In*: D. Hofmann and J. Smyth, eds. *Tracking the Neolithic house in Europe. Sedentism, Architecture, and Practice*. One World Archaeology. New York: Springer, 95–115. Available from: https://doi.org/10.1007/978-1-4614-5289-8 5
- Clark, A., 1996. Seeing Beneath the soil: Prospecting Methods in Archaeology, 2^{nd} ed. London: Batsford.
- Cotiugă, V., 2009. Experimental Archaeology: the burning of the Chalcolithic Dwellings. *In*: V. Cotiugă, F.A. Tencariu and G. Bodi, eds. *Itinera in praehistoria. Studia in honorem magistri Nicolae Ursulecu quinto et sexagesimo anno*. Iași: Editura Universității "Alexandru Ioan Cuza", 303–342.
- Dearing, J., 1999. Environmental Magnetic Susceptibility: Using the Bartington MS2 System, 2nd ed. Bartington Instruments. Available from: https://bartingtondownloads.com/wp-content/uploads/OM0409.pdf
- Dreibrodt, S., Furholt, M., Hofmann, R., Hinz, M. and Cheben, I., 2017. P-ed-XRF-geochemical signatures of a 7300 year old Linear Band Pottery house ditch fill at Vráble-Ve'lké Lehemby, Slovakia House inhabitation and post-depositional processes. *Quaternary International*, 438, 131–143. Available from: https://doi.org/10.1016/j.quaint.2017.03.054

- Forget, M.C.L., Regev, L., Friesem, D.E. and Shahack-Gross, R., 2015. Physical and mineralogical properties of experimentally heated chaff-tempered mud bricks: Implications for reconstruction of environmental factors influencing the appearance of mud bricks in archaeological conflagration events. *Journal of Archaeological Science: Reports*, 2, 80–93. Available from: https://doi.org/10.1016/j. jasrep.2015.01.008
- Hofmann, R., Müller, J., Shatilo, L., Videiko, M., Ohlrau, R., Rud, V., Burdo, N., Dal Corso, M., Dreibrodt, S. and Kirleis, W., 2019. Governing Tripolye: Integrative architecture in Tripolye settlements. *PLoS ONE*, 14 (9), e0222243. Available from: https://doi.org/10.1371/journal.pone.0222243
- Jordanova, N., Jordanova, D., Barrón, V., Lesigyarski, D. and Kostadinova-Avramova, M., 2019. Rock-magnetic and color characteristics of archaeological samples from burnt clay from destructions and ceramics in relation to their firing temperature. *Archaeological and Anthropological Sciences*, 11, 3595–3612. Available from: https://doi.org/10.1007/s12520-019-00782-y
- Khamnueva, S., Mieth, A., Dreibrodt, S., Out, W.A., Madella, M. and Bork, H.-R., 2018. Interpretation of prehistoric reddish pit fillings on Easter Island: A micromorphological perspective. *Spanish Journal of Soil Science*, 8 (2), 236–257. Available from: https://doi.org/10.3232/SJSS.2018.V8.N2.07
- Korvin-Piotrovskiy, A.G., Chabanyuk, V. and Shatilo, L., 2012. Tripolian House Construction: Concepts and Experiments. *In*: F. Menotti and A.G. Korvin-Piotrovskiy, eds. *The Tripolye Culture Giant-Settlements in Ukraine. Formation, Development and Decline*. Oxford: Oxbow Books, 210–229. Available from: https://doi.org/10.2307/j.ctvh1dvmn.14
- Krupskovo and Polupana 1979: Крупского, Н.К. and Полупана, Н.И., eds., 1979. Атлас почв Украинской ССР. Киев: Урожай.
- Le Borgne, E., 1955. Susceptibilité magnétique anormale du sol superficiel. *Annales de Géophysique*, 11, 399–419.
- Le Borgne, E., 1960. Influence du feu sur les propriétés magnétiques du sol et sur celles du schiste et du granite. *Annales de Géophysique*, 16, 159–195.
- Lichter, C., 2016. Burning Down the House Fakt oder Fiktion? *In*: K. Bacvarov and R. Gleser, eds. *Southeast Europe and Anatolia in prehistory: Essays in Honor of Vassil Nikolov on his 65th anniversary*. Universitätsforschungen zur prähistorischen Archäologie 293. Bonn: Dr. Rudolf Habelt, 305–317.
- Lubos, C., Dreibrodt, S. and Bahr, A., 2016. Analysing spatio-temporal patterns of archaeological soils and sediments by comparing pXRF and different ICP-OES extraction methods. *Journal of Archaeological Science: Reports*, 9, 44–53. Available from: https://doi.org/10.1016/j.jasrep.2016.06.037
- Maki, D., Homburg, J.A. and Brosowske, S.D., 2006. Thermally activated mineralogical transformations in archaeological hearths: inversion from maghemite Fe2O4 phase to haematite Fe2O4 form. *Archaeological Prospection*, 13 (3), 207–227. Available from: https://doi.org/10.1002/arp.277
- Martini, S.J., Athanassov, B., Frangipane, M., Rassmann, K., Stockhammer, P.W. and Dreibrodt, S., 2019. A budgeting approach for estimating matter fluxes in archaeosediments, a new method to infer site formation and settlement activity: Examples from a transect of multi-layered Bronze Age settlement mounds. *Journal of Archaeological Science: Reports*, 26, 101916. Available from: https://doi.org/10.1016/j.jasrep.2019.101916
- Mentzer, S.M., 2014. Microarchaeological Approaches to the Identification and Interpretation of Combustion Features in Prehistoric Archaeological Sites. *Journal of Archaeological Method and Theory*, 21, 616–668. Available from: https://doi.org/10.1007/s10816-012-9163-2

- Müller, J., Rassmann, K. and Videiko, M., eds., 2016. *Trypillia Mega-Sites and European Prehistory 4100-3400 BCE*. Themes in Contemporary Archaeology 2. London, New York: Routledge. Available from: https://doi.org/10.4324/9781315630731
- Müller, J., Hofmann, R., Kirleis, W., Dreibrodt, S., Ohlrau, R., Brandtstätter, L., Dal Corso, M., Out, W., Rassmann, K., Burdo, N. and Videiko, M., eds., 2017. *Maidanetske 2013. New excavations at a Trypillia mega-site / Майданецьке 2013. Hoві розкопки великого Трипільського поселення*. Studien zur Archäologie in Ostmitteleuropa 16. Bonn: Dr. Rudolf Habelt.
- Nodarou, E., Frederick, C. and Hein, A., 2008. Another (mud)brick in the wall: scientific analysis of Bronze Age earthen construction materials from East Crete. *Journal of Archaeological Science*, 35 (11), 2997–3015. Available from: https://doi.org/10.1016/j.jas.2008.06.014
- Ohlrau, R., 2020. *Maidanets'ke: Development and decline of a Trypillia mega-site in Central Ukraine*. Scales of Transformation in Prehistoric and Archaic Societies 7. Leiden: Sidestone Press. Available from: https://doi.org/10.59641/h0912kt
- Out, W.A., Mieth, A., Pla-Rabés, S., Madella, M., Khamnueva-Wendt, S., Langan, C., Dreibrodt, S., Merseburger, S. and Bork, H.-R., 2021. Prehistoric pigment production on Rapa Nui (Easter Island), c. AD 1200-1650: New insights from Vaipú and Poike based on phytoliths, diatoms and ¹⁴C dating. *The Holocene*, 31 (4), 592–606. Available from: https://doi.org/10.1177/0959683620981671
- Peters, C., Church, M.J. and Mitchell, C., 2001. Investigation of fire ash residues using mineral magnetism. *Archaeological Prospection*, 8 (4), 227–237. Available from: https://doi.org/10.1002/arp.171
- Pickartz, N., Hofmann, R., Dreibrodt, S., Rassmann, K., Shatilo, L., Ohlrau, R., Wilken, D. and Rabbel, W., 2019. Deciphering archeological contexts from the magnetic map: Determination of daub distribution and mass of Chalcolithic house remains. *The Holocene*, 29 (10), 1637–1652. Available from: https://doi.org/10.1177/0959683619857238
- Rabenhorst, M.C., Schmehling, A., Thompson, J.A., Hirmas, D.R., Graham, R.C. and Rossi, A.M., 2014. Reliability of Soil Color Standards. *Soil Science Society of America Journal*, 79 (1), 193–199. Available from: https://doi.org/10.2136/sssaj2014.10.0401
- Sanmartín, P., Chorro, E., Vázquez-Nion, D., Martínez-Verdú, F.M. and Prieto, B., 2014. Conversion of a digital camera into a non-contact colorimeter for use in stone cultural heritage: The application case to Spanish granites. *Measurement*, 56, 194–202. Available from: https://doi.org/10.1016/j.measurement.2014.06.023
- Stevanović, M., 1997. The Age of Clay: The Social Dynamics of House Destruction. *Journal of Anthropological Archaeology*, 16 (4), 334–395. Available from: https://doi.org/10.1006/jaar.1997.0310
- Tite, M.S. and Mullins, C., 1971. Enhancement of the magnetic susceptibility of soils on archaeological sites. *Archaeometry*, 13 (2), 209–219. Available from: https://doi.org/10.1111/j.1475-4754.1971.tb00043.x
- Viscarra Rossel, R.A., Minasny, B., Roudier, P. and McBratney, A.B., 2006. Colour Space Models for Soil Science. *Geoderma*, 133 (3–4), 320–337. Available from: https://doi.org/10.1016/j.geoderma.2005.07.017

Appendices

Appendix 1: Dataset of results from geochemical and geophysical analyses on experimental daub pieces. Cf. Figure 3.

Т	Time	oxgen	colors						magnetic susceptibility			Fed		
°C	min	access	R avrg	S	G avrg	S	B avrg		mean m lf	S	mean m hf	S	freq dep	mg/kg
40	0	0	348,07	22,22	295,39	17,96	214,46	14,20	17,20	1,83	17,18	2,60	0,06	259,125
550	30	0	335,78	18,67	240,78	13,50	151,00	7,88	156,69	86,19	138,38	74,67	11,68	1213,5
550	60	0	361,44	7,99	255,22	7,65	158,56	5,36	58,36	20,32	51,61	19,29	11,57	1174
550	120	0	315,67	37,02	221,78	25,00	138,89	14,51	55,58	22,97	49,30	19,98	11,30	1475,5
550	180	0	328,22	40,84	225,00	28,49	137,67	16,56	74,81	25,85	67,68	22,73	9,53	1822,5
550	240	0	343,11	5,27	250,00	15,62	155,44	10,36	187,15	70,04	166,45	62,36	11,06	1856
650	30	0	337,11	31,02	240,33	21,70	153,44	12,83	380,55	70,73	338,67	61,60	11,00	1522
650	60	0	338,78	24,88	234,33	17,95	148,22	10,88	44,71	7,72	39,82	6,98	10,94	1632
650	120	0	395,56	61,04	274,00	31,66	175,11	19,39	295,71	66,25	264,89	59,25	10,42	1720
650	180	0	362,00	6,57	253,78	5,42	162,56	3,42	244,77	26,45	218,72	23,67	10,64	1611,333
850	30	0	271,67	5,20	149,22	4,03	85,22	2,83	37,85	1,30	35,00	1,14	7,52	555,75
850	60	0	281,11	15,99	167,22	12,48	100,22	9,34	183,29	54,72	163,69	48,65	10,70	487
850	120	0	312,00	2,00	168,89	1,64	94,22	1,02	36,41	0,82	33,89	0,70	6,92	517
850	180	0	322,67	12,00	182,44	10,22	105,56	7,53	129,51	24,50	115,41	21,32	10,89	464,25
940	30	0	381,00	29,87	250,22	16,25	157,00	9,61	200,15	61,41	178,92	53,89	10,60	704,5
940	60	0	352,22	23,52	235,56	29,73	140,11	7,95	40,09	7,13	36,64	7,52	8,61	640
940	120	0	303,22	13,80	191,00	6,89	119,11	4,86	48,63	9,48	43,54	9,28	10,47	624
940	180	0	295,11	38,24	164,44	23,90	94,56	14,53	251,34	52,66	223,11	45,34	11,23	440
940	240	0	334,33	25,36	214,11	19,57	140,44	13,00	117,36	33,93	104,58	30,11	10,89	653
550	30	R	67,33	4,18	62,56	3,50	54,67	2,85	244,73	77,09	219,76	70,78	10,20	2779
550	60	R	66,33	5,86	61,33	5,29	54,11	4,55	234,16	33,68	212,32	30,60	9,33	2376
550	120	R	81,11	11,10	74,33	9,13	63,44	6,77	238,91	17,98	215,00	16,41	10,01	2672
550	180	R	114,00	1,73	102,67	1,15	81,67	1,15	487,77	108,60	442,30	93,24	9,32	1788
550	240	R	260,33		222,00		160,67		448,11	103,67	397,77	92,80	11,23	1655,5
650	30	R	164,11	19,76	142,89	15,51	108,78	10,19	853,07	28,42	753,67	23,85	11,65	1502
650	60	R	301,06	28,40	230,33	18,53	151,39	8,89	853,07	28,42	753,67	23,85	11,65	1606,4
650	120	R	78,33	0,58	74,67	0,58	66,67	0,58	591,25	303,58	526,57	260,63	10,94	1456
650	180	R	349,22	5,87	263,33	5,49	170,78	3,08	947,91	88,55	833,82	69,80	12,04	1571
850	30	R	300,56	9,97	218,78	7,88	141,33	5,93	941,76	17,67	838,40	16,46	10,98	619
850	60	R	322,78	9,03	227,11	4,03	146,44	1,92	942,07	11,72	836,74	10,64	11,18	611,75
850	120	R	368,89	10,01	248,67	6,77	154,44	5,34	882,10	26,57	781,52	23,51	11,40	535
850	180	R	376,00	10,59	249,00	10,17	157,22	6,35	816,31	28,10	720,26	25,25	11,77	502,25
940	30	R	335,56	21,53	190,56	14,84	109,67	9,33	616,33	69,75	543,15	61,71	11,87	668,5
940	60	R	300,00	24,34	162,89	10,69	91,56	4,74	518,53	77,87	455,64	68,50	12,13	559,5
940	120	R	286,44	5,74	157,44	4,35	91,00	2,65	381,32	42,07	335,34	35,27	12,06	652,5
940	180	R	335,33	53,37	211,33	41,79	133,89	25,72	795,57	40,81	702,62	39,91	11,68	552
940	240	R	320,00	7,22	181,44	5,68	107,11	3,67	519,76	84,47	457,16	76,25	12,05	428

Appendix 2: Dataset of results from geochemical and geophysical analyses on 14 archaeological daub pieces (seven from a communal building, seven from a domestic house). Cf. Figure 4.

Sample ID	Find No.	Structure	ID	Colors						Magnetic susceptibility			Fed		
				Red	S	Green		Blue	S	LF MS	S	HF MS		Freq dep	mg/ kg
1110515a	1110515	mega	1	201,67	1,53	148,67	1,53	99,67	1,53	1154,18	4,39	1054,94	9,41	8,60	480,5
1110515b	1110515	mega	1	200,67	5,13	164,33	4,04	115,67	3,21	337,85	1,29	309,64	1,12	8,35	2040
1110515c	1110515	mega	1	294,67	10,60	226,33	8,50	141,33	5,03	435,91	8,90	389,42	7,43	10,66	3580
1110517a	1110517	mega	2	162,67	3,51	135,67	3,21	95,33	2,08	802,61	5,22	750,86	16,08	6,45	2240
1110517b	1110517	mega	2	108,33	2,52	96,67	2,52	75,33	1,53	544,05	20,51	501,62	20,68	7,81	3136
1110519a	1110519	mega	3	246,00	4,36	194,00	3,46	128,33	3,06	414,47	1,38	374,55	1,34	9,63	1001,5
1110519b	1110519	mega	3	89,67	7,02	80,00	6,56	65,00	4,58	282,96	2,88	258,70	2,62	8,57	1462
1110634Aa	1110634A	mega	4	211,67	4,93	171,00	4,36	120,67	3,21	818,30	12,60	743,55	12,21	9,14	4252
1110634Ab	1110634A	mega	4	124,00	4,36	113,33	4,04	94,67	2,89	260,32	2,37	241,29	2,82	7,31	1597
1110634Ba	1110634B	mega	5	223,67	2,08	175,67	2,08	117,67	1,15	1101,07	3,49	1015,77	2,96	7,75	615,5
1110634Bb	1110634B	mega	5	139,00	6,24	124,67	5,13	99,33	3,06	444,02	3,72	406,36	3,19	8,48	2792
1110636a	1110636	mega	6	261,67	2,52	200,33	3,51	130,33	3,21	303,22	1,81	271,88	1,17	10,34	1557
1110636b	1110636	mega	6	80,67	6,03	71,67	5,03	59,33	3,51	366,54	7,10	332,41	3,03	9,28	2728
1110642a	1110642	mega	7	276,00	12,17	198,33	9,07	137,00	6,56	444,36	2,88	423,18	1,57	4,76	395,5
1110642b	1110642	mega	7	139,00	6,56	124,00	5,57	97,67	4,51	316,82	0,54	284,23	0,63	10,29	403,5
1110642c	1110642	mega	7	236,67	11,02	180,00	7,55	121,67	4,73	827,69	12,64	766,78	11,00	7,36	247
1110644a	1110644	mega	8	277,00	3,00	186,33	1,15	116,00	1,00	907,36	12,58	847,23	10,78	6,63	161
1110644b	1110644	mega	8	271,00	3,00	188,33	2,89	120,67	2,31	992,26	6,72	916,61	5,41	7,62	178
1110646a	1110646	mega	9	264,33	6,51	182,67	5,51	115,33	3,06	1148,60	14,22	1048,57	14,58	8,71	130
1110646b	1110646	mega	9	185,67	8,62	145,67	7,02	99,00	5,57	852,50	7,10	778,16	8,79	8,72	1481
1110648mixa	1110648	mega	10	306,00	14,73	241,67	11,06	152,67	5,51	1056,94	2,73	942,14	3,50	10,86	4450
1110648mixb	1110648	mega	10	251,33	9,45	194,67	7,37	126,67	3,79	518,60	7,70	461,36	6,03	11,04	3370
1111525mixa	1111525	mega	11	152,67	5,03	132,67	4,93	100,33	3,06	324,78	2,81	294,84	2,22	9,22	1832
1111525mixb	1111525	mega	11	229,00	6,24	193,33	4,62	136,67	3,21	522,08	3,27	468,61	2,57	10,24	2264
1111526mixa	1111526	mega	12	108,00	8,89	96,33	8,50	78,33	7,57	290,50	0,77	264,27	0,26	9,03	2174
1111526mixb	1111526	mega	12	100,00	6,24	88,00	5,57	71,33	4,04	218,41	0,96	200,53	0,94	8,18	2508
1111535Aa	1111535A	mega	13	278,33	5,69	240,00	5,20	170,00	3,61	288,40	7,48	281,18	7,22	2,50	535
1111535Ab	1111535A	mega	13	211,00	4,58	165,00	2,65	113,00	1,73	443,08	7,64	429,63	6,77	3,03	922,5
1111535Ac	1111535A	mega	13	208,67	8,50	192,00	7,55	158,33	6,03	199,50	3,87	185,77	4,73	6,89	2672
1111535Ad	1111535A	mega	13	208,67	4,51	154,00	3,00	99,67	1,53	523,05	4,41	505,44	4,19	3,37	262
1111535Ae	1111535A	mega	13	185,33	9,50	155,67	7,64	113,33	5,13	437,32	18,30	405,61	16,19	7,25	687
1111535Ba	1111535B	mega	14	297,00	4,58	202,33	1,53	125,00	1,00	1267,82	4,35	1150,76	4,87	9,23	1193
1111535Bb	1111535B	mega	14	227,00	5,57	170,33	4,04	113,67	2,31	1151,11	0,28	1053,60	1,76	8,47	2260
1111574mixa	1111574	mega	15	195,33	2,31	157,67	2,08	111,00	2,00	523,06	1,31	483,08	0,97	7,64	342
1111574mixb	1111574	mega	15	186,33	5,86	154,00	3,61	111,00	2,65	349,66	5,74	327,46	4,68	6,35	1027,5
1111575mixa	1111575	mega	16	79,67	3,21	71,00	3,61	57,67	3,51	367,04	1,25	336,34	7,11	8,36	2836
1111575mixb	1110575	mega	16	81,00	2,65	74,00	2,65	61,00	1,73	367,39	1,09	329,48	0,73	10,32	3406
51293mix	51293	house	1	140,00	26,46	136,00	24,76	118,33	21,73	29,09	1,97	28,56	1,89	1,82	n.d.

Sample ID	Find No.	Structure	ID	Colors						Magnetic			Fed		
					_	_				susceptibility			_	Freq	mg/
				Red	S	Green	S	Blue	S	LF MS	S	HF MS	S	dep	kg
51366mixa	51366	house	2	217,33	9,45	157,33	8,39	107,33	5,86	358,34	23,69	350,73	23,11	2,12	138
51366mixb	51366	house	2	226,67	9,29	159,67	4,93	105,67	3,21	294,79	31,90	284,29	30,03	3,55	140,5
51371a	51371	house	3	210,00	1,73	140,00	1,00	106,33	0,58	133,91	1,39	126,34	1,22	5,65	n.d.
51371b	51371	house	3	85,00	1,00	81,00	1,00	75,00	0,00	462,41	3,41	459,41	3,43	0,65	n.d.
51371c	51371	house	3	210,00	9,64	202,67	9,29	168,33	6,43	78,19	1,51	76,99	1,44	1,54	n.d.
51371d	51371	house	3	186,67	3,51	178,00	3,61	159,00	3,61	146,35	1,01	144,20	0,92	1,46	n.d.
51371e	51371	house	3	172,67	7,09	132,67	4,51	107,00	3,00	194,01	3,18	187,73	3,15	3,24	n.d.
51372mixa	51372	house	4	218,67	1,53	210,00	1,00	182,33	1,15	48,71	1,44	46,67	1,13	4,18	n.d.
51372mixb	51372	house	4	203,00	5,57	196,67	5,03	175,00	4,58	60,71	2,63	56,97	2,19	6,15	n.d.
51373a	51373	house	5	238,67	15,95	218,33	13,58	167,33	9,45	126,55	0,84	121,65	0,86	3,87	n.d.
51373b	51373	house	5	210,00	6,24	203,67	6,11	183,00	6,00	47,19	0,52	46,65	0,54	1,16	n.d.
51373c	51373	house	5	184,33	27,54	179,33	26,01	157,67	23,50	15,87	0,33	15,77	0,38	0,61	n.d.
51373Bmixa	51373B	house	6	142,33	15,89	129,00	13,86	110,67	10,97	252,89	0,73	245,66	0,94	2,86	n.d.
51373Bmixb	51373B	house	6	145,00	13,89	127,67	11,02	103,67	7,51	281,64	0,86	272,39	1,34	3,28	n.d.
51378a	51378	house	7	186,00	5,57	145,00	5,57	102,67	4,16	392,13	1,82	384,18	3,11	2,03	204,5
51378b	51378	house	7	276,67	2,08	241,33	2,31	164,67	2,08	117,40	1,93	112,30	2,11	4,35	129,5
51378c	51378	house	7	124,67	2,08	115,00	1,73	100,00	1,00	97,62	0,67	94,90	0,82	2,79	108,5
51379mixa	51379	house	8	419,00	37,51	329,67	31,66	223,33	22,37	728,25	4,46	637,55	2,89	12,45	1702,4
51379mixb	51379	house	8	379,33	13,01	294,67	10,02	197,67	6,66	907,83	4,47	795,76	4,64	12,34	2433,3
51386a	51386	house	9	388,33	12,58	336,33	10,26	224,33	7,64	170,53	3,45	166,21	3,10	2,53	278,5
51386b	51386	house	9	344,67	7,57	317,33	8,08	230,67	7,57	100,08	0,53	96,15	0,93	3,93	174
51387a	51387	house	10	231,67	9,02	220,67	8,50	192,33	7,09	48,05	0,98	45,78	0,83	4,72	135,5
51387b	51387	house	10	290,67	9,61	264,67	9,07	192,00	7,21	64,65	1,14	60,21	0,50	6,86	196,5
51390a	51390	house	11	367,33	3,06	333,00	3,00	246,33	2,89	97,69	0,86	93,70	1,05	4,08	103
51390b	51390	house	11	314,33	40,65	291,33	35,73	215,67	27,23	79,69	0,13	76,50	0,28	4,00	99
51391a	51391	house	12	258,33	10,07	171,67	5,51	110,33	4,62	532,95	4,20	515,45	2,76	3,28	43,5
51391b	51391	house	12	284,67	14,01	184,67	9,02	119,33	5,03	425,40	1,75	406,47	1,60	4,45	106,5
51392a	51392	house	13	321,67	21,73	269,33	17,90	186,33	13,05	288,69	1,88	275,60	1,70	4,53	n.d.
51392b	51392	house	13	367,67	24,68	309,33	20,53	206,33	13,05	241,97	2,22	234,69	2,15	3,01	n.d.
51393a	51393	house	14	182,00	13,08	150,00	10,39	104,00	7,00	437,95	3,37	399,47	1,08	8,78	1048,5
51393b	51393	house	14	207,33	5,69	178,33	4,73	128,67	3,21	104,67	0,15	97,66	0,33	6,69	790,5
51393c	51393	house	14	145,67	16,50	130,33	14,01	99,67	10,07	85,68	0,45	80,44	0,19	6,12	490,5
51394a	51394	house	15	346,00	10,54	294,00	9,17	198,00	6,24	166,89	1,29	163,71	0,25	1,91	189
51394b	51394	house	15	353,00	8,54	307,67	6,03	211,67	5,03	161,03	1,83	157,95	1,52	1,91	249
51395a	51395	house	16	170,00	4,58	141,00	4,36	99,00	2,65	358,02	0,92	325,53	0,67	9,07	1617
51395a	51395	house	16	81,33	2,52	75,67	1,53	63,33	0,58	146,96	1,23	135,33	0,67	7,91	799,5
513950 51395mix	51395		16											,	
		house		111,33	2,08	101,00	1,73	79,67	1,53	286,27	3,90	264,11	2,87	7,74	778
51396a	51396	house	17	309,00	14,53	279,67	11,50	193,00	8,54	64,99	1,06	62,91	0,88	3,21	184
51396b	51396	house	17	182,00	5,57	176,00	4,58	155,00	2,65	80,45	2,97	78,29	2,68	2,69	567,5
51400mixa	51400	house	18	425,00	23,64	356,33	18,15	249,00	13,00	289,24	1,21	270,65	0,92	6,43	n.d.

Sample ID	Find No.	Structure	ID	Colors						Magnetic susceptibility			Fed		
				Red	S	Green	S	Blue	S	LF MS	S	HF MS	S	Freq dep	mg/ kg
51400mixb	51400	house	18	454,67	18,50	376,67	16,04	262,67	12,66	296,44	3,14	276,20	2,78	6,83	n.d.
51402a	51402	house	19	406,33	15,37	326,67	11,93	229,33	7,02	332,86	14,80	314,99	14,90	5,38	202
51402b	51402	house	19	393,00	10,39	324,33	8,96	226,67	7,57	448,69	3,52	420,46	2,81	6,29	253,5
51409a	51409	house	20	312,67	20,60	208,33	15,04	140,33	10,07	247,83	6,12	232,30	5,61	6,27	102,5
51409b	51409	house	20	411,00	18,68	334,33	13,65	240,33	10,69	402,52	0,78	374,76	0,63	6,90	14
51413mixa	51413	house	21	356,00	13,75	258,33	12,01	167,00	8,00	461,29	0,06	413,28	1,47	10,41	623
51413mixb	51413	house	21	336,33	16,56	235,33	11,59	151,00	6,56	331,91	2,17	296,53	1,49	10,66	595
51416a	51416	house	22	450,33	17,56	372,00	7,00	271,33	4,04	340,69	16,34	308,99	16,46	9,32	60,5
51416b	51416	house	22	336,67	2,52	230,67	1,53	152,67	0,58	933,22	9,25	832,95	8,16	10,74	43
51416c	51416	house	22	346,67	6,43	255,67	5,69	172,00	4,36	666,94	4,98	584,04	4,92	12,43	68
51416d	51416	house	22	318,33	19,66	211,33	12,70	132,67	8,08	769,35	3,75	706,49	3,09	8,17	179
51613a	51613	house	23	425,67	4,93	371,00	4,36	263,00	3,00	188,75	9,53	181,78	9,48	3,70	47
51613b	51613	house	23	183,67	4,93	147,33	3,79	112,67	2,52	534,18	2,50	525,01	2,35	1,72	179,5
51613Bmixa	51613B	house	24	439,67	9,29	389,67	8,39	271,00	6,24	136,59	2,24	133,04	2,29	2,60	50,5
51613Bmixb	51613B	house	24	454,00	21,17	397,67	18,58	274,00	12,77	140,75	1,22	136,09	1,11	3,31	157,5
51615a	51615	house	25	403,00	38,12	362,33	34,36	255,67	23,69	73,04	1,34	70,87	1,39	2,97	n.d.
51615b	51615	house	25	398,33	23,18	338,33	20,60	231,33	15,04	194,53	1,54	188,98	1,68	2,85	n.d.
51615c	51615	house	25	390,00	15,87	305,33	14,15	216,67	10,21	478,89	1,19	444,91	1,34	7,10	n.d.
51617a	51617	house	26	244,00	2,65	177,00	1,73	114,00	1,73	629,13	3,53	573,41	3,10	8,86	n.d.
51617b	51617	house	26	248,33	10,60	171,33	6,66	110,00	4,00	649,24	3,18	615,86	2,88	5,14	n.d.
51617ox	51617	house	26	267,67	12,01	174,00	8,54	113,00	5,00	529,04	0,71	505,41	1,00	4,47	n.d.
51617red	51617	house	26	220,33	7,09	156,33	5,51	99,00	4,58	586,92	2,41	543,60	2,07	7,38	n.d.
51620a	51620	house	27	261,67	23,03	196,67	17,62	138,33	12,01	285,37	5,46	269,94	4,80	5,40	n.d.
51620b	51620	house	27	438,33	16,77	362,00	13,89	255,67	11,15	225,42	0,87	213,83	1,08	5,14	n.d.
51620c	51620	house	27	304,67	17,24	234,33	12,50	164,00	8,19	322,88	2,46	305,11	2,12	5,50	n.d.
53391a	53391	house	28	252,33	23,07	174,33	15,95	116,67	10,12	554,41	2,34	536,07	2,87	3,31	n.d.
53391b	53391	house	28	247,67	8,14	171,00	5,29	111,67	3,06	599,02	2,48	579,50	1,80	3,26	n.d.

From Ros to Prut:

TRANSFORMATIONS OF TRYPILLIA SETTLEMENTS

Pre-dating the urban revolution in Western Asia, a network of agricultural settlements developed in the forest-steppe zone northwest of the Black Sea in the late 5th and first half of the 4th millennium BCE, some of which are among the largest prehistoric mega-sites in Europe. These enormous so-called Trypillia/Tripolye communities are unique in many respects, and the dynamics of their formation and their development have long been a topic of intensive research. For more than ten years now, research on the transformations of these Chalcolithic societies has been conducted as a Ukrainian-Moldavian-German cooperation. This research does not only focus on some of the largest mega-sites, but also attempts to reconstruct the dynamics of mega-site processes and their economic, social and ideological foundations in different perspectives – local, regional and interregional. Although our research is not yet complete, it is already clear that the emergence of Trypillia/Tripolye mega-sites represented the preliminary culmination of a regionally differentiated and widely interconnected process of settlement formation in the area between the Prut and Ros rivers. These processes were, on the one hand, closely interwoven with Copper Age societies of Southeast Europe and, on the other hand, ushered in the transition to the era characterised by higher settlement mobility.

This volume brings together archaeological, geophysical, archaeobotanical, archaeozoological and geoarchaeological contributions on economy, settlement patterns, material culture and dating from three different test regions in the territory of present-day Ukraine and Moldova. The presentation of our new data contributes decisively to a better understanding of both the enormous variability of settlement trajectories characterising this vast area and to connecting developments throughout time.

Volume 1 contains contributions on the Maidanetske mega-site and the Sinyukha River basin (Dnieper-southern Bug interfluve).

CRC 1266
SCALES OF TRANSFORMATION

